The Determination of Variation in Proximal Femoral Geometry and Shape in Primary Hip Osteoarthritis Using Active Shape Modelling

A dissertation submitted to the University of Oxford



In partial fulfilment of the requirements for the degree of

Master of Science by Research in Musculoskeletal Sciences

By

Christian D. Merle

Wolfson College

and

Nuffield Department of Orthopaedics, Rheumatology and Musculoskeletal Sciences, University of Oxford

Trinity Term 2011

ABSTRACT

The Determination of Variation in Proximal Femoral Geometry and Shape in Primary Hip Osteoarthritis Using Active Shape Modelling

Christian D. Merle MSc by Research

Wolfson College Trinity Term 2011

The success of cementless femoral reconstruction in contemporary total hip arthroplasty is dependent on both an adequate endosteal stem fit and the precise restoration of physiologic joint mechanics. With regard to the rising popularity of cementless fixation, modularity and short stem designs, accurate pre-operative templating has become essential as small inaccuracies in the assessment of proximal femoral shape and geometry may compromise the clinical outcome. In addition, the current knowledge of variation in proximal femoral geometry and canal shape in arthritic hips is limited, and the association of geometry and canal shape is poorly understood. Therefore, the broad aims of this thesis were (1) to improve pre-operative planning in hip arthroplasty and (2) to provide information for future femoral component design accounting for individual patient anatomy.

Based on a large (n=345) retrospective cohort of patients with primary end-stage hip osteoarthritis the differences in the assessment of femoral offset (FO) on corresponding AP ***pelvis*** radiographs, AP ***hip*** radiographs and CT scans were examined. FO was used as a surrogate parameter to represent proximal femoral geometry. Active Shape Modelling (ASM) was performed to assess differences in the radiographic appearance of the proximal femoral canal on corresponding modes of imaging, and to determine the variation and underlying patterns in proximal femoral anatomy.

It was demonstrated that - in contrast to AP pelvis radiographs - measurements on standardised AP hip radiographs provide a more accurate and reliable assessment of FO and canal shape of the proximal femur, comparable to 3D measurements performed on CT. A linear relationship between FO measurements on corresponding modes of imaging was observed which allowed gender specific regression equations to be established in order to predict 3D FO from AP pelvis radiographs. ASM revealed an association between endosteal canal shape and joint geometry. Ten distinct shape patterns of the proximal femoral canal were identified and each pattern was associated with a specific set of geometric parameters. Variations in canal shape shape were independent of femoral head size, BMI, gender or age.

In conclusion, orthopaedic surgeons need to be aware that the assessment of proximal femoral geometry and canal shape may be misleading on AP pelvis radiographs. Standardised AP hip radiographs are a practical, cost-effective and readily available method which allows accurate and reliable assessment of joint geometry and canal shape without the routine performance of CT. When AP hip radiographs are not available for templating, the provided regression equations can be used to compensate for the adverse effects of positioning inconsistencies and beam divergence in the assessment of FO on AP pelvis radiographs. The present findings have the potential to aid surgeons in selecting an appropriate implant design and size, and assist in planning the intra-operative position of femoral components.

The findings further provide a comprehensive classification of proximal femoral geometry and shape in patients with primary hip OA. The identification of distinct shape patterns has implications for future cementless femoral component designs that aim for optimal metaphyseal stem fit and concomitant restoration of individual patient anatomy.

Table of Contents

1. INTRODUCTION ..... - 6 -

1.1 Background ..... - 6 -
1.2 Study Rationale ..... - 7 -
1.3 Objectives of the Thesis ..... - 9 -
1.3.1 Overall scope ..... - 9 -
1.3.2 Specific aims ..... - 9 -

2. LITERATURE REVIEW ..... - 10 -

2.1 Hip Osteoarthritis ..... - 10 -
2.1.1 Definition ..... - 10 -
2.1.2 Aetiology of Hip Osteoarthritis ..... - 10 -
2.1.3 Epidemilogy and Socio-economic Impact of Osteoarthritis ..... - 13 -
2.2 Total Hip Arthroplasty ..... - 14 -
2.2.1 Historical Background ..... - 14 -
2.2.2 Epidemiology of Total Hip Arthroplasty ..... - 16 -
2.2.3 Cemented and Cementless Femoral Component Fixation ..... - 16 -
2.2.4 Functional Anatomy and Biomechanics of THA ..... - 18 -
2.2.5 Pre-operative Imaging and Planning ..... - 19 -
2.2.6 Femoral Implant Design ..... - 21 -
2.3 Active Shape Modelling ..... - 23 -
2.4 Summary and Outline of the Remaining Thesis ..... - 24 -

3. ASSESSMENT OF FEMORAL OFFSET ..... - 26 -

3.1 Introduction ..... - 26 -
3.2 Materials and Methods ..... - 27 -
3.2.1 Study Cohort ..... - 27 -
3.2.2 Radiographic Protocol ..... - 28 -
3.2.3 Computed Tomography Protocol ..... - 29 -
3.2.4 Radiographic Measurements ..... - 29 -
3.2.5 CT Measurements ..... - 30 -
3.2.6 Measurement Reliability ..... - 31 -
3.2.7 Statistical Analysis ..... - 32 -
3.3 Results ..... - 32 -
3.3.1 Measurement Reliability ..... - 32 -
3.3.2 Radiographic Findings ..... - 33 -

3.3.3 CT Findings ..... - 34 -
3.4 Discussion ..... - 38 -
3.5 Summary ..... - 43 -

4. PREDICTION OF 3D FEMORAL OFFSET FROM AP PELVIS RADIOGRAPHS ..... - 45 -

4.1 Introduction ..... - 45 -
4.2 Materials and Methods ..... - 45 -
4.2.1 Study Cohort ..... - 45 -
4.2.2 Imaging Protocols ..... - 47 -
4.2.3 Radiographic Measurements ..... - 47 -
4.2.4 CT Measurements ..... - 48 -
4.2.5 Measurement Reliability ..... - 48 -
4.2.6 Statistical Analysis ..... - 48 -
4.3 Results ..... - 49 -
4.3.1 Measurement Reliability ..... - 49 -
4.3.2 Radiographic and CT Findings ..... - 49 -
4.3.3 Regression and Prediction Analysis ..... - 52 -
4.4 Discussion ..... - 58 -
4.5 Summary ..... - 60 -

5. ASSESSMENT PROXIMAL FEMORAL CANAL SHAPE ..... - 62 -

5.1 Introduction ..... - 62 -
5.2 Materials and Methods ..... - 63 -
5.2.1 Study Cohort ..... - 63 -
5.2.2 Imaging Protocols ..... - 63 -
5.2.3 Active Shape Modelling ..... - 63 -
5.2.3 Curve Fitting ..... - 65 -
5.2.4 Measurement Reliability ..... - 66 -
5.2.5 Statistical Analysis ..... - 66 -
5.3 Results ..... - 67 -
5.3.1 Measurement Reliability ..... - 67 -
5.3.2 Active Shape Modelling ..... - 67 -
5.3.3 Curve fitting ..... - 70 -
5.4 Discussion ..... - 71 -
5.5 Summary ..... - 75 -

6. VARIATION AND PATTERNS OF PROXIMAL FEMORAL SHAPE AND GEOMETRY- 76 -

6.1 Introduction ..... - 76 -
6.2 Materials and Methods ..... - 77 -
6.2.1 Study Cohort ..... - 77 -
6.2.2 Imaging Protocols ..... - 77 -
6.2.3 Active Shape Modelling ..... - 77 -
6.2.4 Cluster Analysis ..... - 78 -
6.2.5 Canal Flare ..... - 78 -
6.2.6 CT measurements ..... - 80 -
6.2.7 Measurement reliability ..... - 80 -
6.2.8 Statistics ..... - 81 -
6.3 Results ..... - 82 -
6.3.1 Measurement reliability ..... - 82 -
6.3.2 Radiographic and CT measurements ..... - 82 -
6.3.3 Active Shape Modelling ..... - 84 -
6.3.4 Cluster Analysis ..... - 86 -
6.4 Discussion ..... - 89 -
6.5 Summary ..... - 94 -

7. CONCLUSIONS, CLINICAL RELEVANCE AND FUTURE WORK ..... - 95 -

7.1 Review of Objectives and Conclusions ..... - 95 -
7.2 Clinical Relevance ..... - 96 -
7.3 Strengths and Limitations ..... - 98 -
7.4 Future work ..... - 99 -

References ..... - 101 -

List of Tables ..... - 111 -

List of Figures ..... - 112 -

Appendix A ..... - 113 -

Appendix B ..... - 114 -

Acknowledgements ..... - 115 -

1. INTRODUCTION

1.1 Background

The original goal of total hip arthroplasty (THA) was to provide pain relief and durable implant fixation in the long-term. Indications for THA were initially restricted to elderly patients with low physical activity, or patients with other major locomotor impairments. Since the revolutionary introduction of Sir John Charnley's low friction arthroplasty in the late 1950s and early 1960s[1], THA has undergone a rapid technical development, and for its great success, it has been termed "the operation of the century"[2,3]. The numbers of total hip replacements performed have increased remarkably over the last decade[4,5], and future predictions suggest that the demand for primary THA might further increase over the next two decades[6].

The high technical standard of THA and its predictable clinical outcome have consequently led to a rising number of procedures performed in young and more active patients. With extension of THA indications, the expectations of patients have changed fundamentally, especially with regard to physical activity levels and quality of life issues[7,8]. In addition to long-term implant fixation and pain relief, patients expect the surgery to provide good post-operative joint function regarding muscle strength and range of motion (ROM). Moreover, leg length discrepancies after THA are a major factor contributing to dissatisfaction of patients, as they have been associated with complications such as nerve palsy, low back pain and abnormal gait patterns[9-12].

Promising long-term survival rates of cementless femoral reconstruction have been recently reported in single retrospective cohort studies[13-15]. However, wear-related complications such as aseptic loosening and osteolysis continue to be the major modes of

failure in the long-term, and there is an on-going debate on whether failure of the femoral component is more likely to occur in young and/or active patients[16-18]. Moreover, there is concern that stress-shielding and progressive peri-prosthetic bone loss as a result of distal load transfer may adversely affect the clinical outcome of THA[19].

As a consequence, the individual restoration of physiological joint mechanics with high accuracy has become a major focus in contemporary THA because it provides patients with a better functional outcome[20,21] and minimises the risk of post-operative complications such as limp, dislocation or wear-related implant failure[22-24].

In cementless THA, which has become increasingly popular, the ideal femoral component should achieve a close geometric fit between the implant and the endosteal surface of the proximal femoral meta- and diaphysis to obtain primary and secondary stability[25,26]. Simultaneously, it should allow accurate restoration of physiologic joint geometry. In clinical practise, these demands are often compromised as a result of inaccurate pre-operative planning and a high individual variability in proximal femoral anatomy[27-29].

1.2 Study Rationale

Adequate stem fixation and the individual restoration of physiological joint mechanics are two major factors that determine the success of contemporary THA.

Accurate pre-operative templating is an essential requirement for successful THA as it aids the surgeon in the selection of appropriate implant geometry and size, and suggests intra-operative positioning of prosthetic components[30,31]. In clinical practise, pre-operative templating is widely performed on anteroposterior (AP) pelvis radiographs which provide essential information regarding pelvic and contralateral hip anatomy, and allow evaluation of leg length discrepancies[32]. However, several studies over the past two decades have

described limited accuracy of radiographic geometry measurements on AP pelvis radiographs as a result of the difficulty to position the femoral neck in the coronal plane. This has been attributed to a high variability in femoral anteversion (FA)[29,33], and the presence of external rotational contractures which are frequently seen in patients with end-stage osteoarthritis (OA)[34,35]. For the same reasons, the assessment of canal shape on plain radiographs, which is essential to template stem fit, may be misleading[36].

Consequently, some authors have proposed pre-operative computed tomography (CT) as a routine procedure[29,33]. Although CT is considered as gold standard for pre-operative templating[37,38], its routine performance is questionable because of higher radiation doses, higher costs, limited availability and a lack of evidence for improved clinical outcome in the long-term.

In contrast to AP ***pelvis*** radiographs, AP ***hip*** radiographs have the potential for better control of femoral rotation and theoretically limit the projection effects caused by radiographic beam diversion. There are no previous studies in the literature that have investigated the accuracy and reliability of geometric and canal shape measurements on standardised AP ***hip*** radiographs in comparison to AP ***pelvis*** radiographs and CT in pre-operative THA planning.

Secondly, the variation in proximal femoral anatomy and the relationship between femoral canal shape and joint geometry of the hip in patients with end-stage hip OA is poorly understood. Most published studies describe proximal femoral anatomy on the basis of conventional radiography or on observations made in cadaveric specimens[39,40]. There are few studies on relevant anatomic differences between males and females[41-43], and the influence of patient age on proximal femoral anatomy remains controversial[41,42]. In particular, information on the three dimensional morphology of the proximal femur in

degenerative hip conditions is very limited[27,44,45]. Little is known about the range of individual variation in proximal femoral anatomy, and potential associations between shape of the proximal femoral canal and joint geometry have not been investigated.

1.3 Objectives of the Thesis

1.3.1 Overall scope

To improve pre-operative planning and provide information for future femoral component design accounting for individual patient anatomy in THA.

1.3.2 Specific aims

To assess differences in proximal femoral geometry and canal shape on corresponding AP pelvis radiographs, AP hip radiographs and CT scans in primary end-stage hip osteoarthritis.

To quantify the variation in proximal femoral canal shape and its association with geometric and anthropometric parameters in primary end-stage hip osteoarthritis.

2. LITERATURE REVIEW

2.1 Hip Osteoarthritis

2.1.1 Definition

Osteoarthritis is a progressive joint disease and a major cause of musculoskeletal pain and physical disability in middle-aged and elderly adults worldwide[46]. Although the term 'osteoarthritis' was first used in the 1860's to describe a condition of chronic arthritis[47], there is currently no unequivocal definition of osteoarthritis[48]. A contemporary definition may describe OA as progressive and multifactorial articular cartilage degeneration with associated structural changes in the underlying bone and limited inflammation of the synovium.

2.1.2 Aetiology of Hip Osteoarthritis

The aetiology of OA has been historically classified into two major subsets: *Primary* or *idiopathic* osteoarthritis is a condition in which the cause of the joint degeneration is not known or obvious; *secondary* osteoarthritis on the other hand, is associated with a pre-existing pathology that can be causally related to the destruction of the joint, such as trauma, dysplasia, avascular necrosis of the femoral head, or slipped capital femoral epiphysis.

The American College of Rheumatology aimed to classify OA into subsets of primary and secondary OA[49] (Table 2.1).

In 1965, Murray was the first to suggest that subtle and often unrecognised anatomical variations of the hip joint lead to abnormal joint mechanics with incongruity of the articular surfaces which "makes the development of degenerative change more likely than

a joint having normal anatomical structure"[50]. This theory was further extended by Solomon, Harris and Ganz[51-53] and today, the concept of femoro-acetabular impingement (FAI) as a mechanical cause of hip OA is well-recognised[54].

However, the aetiology of primary OA is remains controversial. Scientific approaches to identify causal factors vary considerably, and have identified further risk factors for primary OA, such as obesity[55,56], genetics[57-60], hormones[61] and ageing[62]. This suggests that OA is likely to represent the end-point of a variety of different conditions[63] which can affect all the tissues of the diathrodial joint (i.e. cartilage, sunchondral bone, ligaments, synovium)[64].

In the last two decades, there has been a growing understanding that OA is not only a "wear and tear" disease, but a complex multifactorial disorder in which ageing, genetic, hormonal and mechanical factors are all potential contributors to the onset and progression of OA[49,56,62,64-66].

I. Primary OA
A. Localised
1. Hands: e.g. Heberden's and Bouchard's nodes
2. Feet: e.g. hallux valgus, hallux rigidus
3. Knee:
4. Hip:
a. Eccentric (superior)
b. Concentric (axial, medial)
c. Diffuse (coxae senilis)
5. Spine:
6. Other single sites: e.g. shoulder
B. Generalised
1. Small and spine
2. Large and spine
3. Mixed and spine
II. Secondary OA
A. Posttraumatic
B. Congenital or developmental disorder
1. Localised
a. Hip disease: e.g. Legg-Calve-Perthes, developmental dysplasia
b. Mechanical and local factors: e.g. unequal lower extremity length
2. Generalised
a. Bone dysplasia: e.g. epiphyseal dysplasia
b. Metabolic diseases: e.g. hemochromatosis
C. Calcium Deposition Disease
D. Other Bone and Joint Disorders: e.g. avascular necrosis
E. Other Diseases
1. Endocrines diseases: e.g. diabetes mellitus
2. Neuropathic arthropathy
3. Miscellaneous

Table 2.1

ACR classification for subsets of osteoarthritis, modified from Altman et al., 1991[67].

2.1.3 Epidemilogy and Socio-Economic Impact of Osteoarthritis

Osteoarthritis is the most prevalent joint disease in humans[68], and it is present in all human races[69-72]. Among the large joints, the hip and knee are most commonly affected by OA[73,74].

A precise estimation of the prevalence of OA is difficult because the prevalence of pain associated with radiographic evidence of joint degeneration varies considerably among individuals. It has been shown that some patients with advanced radiographic joint degeneration have only minimal pain and disability[46]. Furthermore, estimates of the prevalence vary depending on whether it is chosen to include mild or only moderate and severe radiographic changes. In 2005, Lawrence and co-workers estimated the prevalence of symptomatic OA in the United States up to nearly 27 million[68], compared to 21 million in 1995[75]. The increase over ten years corresponds with the increase in average age of the population. Jordan et al. reported similar results for symptomatic hip OA (approximately 10%) based on the Johnston County Osteoarthritis Project, a study of hip and knee OA in >3,000 African American and white adults of age greater than 45 years old in a rural county in North Carolina[76]. Finally, an estimate in Germany showed that approximately 15% to 20% of the population were diagnosed with osteoarthritis[77].

Osteoarthritis is a major worldwide cause of economic loss[78]. Based on the Medical Expenditure Panel Survey (MEPS) data on US adults with health insurance, estimates for annual OA-attributable medical expenditures range from 10% ($805 billion in 2003 MEPS)[79] to 19% ($994 billion in 2005 MEPS)[80] of all aggregate medical expenditures.

At an individual level, the indirect costs of OA should not be neglected. It is responsible for work-related problems, leads to lost opportunities for increased productivity, decreased ability to participate in regular exercise which could improve general health, and raises

costs to family members who provide care for patients with OA. Moreover, OA has severe adverse effects on the patients' quality of life[81,82].

In Summary, OA represents a major burden for society.

2.2 Total Hip Arthroplasty

Total hip arthroplasty is the reconstructive surgical replacement of the hip joint with an artificial prosthesis. THA is considered as a highly effective and reliable treatment in patients with end-stage hip OA who do not longer benefit from conservative treatment options[73,83].

2.2.1 Historical Background

As early as 1890, Gluck performed the first recorded attempt in hip arthroplasty, using an ivory femoral component to replace the femoral head[84]. Hip replacement surgery initially expanded after the Second World War, following the introduction of the Austin Moore and Thompson hemi-arthroplasties. Other early pioneers developed replacements made of various materials, including acrylic cement, ceramics, metal and polyethylene. Smith-Petersen covered the re-shaped femoral head with a vitallium cup. Judet devised a partial replacement using acrylic, primarily for fractures. McKee and Watson-Farrer introduced a metal on metal hip replacement. These early arthoplasties were successful in providing pain relief, but showed high failure rates in the short- and mid-term[84].

The first reliable THA was promoted around 1960 by Sir John Charnley, who started to develop a prosthesis that consisted of a metallic femoral component articulating with a plastic (*Teflon*) acetabular component[85]. Charnley also introduced methylmethacrylate, bone cement, to achieve durable component fixation. The design of his *low-friction*

arthroplasty has formed the basis for the development of modern endoprotheses as we recognise them today (Figure 2.1).

The occurrence of aseptic loosening in cemented THA was initially poorly understood, and regarded as 'cement disease'. This led to the development of cementless THA. During the 1970s, the Judet brothers in Paris started to implant total hips designed for use without cement[86]. The prosthesis surface featured large irregularities to stimulate bone ingrowth (Figure 2.1). Initially, these femoral implants appeared to work well, but showed unacceptably high failure rates after five to ten years.

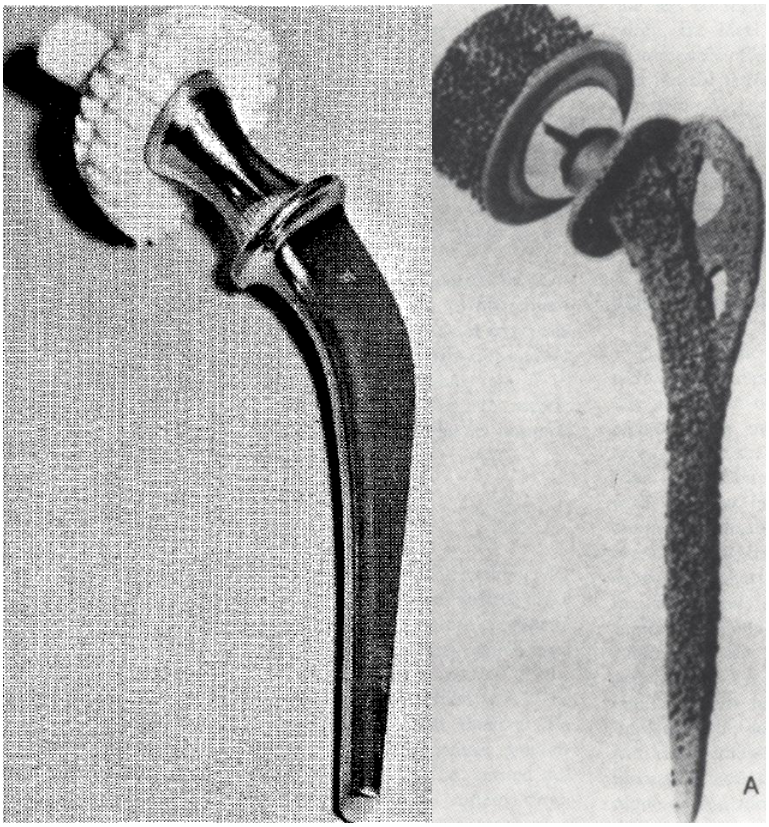


Figure 2.1

Left: Charnley's low-friction arthroplasty. Right: Judet prosthesis with textured surface and a large trochanteric 'fin'. (source left image: Charnley, J., 1961[1]; source right image: Steinberg, M. (Ed.). 'The Hip and its Disorders', page 989[87])

2.2.2 Epidemiology of Total Hip Arthroplasty

Total hip arthroplasty is one of the most widely performed surgical interventions for OA[6]. Kurtz et al. estimated that approximately 250,000 primary THA surgeries were performed in the United States in 2010[6]. In Germany, even higher operation rates per capita of approximately 200,000 THAs were estimated in 2010[88]. In the UK, less THAs per capita are performed compared to Germany, but the numbers of hip replacements have increased considerably by approximately 50% over the last ten years[4,5]. Kurtz et al. furthermore estimated that by 2030, the demand for primary THAs in the US may grow by as much as 174%, and for THA revisions by 137%[6]. These predictions seem realistic, firstly because of the population distributions in Western countries like Germany where currently 56% of the population is over 40 years old[89] and secondly, because of the increase in life expectancy[90].

2.2.3 Cemented and Cementless Femoral Component Fixation

The survival rates of the Charnley low-friction arthroplasty[91] lay the basis for the popularity of cemented implant fixation. Charnley´s low-friction arthroplasty is still considered by many surgeons to be the gold standard in THA, but the best option for a durable implant fixation has been subject of much controversial debates.

In recent years, however, cementless femoral reconstruction has increasingly been used world-wide[92]. The National Joint Registry (NJR) of England and Wales reported that of the 65,229 primary hip procedures undertaken in 2009, 36% were cemented total hip replacements (THR), 39% were cementless THRs and 16% were hybrids or reverse hybrid THRs. Registry data and meta-analyses comparing cemented and cementless fixation with a minimum of 10-year follow-up have been published[93,94]. It has been discussed that younger patients (<55 years) still have a more active bone metabolism and hence

cementless implants, which rely on a biological fixation, should be favoured. Shorter operation times are another advantage of cementless implants. On the other hand, there seems to be an eight-fold higher risk for early revisions within the first two years after index surgery using cementless stems, suggesting a high incidence of unrecognised intra-operative fractures[95]. Concerning cemented implants, it has been suggested that they provide more flexibility in the restoration of femoral version and leg length as the stem position can be relatively easily adjusted within the cement mantle after insertion. Evaluations of the Swedish Hip Arthroplasty Register[95] recently described superior survival rates of cemented THA, compared to uncemented THA. In uncemented THA, the acetabular component was associated with an increased risk of revision. In contrast to the inferior performance of uncemented cups, uncemented stems showed superior survival. These findings correspond with 15-year survival rates of >90% for selected cementless stems with certain design criteria[96].

Unlike cemented femoral components, in which a geometric mismatch between the femoral component and the medullary canal of the proximal femur is required for fixation, cementless femoral reconstruction aims for a close geometric fit between the implant and the endosteal surface of the proximal femur[97,98]. Primary stable fixation is achieved by press-fit implantation of a slightly oversized implant into the prepared medullary canal[99]. Primary stability is crucial to minimise micro-motion at the implant bone interface which subsequently allows secondary biologic fixation by osseous ongrowth of bone to the implant surface (osteointegration)[25,26]. A number of investigations have highlighted the importance of metaphyseal stem fit to reduce micro-motion at the implant bone interface[97,100], and to minimise stress-mediated proximal bone resorption (stress-shielding)[101,102]. Despite promising long-term results of some cementless stems[103,104], an

increased risk of aseptic loosening has been reported for undersized femoral components[105] and there is still is concern that progressive peri-prosthetic bone loss may compromise long-term stem performance[19]. This is particularly important with regard to a rising number of THAs performed in young and active patients[106].

2.2.4 Functional Anatomy and Biomechanics of THA

The hip is a highly congruent, multi-axial ball and socket joint and composed of osseous, muscular and ligamentous structures. The joint is responsible for transferring the weight of the body from the axial skeleton into the lower extremities, and for forces which balance the upper body during the gait cycle[107]. It acts as a fulcrum in which the body weight and the opposing hip abductors are in a state of equilibrium to level the pelvis in stance and throughout the gait cycle.

Hip joint forces vary with specific activity. During normal gait, cyclic loading can place forces on prosthetic components that are two to five times the body weight[108]. During more strenuous activity, such as running or stumbling, the joint is exposed forces as high as eight times the body weight[109].

The main biomechanical determinants of stability, leg-length, range of motion, muscle function and joint forces following THA are the location of the centre of rotation (COR) in relation to the pelvis, femoral offset (FO), anteversion (FA) and neck-shaft-angle (NSA), as well as the individual anatomy of muscular and other soft tissues. Variations in the overall geometry of a THA have a significant influence on the resultant joint reaction force (JRF)[110]. It has been shown that a decreased NSA increases the mechanical advantage of the abductors, whilst reducing the JRF and directing it more medially[110].

In clinical practise, several advantages are associated with the reproduction of physiological hip anatomy after THA. Appropriate offset- and leg length reconstruction in THA are known to improve the functional outcome while minimizing the risk of complications such as limp, dislocation or wear-related implant failure[22,111].

FA is a variable that affects the range of motion (ROM) before component impingement occurs[112,113]. Inadequate femoral version may therefore lead to impingement, subsequent dislocation and accelerated wear[114,115].

Increased FO after THA allows both an increased range of abduction and greater abductor muscle strength post-operatively[21,111]. A decreased polyethylene (PE) wear rate was observed for the use of high offset components in comparison to standard offset components[24]. Similarly, accurate restoration of femoral offset was reported to decrease polyethylene wear[116,117].

2.2.5 Pre-operative Imaging and Planning

Besides the assessment of characteristic symptoms and a thorough clinical examination of the affected joint, the gold standard for the diagnosis of hip OA is radiography. In conventional radiography, the following joint alterations are observed with progression of the disease:

- joint space narrowing
- subchondral sclerosis
- osteophytes
- subchondral cysts
- malalignment/deformity

The Tönnis classification[118] is commonly used to grade the extent of hip OA on conventional radiographs (Table 2.2).

Grade	Radiographic Findings
0	No sign of osteoarthritis
1	Increased sclerosis of the head and acetabulum, slight narrowing of the joint space, and slight lipping at the joint margins
2	Small cysts in the head or acetabulum, increasing narrowing of the joint space, and moderate loss of sphericity of the head
3	Large cysts in the head or acetabulum, severe narrowing or obliteration of the joint space, severe deformity of the head, and necrosis

Table 2.2

Radiographic Tönnis classification for osteoarthritis of the hip[118].

In contemporary hip arthroplasty, pre-operative planning after careful review of the clinical and radiographic findings is of paramount importance in order to perform the procedure precisely, to anticipate potential intra-operative complications, and to achieve reproducible results. Templating the femoral side for cemented and cementless implants should aim to optimize limb length and femoral offset, thereby restoring physiologic biomechanics of the hip joint[30].

Conventionally, most surgeons use plain radiographs in two planes for pre-operative planning. However, several studies showed that radiographic evaluation of the hip has limited reliability with regard to the estimation of morphologic parameters[119]. Surgeons should take into consideration that conventional radiography has limitations with regard to

planning the version of the prosthetic components and assessing the rotation of the lower limb[111]. On AP pelvis radiographs, femoral offset is frequently underestimated which may lead to inadequate soft-tissue balancing[22].

It has been shown, that CT scanning allows a precise, three-dimensional (3D) evaluation both of the proximal femur as well as of the acetabulum and may improve pre-operative templating with regard to intra-operative component positioning and the implant selection[33].

2.2.6 Femoral Implant Design

The original Charnley low-friction arthroplasty consisted of a monobloc metallic femoral component with a small head (22 mm). In Switzerland, Müller altered Charnley's prosthesis fundamentally in 1968. The modifications of the Müller prosthesis were firstly, the availability of different neck lengths to accurately restore leg length and tension, secondly a larger head diameter of 32 mm, and thirdly a curved stem that allowed insertion without osteotomy of the greater trochanter. The new prosthesis became very popular but soon increased loosening rates compared to the original Charnley THA were reported[87]. Further developments in THA design followed in the 1980s; in addition to previous head diameters (22 mm and 32 mm), prostheses with 26 mm and 28 mm head diameters became available. Most femoral components became available in modular form at the head-neck junction, and acetabular components allowed the removal and replacement of plastic liners[87].

Contemporary third generation implants are designed to closely approximate the functional anatomy of a normal hip joint. Many considerations including implant materials, manufacturing technology and current knowledge of proximal femoral anatomy dictate the design of prosthetic components[120]. However, the previously described limited knowledge

of variation in femoral anatomy, especially in patients with end-stage OA, may potentially compromise the achievement of this goal.

Several concepts of femoral component designs have been introduced in order to account for anatomical variations in the proximal femur. Aldinger et al. developed custom-made cementless stems in 1988[121] which proved to have remarkable survival rates[122]. Yet, custom made implants require routine CT and are more expensive, so that their use in primary OA is controversial. Similarly, off-the-shelf implants with multiple shape options have been recently introduced to account for individual patient anatomy[123,124], but long-term follow up data for these novel components is not available.

Another innovation in the design of femoral components has been the introduction of neck-stem modularity which permits intra-operative adjustment of soft-tissue tension and leg length. Modularity at the neck-stem junction allows independent adjustment of stem fixation and reconstruction of geometry, and hence, modular hip stems have gained growing popularity[123,125]. However, concerns have been raised that, as with any metal-on-metal modular junction, there is an increased risk of fretting corrosion, concomitant metal ion release and early implant failure[126,127] .

In addition, there has been a recent interest in bone preserving and minimally invasive procedures[128] which has led to the development of novel “short” stem designs which aim to obtain metaphyseal fixation and to preserve the femoral neck[129]. Several theoretical advantages have been advocated in favour of short stems; the key advantages are that short stems preserve the proximal femoral bone stock and facilitate minimally invasive surgical procedures. Moreover, due to proximal fixation, they have the potential to decrease stress-shielding and the occurrence of thigh pain. An easier revision has also been

postulated[130,131]. There is very limited data on mid- and long-term performance of short stems[130,132], and early failures of some designs have been reported[133,134].

In summary, the issue of identifying the optimal femoral component has not yet been resolved.

2.3 Active Shape Modelling

The proximal femur is a complex object that varies considerably in shape, not only between individuals, but also between modes of imaging, i.e. between two radiographic projections. In addition to the assessment of single geometric measures (i.e. femoral offset), the present work aims to characterise the shape of the proximal femoral canal using a more abstract, yet powerful technique, Active Shape Modelling (ASM).

ASM is a statistical model to represent shape that describes the global shape of an object and enables identifying or segmenting of objects in images. It was developed by Cootes and Taylor in 1995[135,136]. ASM works by calculating distances of an individual set of landmark points that define the outline of an object of interest from the mean position of equivalent points marked in a whole set of images. This is done following a set of affine transformations (Procrustes analysis[135]) which align all objects of interest as closely as possible to ensure that differences in point placement are genuinely due to variation in shape, rather than in size, position, or rotation of the object. Thereafter, principal component analysis (PCA)[135], a dimension reduction technique, is used to generate modes of variation that describe the variation of shape in the given dataset. Variation in shape is expressed by a series of modes of variation (shape modes). Each shape mode is orthogonal to all the others, and therefore, each shape mode is an independent descriptor of shape.

ASM has several advantages: It allows not only a global representation of variation in complex shape, such as in the proximal femur, but also enables comparison of actual shape independently of size and orientation which are removed during the normalisation process. The ASM model can be trained on a suitable dataset which allows semi-automated identification of the object of interest in larger datasets. Therefore, it can be considered as a widely applicable and time-saving method. On the other hand, interpretation of results obtained by ASM is less intuitive than interpretation of geometrical measurements[137].

ASM has recently been used to examine the shape of the proximal femur and to investigate its relationships with the incidence of hip fracture or the progression and clinical presentation of OA[137-139].

2.4 Summary and Outline of the Remaining Thesis

The review of the literature demonstrated that the success of primary THA is dependent on stem fixation and the restoration of physiologic joint mechanics, and that accurate pre-operative assessment of proximal femoral canal shape and geometry is essential. It has been shown that pre-operative planning performed on AP pelvis radiographs has limited reliability. Despite an increasing popularity of cementless femoral reconstruction and the development of novel short and modular stem designs, the current knowledge of the variation in proximal femoral geometry and canal shape in arthritic hips is very limited. Additionally the association between femoral geometry and canal shape is poorly understood.

The aims of the present work are (1) to improve pre-operative planning in THA and (2) to provide information for future femoral component design accounting for individual patient anatomy in THA. Therefore, the remaining chapters are structured as follows:

Chapter 3 assesses differences in femoral offset on corresponding AP ***pelvis*** radiographs, AP ***hip*** radiographs and CT scans in patients with primary end-stage hip osteoarthritis.

Chapter 4 aims to provide gender specific regression equations to predict 3D femoral offset from AP pelvis radiographs.

In Chapter 5, Active Shape Modelling is used to determine differences in the radiographic appearance of the proximal femoral canal between AP hip and AP pelvis radiographs with reference to CT.

In Chapter 6, a second ASM study aims to determine the variation and underlying patterns in proximal femoral anatomy in patients with primary OA, further investigating the association between endosteal canal shape, joint geometry and anthropometric parameters.

Chapter 7 summarises the conclusions of the present work, highlights its clinical relevance, and provides recommendations for future research.

3. ASSESSMENT OF FEMORAL OFFSET

3.1 Introduction

Accurate restoration of femoral offset (FO) in total hip arthroplasty provides patients with a better functional outcome in terms of improved abductor muscle strength[20,21] and greater range of motion[21,22,140,141], and helps to minimise the risk of post-operative complications such as limp, dislocation or wear-related implant failure in the long-term[22,24,142,143].

A mandatory pre-requisite for accurately restoring individual patient anatomy is precise pre-operative planning, in which FO is an essential parameter. In clinical practise, pre-operative templating in THA is widely performed on anterior-posterior (AP) pelvis radiographs, even though several studies over the past two decades have described limited reliability for measuring FO on AP pelvis radiographs compared to computed tomography (CT)[29,33-35]. Femoral anteversion (FA)[29,33] and external rotational contractures in patients with end-stage osteoarthritis (OA)[34,35] were identified as main reasons for underestimating FO on AP pelvis radiographs and consequently, some authors have proposed pre-operative CT as a standard procedure[29,33]. Although CT is considered as gold standard for FO assessment[37,38] its routine performance is questionable because of higher radiation doses, higher costs and limited availability. To date, there are no previous studies in the literature that have investigated the accuracy and reliability of FO measurements on AP ***hip*** radiographs with reference to CT in pre-operative THA planning.

The aim of the present chapter was to evaluate differences in FO when measured on standardised corresponding AP ***pelvis*** radiographs, AP ***hip*** radiographs and CT scans of patients with primary hip OA. The first hypothesis was that FO as measured on AP pelvis radiographs is significantly underestimated compared to FO as measured on AP hip

radiographs. The second hypothesis was that there is no clinically relevant difference in FO measurements between AP hip radiographs and CT scans.

3.2 Materials and Methods

3.2.1 Study Cohort

Between July 2009 and December 2009 a consecutive series of 152 patients who had undergone primary THA for end-stage hip osteoarthritis (OA) with a custom-made cementless femoral implant[122] was retrospectively evaluated. For each patient, a pre-operative AP pelvis radiograph, an AP hip radiograph and a CT scan of the affected hip had been routinely obtained and all images were retrieved in DICOM format.

Patients with secondary forms of hip osteoarthritis, medication affecting bone metabolism or radiographs without calibration marker were excluded from the study. Patients in whom THA was performed bilaterally during the study period were only included with the first procedure side. Fifty-two patients were excluded according to the criteria stated above, leaving 100 patients (43 males, 57 females, mean age 61 (range: 45-74) years, mean body-mass- index (BMI) 27 (range: 20-45) kg/m², Table 3.1) that were included in the present study. In all cases, the diagnosis leading to THA was primary OA.

	Entire Cohort (n=100)	Males (n= 43)	Females (n= 57)
Age (years)	60.8 (45-74) (95%CI: 59.4- 62.2)	61.0 (45-72) (95%CI: 58.7- 63.3)	60.7 (45-74) (95%CI: 58.8-62.6)
Weight (kg)	79.7 (48.0-125.0) (95%CI: 76.6-82.9)	87.0 (60.0-125.0) (95%CI: 82.2-91.9)	74.2 (48.0-120.0) (95%CI:70.6-77.7)
Height (meters)	1.70 (1.53-1.91) (95%CI: 1.68-1.72)	1.77 (1.60-1.91) (95%CI: 1.75-1.79)	1.65 (1.53-1.76) (95%CI: 1.63-1.66)
BMI (kg/m²)	27.5 (20.3-44.6) (95%CI: 26.6-28.4)	27.7 (20.3-42.2) (95%CI: 26.3-29.1)	27.3 (20.5-44.6) (95%CI: 26.1-28.5)

Table 3.1

Demographic data (range) of the study cohort, male patients and female patients with 95% CI.

3.2.2 Radiographic Protocol

In all patients, a standardised radiographic protocol was administered to achieve reproducible projection. Low-centred AP pelvis and AP hip radiographs were taken in supine position. To correct for effects of magnification, a metal calibration sphere of 25 mm was positioned on the inner thigh at the anterior-posterior level of the femoral head. During the study period, two different x-ray tubes were in use: Canon CXDI series [Canon Inc., Tokyo, Japan] and Philips Bucky Diagnost VE VT [Royal Philips Electronics Inc., Amsterdam, Netherlands]. The tube-to-film distance was 1150 mm, with the tube orientation perpendicular to the table.

On AP pelvis radiographs, both legs were internally rotated by 15 degrees using a leg retainer and the crosshair of the beam was centred on the pubic symphysis.

For AP hip radiographs, the crosshair of the beam was directed to the midpoint between the anterior superior iliac spine and the symphysis to centre the beam on the centre of the femoral head of the affected hip. The affected leg was internally rotated and retained so that the greatest prominence of the greater trochanter was palpated at its most lateral

position to bring the femoral neck into the coronal plane. When internal rotation of the leg was not sufficient due to external rotation contracture, the affected hip was additionally elevated on the AP hip view using a wedge.

3.2.3 Computed Tomography Protocol

All hip CT scans were performed pre-operatively using a Toshiba Aquilion 16 CT scanner [Toshiba Corp., Tokyo, Japan]. Patients were positioned supine with legs retained in neutral rotation as confirmed by scout views. The scans were obtained in three sets: (1) from the cranial aspect of the acetabulum to below the lesser trochanter, (2) from below the lesser trochanter to a point 50 mm distally of the femoral isthmus and (3) 4-6 slices of the knee. Slice spacing of 4 mm, 8 mm and 2 mm were used, respectively. All scans were recorded with gantry tilt 0, 120 kV and a field of view (FOV) of 250 mm.

3.2.4 Radiographic Measurements

A validated MATLAB programme[144] [version 7.10, The MathWorks Inc., MA, USA] was used to determine the centre of the femoral head (HC), the head diameter (HD) and the femoral shaft axis on AP pelvis and AP hip views. On the femoral diaphysis, two points on the medial and lateral cortex 20 mm below the lesser trochanter, and two points on the medial and lateral cortex at the level of the femoral isthmus were defined. The midpoints of these point pairs determined the femoral shaft axis. A circle tool was used to define the head diameter and the co-ordinates of its centre. FO was calculated as the perpendicular distance from the centre of the femoral head to the femoral shaft axis. Measurements on AP pelvis radiographs were labelled FO_p and HD_p and on AP hip radiographs FO_h and HD_h, respectively (Figure 3.1). On AP pelvis radiographs, the distance from the midpoint of both tear drops to the centre of the femoral head (x) was calculated.

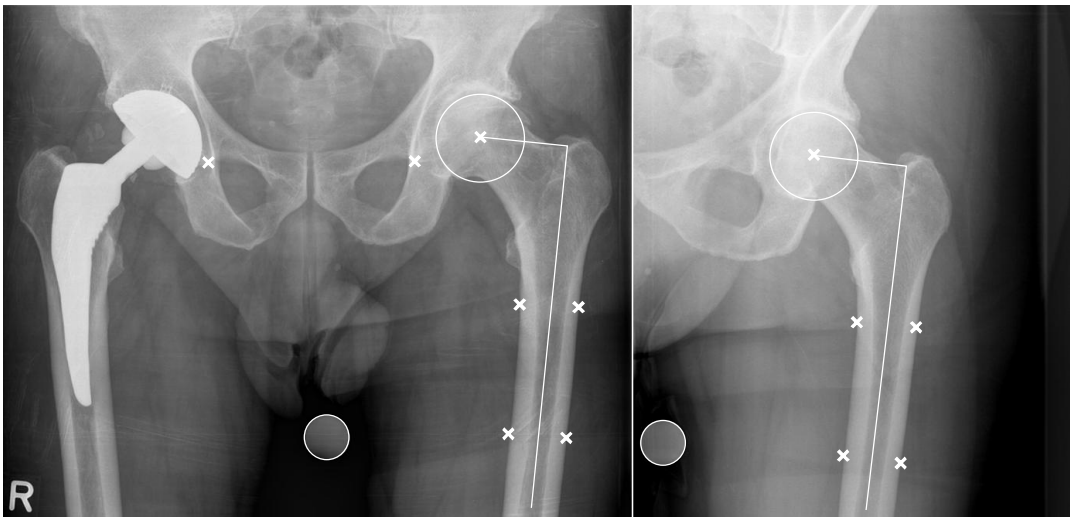


Figure 3.1

Radiographic measurements:
Femoral offset (FO) measurements on standardised AP pelvis (FOp) and AP hip (FOh) radiographs for a 71 year-old male patient with primary OA of the left hip.

3.2.5 CT Measurements

In addition to the 2D measurements, a second MATLAB programme* [version 7.10, The MathWorks Inc., MA, USA] was used to measure FO and FA. The programme enabled the user to select points from pre-selected axial CT slices and performed calculations in the three dimensional (3D) co-ordinate system of the CT scanner. For the 3D calculation of FO (FO_c) and head diameter (HD_c), three axial slices were selected (s1, s3, s4, Figure 3.2). HD_c and the centre of the femoral head were determined on the slice with the femoral head at its largest diameter (s1) using a circle tool. The femoral shaft axis was defined by the centroid of the proximal femoral metaphysis[145,146] (s3) and the centre of the isthmus (s4); FO_c was then calculated as the perpendicular distance from the femoral shaft axis to the centre of the femoral head. For the calculation of FA, the femoral neck axis (s2, Figure 3.2) was defined using the single slice method as described by Sugano[147], and the posterior

* The programme was developed by Elise Pegg, PhD, engineer at the Nuffield Department of Orthopaedics, Rheumatology and Musculoskeletal Sciences, University of Oxford and validated as described in section 3.2.6.

condylar axis (s5) was defined by the most posterior aspects of the lateral and medial condyles. The angle between the femoral neck axis and the posterior condylar axis represented FA.

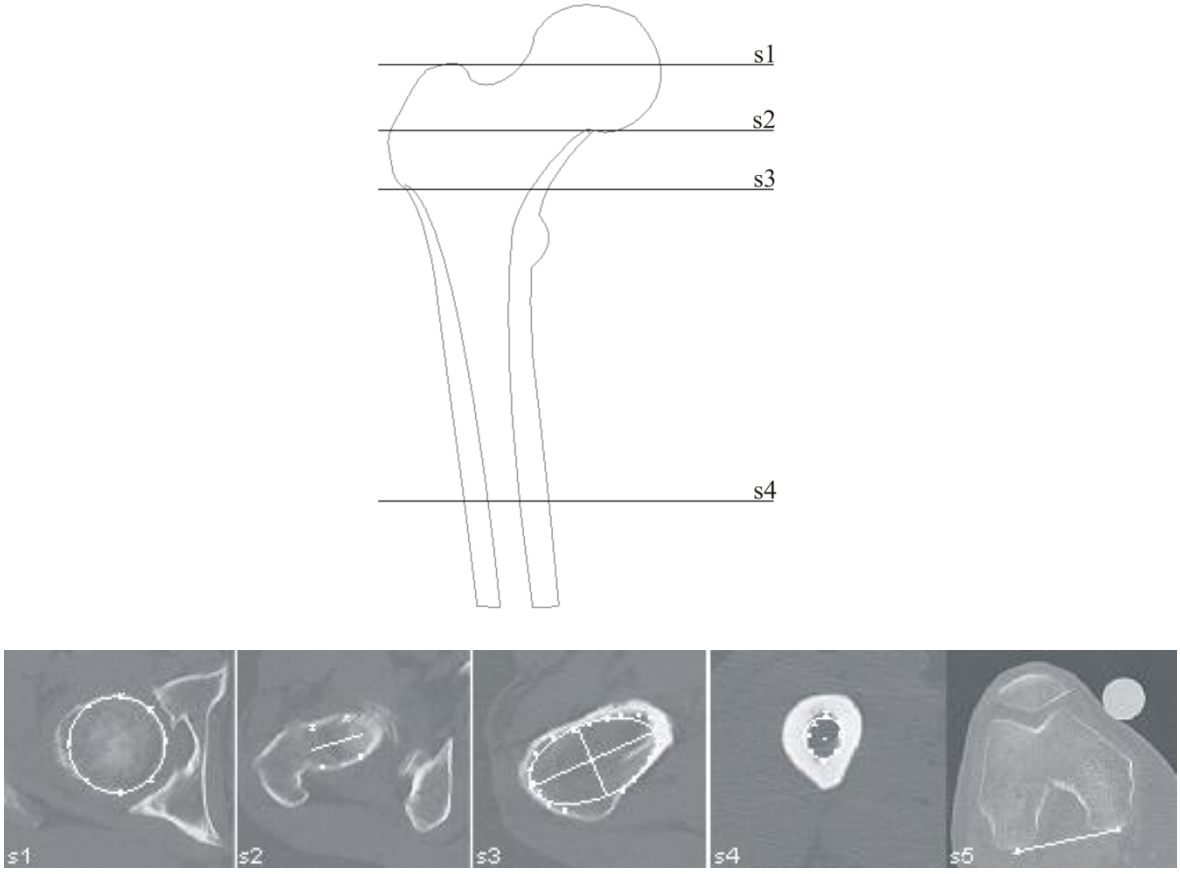


Figure 3.2

Selection of CT slices of the proximal femur for 3D calculation of femoral offset (FO) and femoral anteversion (FA) based on CT: Centre of the femoral head (s1), femoral neck axis (s2), centroid of the proximal femoral metaphysis (s3), centre of femoral isthmus (s4), posterior condylar axis (s5).

3.2.6 Measurement Reliability

Intra- and inter-observer reliabilities for 20 randomly selected corresponding AP pelvis radiographs, AP hip radiographs and CT scans were evaluated by two independent and blinded observers using single-measure intra-class-correlation coefficients (ICC) with a two-way-random effects model for absolute agreement.

3.2.7 Statistical Analysis

The distributions of variables were examined in exploratory data analysis, and tested for normality using Kolmogorov-Smirnov tests. All variables (FO_p, FO_h, FO_c, HD_p, HD_h, HD_c and FA) were normally distributed (range: p=0.06-0.20). For descriptive analysis, absolute mean values and differences of FO were expressed in mm with 95% confidence intervals (95%CI). FA was expressed in degrees with 95%CI. Distributions of FO values were compared using paired-samples *t*-tests for paired observations and independent-samples *t*-tests for unpaired observations. Pearson's correlation coefficient (r) was used to evaluate associations between continuous variables. Correlation was characterised as poor (0.00-0.20), fair (0.21-0.40), moderate (0.41-0.60) good (0.61-0.80), or excellent (0.81-1.00). Results with p values <0.05 were considered as significant, p values of <0.001 were considered as highly significant. Differences in FO measurements on all three modes of radiographic imaging were analysed using Bland-Altman plots[148]. Linear regression was performed to relate corresponding FO measurements. Statistical analysis was carried out using PASW Statistics 18 [SPSS Inc. an IBM company, IL, USA] and Sigmaplot 12.0 [Systat Inc., San Jose, CA, USA].

3.3 Results

3.3.1 Measurement Reliability

Excellent intra-observer ICC was seen for all analysed parameters: FO_p (0.993), FO_h (0.990), FO_c (0.990), HD_p (0.886), HD_h (0.906), HD_c (0.933) and FA (0.984).

Inter- observer ICC also showed similar correlations for all parameters: FO_p (0.986), FO_h (0.977), FO_c (0.991), HD_p (0.812), HD_h (0.848), HD_c (0.866) and FA (0.950).

3.3.2 Radiographic Findings

In the entire cohort, mean FO_p was 39.0 mm (95%CI: 37.4 to 40.6 mm), compared to mean FO_h of 44.0 mm (95%CI: 42.4 to 45.6 mm, Table 3.2). FO_p was significantly lower than FO_h ($p<0.001$) with a mean difference of 5.0 mm (95%CI: 4.3 to 5.7 mm) or 11%, respectively (Table 3.3, Figure 3.3). The difference between FO_p and FO_h was slightly higher in males (5.8 mm, 14%) than in females (4.4 mm, 12%, p=0.45, Table 3.3).

A fair correlation between the difference in mean FO on corresponding radiographs and *x* was observed ($r=0.37$, $p<0.001$). No correlation between the difference in mean FO on corresponding radiographs and FA ($r=0.18$, $p=0.07$) was found.

	Entire cohort (n=100)	**Males (n= 43)**	**Females (n= 57)**
FO_p (mm)	39.0 (10.2-54.7) (95%CI: 37.4-40.6)	41.9 (18.4-54.7) (95%CI: 39.6-44.2)	36.8 (10.2-50.7) (95%CI: 34.7-38.9)
FO_h (mm)	44.0 (19.7-61.2) (95%CI: 42.4-45.6)	47.7 (26.2-61.2) (95%CI: 45.5-49.9)	41.2 (19.7-57.9) (95%CI: 39.3-43.2)
FO_c (mm)	44.7 (29.0-61.2) (95%CI: 43.5-45.9)	48.2 (40.2-61.2) (95%CI: 46.6-49.9)	42.0 (29.0-54.0) (95%CI: 40.7-43.3)
HD_p (mm)	47.2 (38.8-57.7) (95%CI: 46.4-48.1)	50.6 (43.7-57.7) (95%CI: 49.6-51.6)	44.7 (38.8-51.7) (95%CI: 43.9-45.4)
HD_h (mm)	48.2 (40.9-59.0) (95%CI: 47.3-49.1)	51.9 (45.2-59.0) (95%CI: 50.9-52.9)	45.4 (40.9-52.9) (95%CI: 44.6-46.3)
HD_c (mm)	46.0 (34.7-57.5) (95%CI: 45.0-47.0)	49.5 (36.8-57.5) (95%CI: 48.3-50.7)	43.3 (34.7-54.9) (95%CI: 42.3-44.4)
FA (degrees)	14.9 (-6.7-56.8) (95%CI: 12.6-17.1)	13.2 (-3.0-30.2) (95%CI: 10.5-15.9)	16.1 (-6.7-56.8) (95%CI: 12.7-19.6)

Table 3.2

Mean values (range) for FO, HD and FA with 95% CI for the study cohort, male patients and female patients.

	Entire cohort (n=100)	Males (n= 43)	Females (n= 57)
FO_p to FO_h (mm)	5.0 (-2.1-16.5) (95%CI: 4.3-5.7)	5.8 (-0.8-16.5) (95%CI: 4.8-6.8)	4.4 (-2.1-15.2) (95%CI: 3.5-5.3)
FO_p to FO_h (%)	11	12	11
FO_P to FO_c (mm)	5.7 (-6.7-23.7) (95%CI:4.5-6.9)	6.3 (-5.2-21.8) (95%CI: 4.5-8.1)	5.2 (-6.7-23.7) (95%CI: 3.6-6.8)
FO_P to FO_c (%)	13	13	12
FO_h to FO_c (mm)	0.7 (-10.1-20.1) (95%CI:-0.3-1.7)	0.5 (-10.1-14.0) (95%CI: -1.1-2.2)	0.8 (-8.5-20.1) (95%CI: -0.5-2.1)
FO_h to FO_c (%)	2	1	2

Table 3.3

Mean differences in FO between AP pelvis (FOp) and AP hip (FOh) radiographs, and between radiographs and CT (FOc) given in absolute (mean (range), 95%CI) and relative (%) values.

3.3.3 CT Findings

Mean FO_c was 44.7 mm (95%CI: 43.5 to 45.9 mm, Table 3.2). FO_p was underestimated by 5.7 mm (95%CI: 4.5 to 6.9 mm) or 13% with reference to FO_c ($p<0.001$). FO_c and FO_h were comparable ($p=0.191$) with a mean difference of 0.7 mm (95%CI: -0.3 to 1.7 mm, Table 3.3, Figure 3.3). Bland-Altman plots for the agreement between radiographs and CT are presented in Figures 3.5 and 3.6. Comparing males and females, differences between FO_h and FO_c were similar ($p=0.79$, Table 3.3).

We observed a good correlation between FO_p and FO_c ($r=0.687$, $p<0.001$) and between FO_h and FO_c ($r=0.767$, $p<0.001$, Figure 3.4).

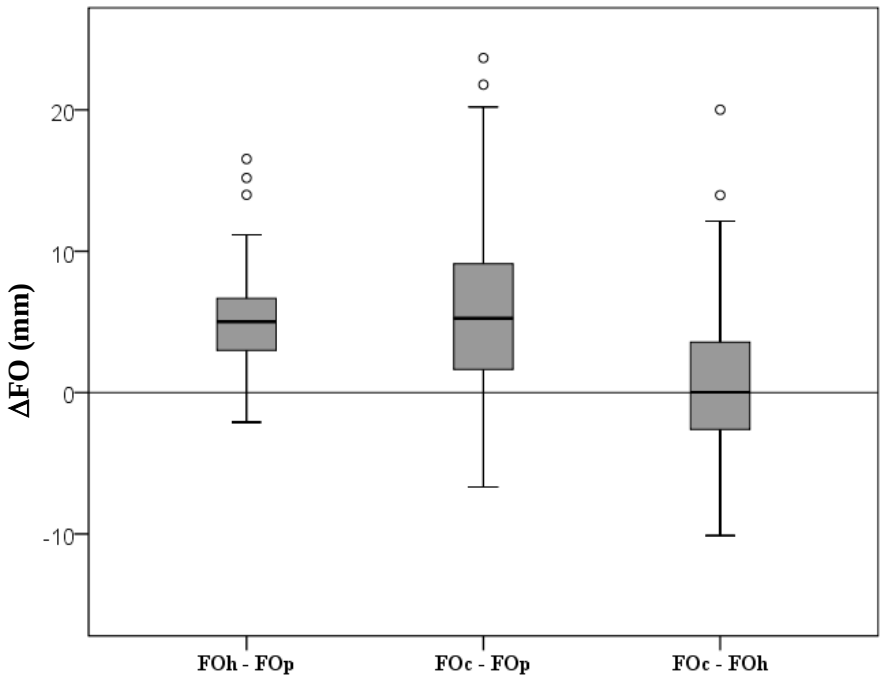


Figure 3.3

Differences (mm) of femoral offset (FO) between AP hip and AP Pelvis radiographs (FOh-FOp), AP pelvis radiographs and CT (FOc-FOp), and AP hip radiographs and CT (FOc-FOh) as boxplots.

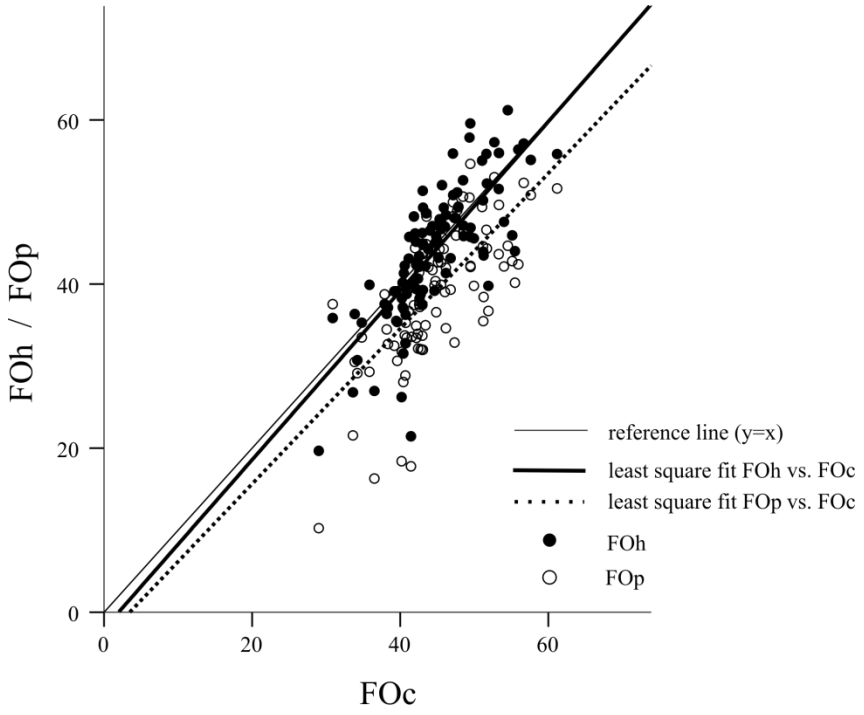


Figure 3.4
Overlay scatter plot illustrating the relationship between FO as measured on AP pelvis radiographs (FOp), AP hip radiographs (FOh) and CT (FOc) in mm. The least square fit lines suggest a good correlation of AP hip and CT values (R^2=0.588)

With reference to CT, disagreement in FO assessment was within ± 5 mm in 44 % (44 patients) of cases for AP pelvis radiographs and 74% (74 patients) for AP hip radiographs (Figures 3.5 and 3.6). With use of regression analysis, the following equations were derived to predict true FO as measured on CT from FO measurements performed on AP pelvis and AP hip views:

$$FO_c = 0.50 * FO_p + 25.22 \ (R^2 = 0.472) \qquad \text{Equation (1)}$$

$$FO_c = 0.57 * FO_h + 19.58 \ (R^2 = 0.588) \qquad \text{Equation (2)}$$

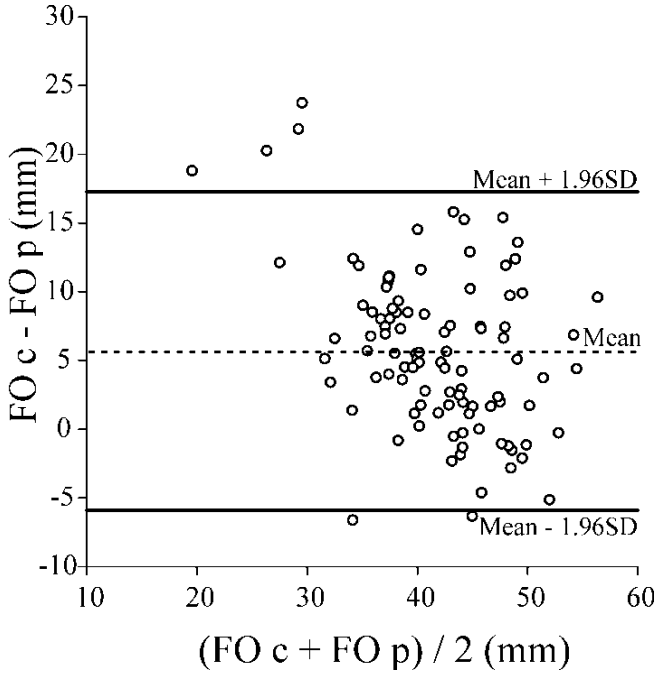


Figure 3.5

Bland-Altman plot illustrating the agreement between FO as measured on AP pelvis radiographs (FOp) and CT (FOc) in mm.

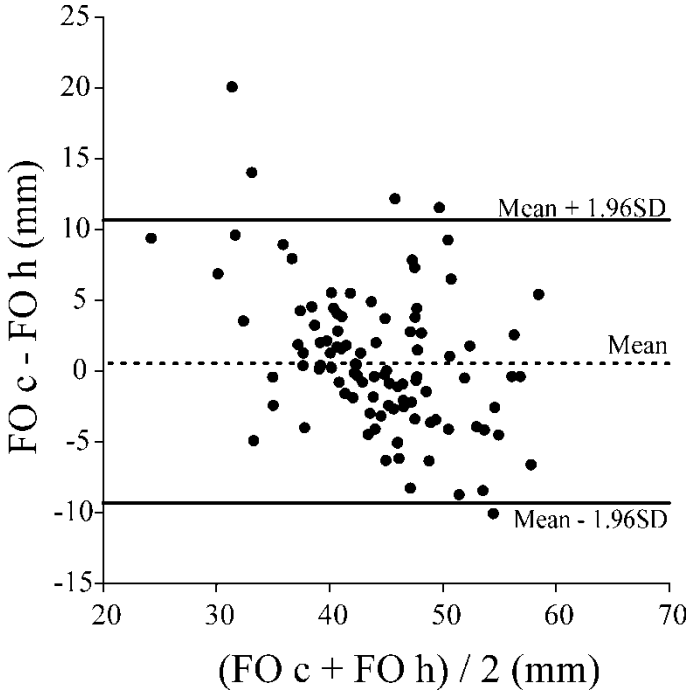


Figure 3.6
Bland-Altman plot illustrating the agreement between FO as measured on AP hip radiographs (FOh) and CT (FOc) in mm.

3.4 Discussion

Accurate and reliable assessment of FO is a key element in pre-operative planning for THA as it determines the selection and positioning of appropriate prosthetic components. Restoration of FO is essential to achieve a stable articulation[149] and to provide good range of motion[21], muscle function[20,21], and equal limb length[22]. The importance of FO restoration to prevent long-term adverse effects related to impingement[150] and wear[23,24] is well-accepted.

Despite the lower accuracy of plain radiography in comparison to 3D techniques based on CT[29], AP pelvis radiographs are widely used for pre-operative templating in hip OA as they provide essential information regarding pelvic and contralateral hip anatomy, and allow evaluation of leg length discrepancies. It is well established that femoral rotation influences the radiographic appearance of proximal femoral anatomy[36] and that failure to correct for femoral anteversion and external rotation contracture results in underestimation of FO[27,29]. Consequently, clear recommendations to optimise conventional radiographic projection of the femoral neck by internally rotating the lower limb during radiography have been made[151]. However, little attention has been given to potential differences in the accuracy of FO assessment on corresponding AP pelvis and AP hip radiographs. In contrast to AP pelvis radiographs, AP hip radiographs theoretically allow a full correction of femoral anteversion in the presence of external rotation contractures as the hip can be elevated and symmetry is not an issue. Moreover, the centre of the beam is directed to the centre of rotation of the diseased hip which minimises projection effects caused by beam divergence.

The present study evaluated differences in FO measurements performed on standardised AP pelvis and AP hip radiographs in patients with primary end-stage hip OA and

compared these measurements to true, 3D FO values obtained from corresponding CT scans. To minimise misleading projection effects of FA and external rotation contracture a standardised positioning protocol was used. All images were calibrated using a metal sphere which was reproducibly placed on the inner aspect of the thigh to compensate for potential errors of magnification in each radiograph. A significant underestimation of FO with a mean of 5.0 mm (95%CI: 4.3 to 5.7 mm) comparing AP pelvis to AP hip views was observed. Comparing AP hip to CT based FO values, a difference of 0.7 mm (95%CI: -0.3 to 1.7 mm) was seen. In 74% of cases AP hip derived FO measurements were within ±5 mm of the CT measurements suggesting that FO measurements performed on standardised AP hip views allow an accurate representation of 3D FO.

The difference in FO measurements observed between AP pelvis and AP hip radiographs can be represented mathematically, considering the trigonometric relation between the focal length (*f*), the angle between the femoral neck and the focal plane (θ), the distance between the centre of the femoral head and the x-ray source (*x*), the true offset (*l*) and the distance between the femoral head and the focal plane (*h*) (Figure 3.7). The complete formulation developed to model the relationship between the parameters is given in Appendix A.

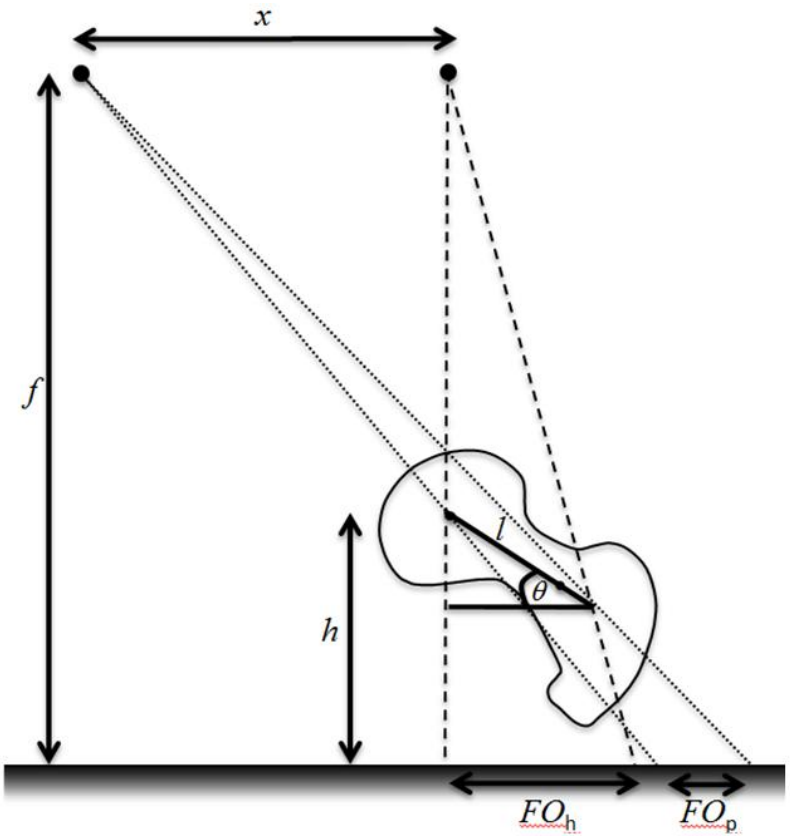


Figure 3.7

Unscaled geometrical illustration for the difference in femoral offset (FO) measurement on AP pelvis (FO_p) and AP hip (FO_h) radiographs: focal length (*f*), angle between the femoral neck and the focal plane (θ), distance between the centre of the femoral head and the x-ray source (*x)*, true offset (*l*), and the distance between the femoral head and the focal plane (*h*).

By establishing the partial derivative of FO_p with respect to *x*, it is possible to conclude that the effect that change in *x* has on the offset value is inversely proportional to sin θ (Equation (3)).

$$\frac{\partial FOp}{\partial x} \propto -\sin\theta \qquad \text{Equation (3)}$$

It has therefore been shown that (1) it is important to minimise x to ensure accurate determination of FO and that (2) the effect x will have on the FO measurement will be greater when the angle between the femoral neck and the focal plane is larger.

The present study has the following limitations:

First, the linear correlation between the difference of FO_p and FO_h and the magnitude of x was weak, and the individual effects of positioning and beam centration cannot be retrospectively quantified. The linear relationship assumes that h and θ are constant; but it is known that both will vary depending on individual patient anatomy and positioning. However, if these values could be recorded then it is thought that a stronger correlation would be found. Although a standardised positioning protocol was administered, the method for obtaining the radiographs is a potential source of bias as it depends on the judgment of the technician and the variability in individual femoral anatomy such as the magnitude of femoral anteversion or contracture.

Second, internal rotation of retroverted femora during radiography positioning might have exaggerated measurement errors of FO. There were 7 retroverted femora in the present cohort which showed a slight mean retroversion of -2.7° (95%CI: -4.5 to (-0.9)°).

Third, the true axis of the femoral neck to evaluate 3D FA can only be determined by means of a 3D reconstruction of the neck portion which was limited with the present CT protocol as a 1 mm slice interval is required for this purpose. However, the selected single slice method chosen in this study has demonstrated sufficient accuracy for FA measurements when the slice for determining the femoral neck axis is chosen just below the femoral head[147]. Moreover, patients with head or neck deformity associated with secondary OA were excluded.

Lastly, the present calculations did not use the long axis of the femur (centroid of metaphysis to centre of knee) as reported previously for FO measurements on CT [152]. FO measurements in the present study were performed based on the longitudinal axis of the proximal femur (centroid of metaphysis to centre of isthmus) in order to replicate offset measurements as performed on plain radiography.

As a consequence of the reported limited accuracy and reliability of conventional radiographic measurements, the routine performance of CT scans for optimised pre-operative FO assessment has been suggested[29,33]. The results of the present study question this consideration in primary OA, as there was no clinically relevant difference in FO values comparing measurements made on AP hip radiographs compared to those made on CT. The obtained mean values for FO (44.0 mm) on AP hip views and FO (44.7 mm) and FA (14.9°) on CT scans compare well with reported values in the literature[29,39,153]. Moreover, the present study suggests that 3D FO may potentially be predicted from FO measurements performed on AP pelvis views with use of the provided regression equations. However, larger patient series are required to confirm this finding and to obtain more powerful and gender specific correction factors.

A decrease in FO of approximately 12% has been reported to cause abductor weakness[20] which indicates that the level of observed underestimation of FO (13%) comparing AP pelvis and AP hip views in this study is of clinical relevance. The difference between AP hip and CT values (2%) is of minor clinical importance. The observed differences in FO were consistent when considering male and female patients separately, suggesting that the present findings are independent of gender related variability in proximal femoral anatomy[28,154].

In conclusion, femoral offset is significantly underestimated on AP pelvis radiographs but can be reliably and more accurately assessed on standardised AP hip radiographs with correction for femoral anteversion and external rotation contracture in patients with primary end-stage hip osteoarthritis. AP hip radiographs reduce radiation exposure compared to CT and are a practical, cost-effective and available method which improves pre-operative templating and aids in the selection of appropriate implants. Although the ultimate decision of implant design, size and position must still be made intra-operatively, it is recommended to routinely obtain additional AP hip radiographs for pre-operative assessment of femoral offset in patients with primary OA.

3.5 Summary

The aim of this retrospective cohort study was to evaluate differences in femoral offset when measured on corresponding pre-operative AP pelvis radiographs, AP hip radiographs and CT-scans of a consecutive series of 100 patients with primary end-stage hip osteoarthritis.

AP pelvis based FO was underestimated by 13% compared to CT based FO. No difference in mean FO between AP hip radiographs and CT was observed.

The work presented in this chapter suggests that femoral offset is significantly underestimated on AP pelvis radiographs but can be reliably and more accurately assessed on AP hip radiographs in patients with primary end-stage hip osteoarthritis. Thus, it can be recommended to routinely obtain additional AP hip radiographs for pre-operative assessment of femoral offset in THA templating.

As a linear relationship between corresponding FO measurements was identified, and the next chapter aims to determine whether 3D FO can be accurately and reliably predicted from AP pelvis radiographs.

4. PREDICTION OF 3D FEMORAL OFFSET FROM AP PELVIS RADIOGRAPHS

4.1 Introduction

In Chapter 3, it has been reported that femoral offset is significantly underestimated on AP ***pelvis*** radiographs but can be accurately and reliably assessed on standardised AP ***hip*** radiographs compared to CT in patients with primary end-stage hip OA. Moreover, a linear relationship between corresponding FO measurements performed on AP pelvis radiographs, AP hip radiographs and CT scans has been suggested.

Therefore, the work presented in this chapter aimed to determine (1) whether three-dimensional femoral offset as measured on CT scans can be reliably and accurately predicted from FO measurements performed on AP ***pelvis*** views, and (2) whether predicted FO values compare favourably to measurements performed on AP ***hip*** views.

4.2 Materials and Methods

4.2.1 Study Cohort

In a retrospective cohort study, a consecutive series of 597 patients who had undergone primary THA for end-stage hip osteoarthritis (OA) was reviewed. All patients received a custom-made cementless femoral component[122] between June 2008 and December 2009. Standardised AP pelvis radiographs, AP hip radiographs and a CT scans of the affected hip were performed pre-operatively as described in section 3.2.2 and 3.2.3.

In order to obtain normative values of FO measurements on the three corresponding modes of imaging, only patients with primary hip osteoarthritis were included. In cases of bilateral THA, patients were only included with the first procedure side. Patients with a

history of trauma, infection, rheumatic disease, developmental dysplasia of the hip (DDH), previous pelvic and/or femoral osteotomy, avascular necrosis (AVN) of the femoral head, Legg–Calvé–Perthes disease, or slipped capital femoral epiphysis (SCFE) were excluded from the present study. To quantitatively identify patients with acetabular undercoverage, further exclusion criteria were defined as a center-edge angle (CE) < 20°[155], an acetabular angle (AA) > 42°[156] and an acetabular index (AI) < 38%[157].

According to the criteria stated above, 252 patients were excluded from the initial cohort, leaving 345 patients (146 males, 199 females, mean age 60 (range: 40-79) years, mean body-mass-index (BMI) 27 (range: 19-56) kg/m², Table 4.1) that were included in the present study. The study was approved by the institutional review board (reference S-272/2009).

	Entire cohort (n=345)	**Males (n=146)**	**Females (n=199)**
Gender in cohort (%)	100.0	42.3	57.7
Age (years)	60.4 (range: 40-79) (95%CI: 59.6-61.1)	60.5 (range: 43-72) (95%CI: 59.3-61.6)	60.3 (range: 40-79) (95%CI: 59.3-61.3)
Weight (kg)	78.5 (range: 46-173) (95%CI: 76.8-80.1)	85.3 (range: 54-138) (95%CI: 83.1-87.5)	73.3 (range: 46-173) (95%CI: 71.2-75.4)
Height (meters)	1.70 (range: 1.46-1.97) (95%CI: 1.69-1.71)	1.77 (range: 1.60-1.97) (95%CI: 1.76-1.78)	1.65 (range: 1.46-1.88) (95%CI: 1.64-1.66)
BMI (kg/m²)	27.0 (range: 19.2-56.5) (95%CI: 26.5- 27.5)	27.1 (range: 19.8-42.6) (95%CI: 26.5-27.8)	26.9 (range: 19.2-56.5) (95%CI: 26.2-27.7)

Table 4.1

Demographic data of the entire cohort, male patients and female patients.

To evaluate the validity and accuracy of predicting 3D FO as measured on CT from FO measurements performed on AP pelvis views, the study cohort of 345 patients was randomly split into two groups. Group A comprised 245 patients (101 males, 144 females, mean age 60 (range: 40 to 79) years, mean BMI 27 (range: 19 to 56) kg/m²); and group B comprised 100 patients (45 males, 55 females, mean age 60 (range: 44 to 72) years, mean BMI 27 (range: 19 to 41) kg/m²). In group A, corresponding FO measurements on AP pelvis radiographs (FO_p) and CT scans (FO_c), were used to derive regression equations for the entire group, and for males (n=45) and females (n=55) separately, in order to predict 3D FO from AP pelvis views (FO_{pred}). Derived regression equations from measurements in group A were applied to FO_p measurements in group B.

The validity and accuracy of mean FO_{pred} for was assessed in group B with reference to FO_c for all patients, and for genders separately. In order to compare FO_{pred} to FO_h, the frequencies of clinically significant over- or underestimation (>12%) with reference to FO_c were evaluated[20]. Agreement between corresponding FO values was assessed using Bland-Altman plots[148].

4.2.2 Imaging Protocols

Details of the radiographic and CT protocols are described in section 3.2.2 and 3.2.3.

4.2.3 Radiographic Measurements

A commercially available templating programme, *TraumaCad* [version 2.2, Voyant Health, Petach-Tikva, Israel] [158], was used to measure CE[155], AA[156] and AI[157] on AP pelvis radiographs.

A validated custom MATLAB programme[144] [version 7.10, The MathWorks Inc., MA, USA] was used to determine FO and NSA on corresponding AP pelvis and AP hip

radiographs. Details of the radiographic measurements have been previously provided in section 3.2.4. In brief, FO was calculated as the perpendicular distance from the centre of the femoral head to the femoral shaft axis. NSA was calculated as the angle between the femoral shaft axis and the femoral neck axis. Measurements were labelled FO_p, NSA_p, and HD_p for AP pelvis measurements, and FO_h, NSA_h and HD_h, for AP hip measurements, respectively.

4.2.4 CT Measurements

FO_c and FA were measured on the CT image set. The identical measurement protocol as described in section 3.2.5 was used.

4.2.5 Measurement Reliability

Intra- and inter-observer reliabilities for 20 randomly selected corresponding AP pelvis radiographs, AP hip radiographs and CT scans were evaluated by two independent and blinded observers using single-measure intra-class-correlation coefficients (ICC) with a two-way-random effects model for absolute agreement.

4.2.6 Statistical Analysis

The distributions of variables were examined in descriptive histograms and box plots, and a Kolmogorov-Smirnov test was used to identify normal distribution of the variables. For descriptive analysis, absolute mean values for FO were expressed in mm with 95% confidence intervals (95%CI). Differences in mean FO were expressed in absolute (mm, 95%CIs) and relative (%) values. Distributions of FO values were compared using paired-samples t-tests for paired observations and independent-samples t-tests for unpaired observations. Results with p values <0.05 were considered as significant, p values of <0.001 were considered as highly significant. Scatter plots and Pearson's correlation coefficient (r) were used to evaluate associations between continuous variables.

Correlation was characterised as poor (0.00-0.20), fair (0.21-0.40), moderate (0.41-0.60) good (0.61-0.80), or excellent (0.81-1.00) [159]. Simple linear regression was performed to predict FO_c from FO_p. Stepwise multiple linear regression with FO_c as the dependent variable and FO_p, NSA_p HD_p, BMI, height, weight and age as the independent variables was used to determine additional significant predictor variables from the dataset. Statistical analysis was performed using PASW Statistics 18 [SPSS Inc. an IBM company, IL, USA].

4.3 Results

4.3.1 Measurement Reliability

Intra-observer ICC was good for NSA_h (0.797) and excellent for all other parameters. Inter-observer ICC also showed good correlation for NSA_h (0.751) and excellent correlation for all other parameters (Table 4.2).

	INTER-observer ICC	**INTRA-observer ICC**		**INTER-observer ICC**	**INTRA-observer ICC**
CE	0.955	0.965	**HD_p**	0.812	0.886
AA	0.890	0.964	**HD_h**	0.848	0.906
AI	0.831	0.937	**HD_c**	0.866	0.933
FO_p	0.986	0.993	**NSA_p**	0.887	0.926
FO_h	0.977	0.990	**NSA_h**	0.751	0.797
FO_c	0.991	0.990	**FA**	0.950	0.984

Table 4.2

Inter-observer and intra-observer ICC (n=20) for all analysed parameters.

4.3.2 Radiographic and CT Findings

In the entire cohort, mean CE was 40.3º (95%CI: 39.2º to 41.4º), mean AA was 34.8º (95%CI: 34.3º-35.2º) and mean AI was 50.4% (95%CI: 49.5% to 51.4%).

Mean FO_p (39.2 mm, 95%CI: 38.5 to 40.0 mm) was significantly lower than mean FO_h (44.1 mm, 95%CI: 43.4 to 44.9 mm, $p<0.001$) with mean difference of 4.9 mm (95%CI: 4.6 to 5.3 mm, 13%, Table 4.3). An excellent correlation between mean FO_p and FO_h ($r=0.885$, $p<0.001$) was observed.

With reference to mean FO_c (44.6 mm, 95%CI: 44.0 to 45.2 mm), FO_p was under-estimated by 5.4 mm (95%CI: 4.8 to 6.0 mm, 13%) and FO_h by 0.4 mm (95%CI: -0.1 to 0.9 mm, 1%). There was a highly significant difference between mean FO_c and FO_p ($p<0.001$); no significant difference between FO_c and FO_h ($p=0.092$) was observed (Table 4.3).

	Entire cohort (n=345)	Males (n=146)	Females (n=199)
FO_p (mm)	39.2 (range: 15.9-59.1) (95%CI: 38.5-40.0)	41.5 (range: 18.4-59.1) (95%CI: 40.4-42.7)	37.5 (range: 15.9-51.9) (95%CI: 36.6-38.4)
FO_h (mm)	44.1 (range: 21.4-61.5) (95%CI: 43.4-44.9)	47.6 (range: 26.2-61.5) (95%CI: 46.6-48.7)	41.6 (range: 21.4-57.9) (95%CI: 40.7-42.5)
FO_c (mm)	44.6 (range: 26.9-66.2) (95%CI: 44.0-45.2)	48.0 (range: 33.9-66.2) (95%CI: 47.1-48.8)	42.1 (range: 26.9-61.0) (95%CI: 41.4-42.7)
HD_p (mm)	46.8 (range: 36.5-57.7) (95%CI: 46.3-47.2)	49.7 (range: 41.1-57.7) (95%CI: 49.2-50.3)	44.6 (range: 36.5-57.6) (95%CI: 44.1-45.0)
HD_h (mm)	47.7 (range: 35.0-59.8) (95%CI: 47.3-48.2)	51.2 (range: 41.4-59.8) (95%CI: 50.6-51.8)	45.2 (range: 35.0-53.8) (95%CI: 44.8-45.7)
HD_c (mm)	45.8 (range: 34.7-61.6) (95%CI: 45.3-46.3)	49.3 (range: 36.8-61.0) (95%CI: 48.6-49.9)	43.2 (range: 34.7-61.6) (95%CI: 42.7-43.7)
NSA_p (º)	130.8 (range: 113.0-157.6) (95%CI: 130.0-131.6)	131.5 (range: 113.0-157.6) (95%CI: 130.3-132.6)	130.3 (range: 113.6-153.7) (95%CI: 129.3-131.4)
NSA_h (º)	125.3 (range: 111.4-148.9) (95%CI: 124.7-125.9)	125.2 (range: 113.5-143.6) (95%CI: 124.3-126.1)	125.4 (range: 111.4-148.9) (95%CI: 124.5-126.3)
FA (º)	14.0 (range: -6.7-56.82) (95%CI: 13.0-15.0)	13.3 (range: -3.0-35.85) (95%CI: 11.9-14.6)	14.5 (range: -6.7-56.8) (95%CI: 13.1-16.0)

Table 4.3

Mean values (range) for FO, HD, FA and NSA with 95% CI for the entire cohort, male patients and female patient.

4.3.3 Regression and Prediction Analysis

In group A, a good correlation between FO_p and FO_c was observed (r=0.642, p<0.001, Figure 4.1).

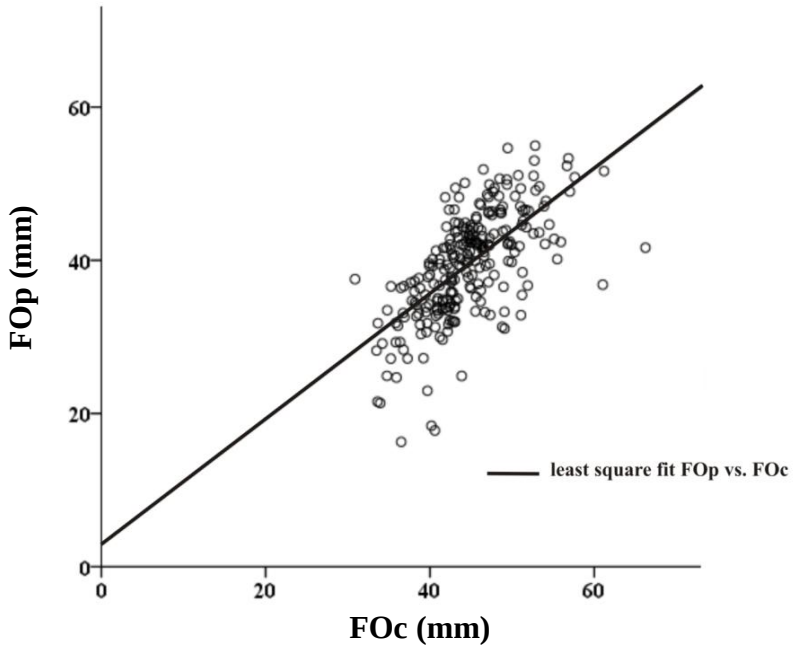


Figure 4.1

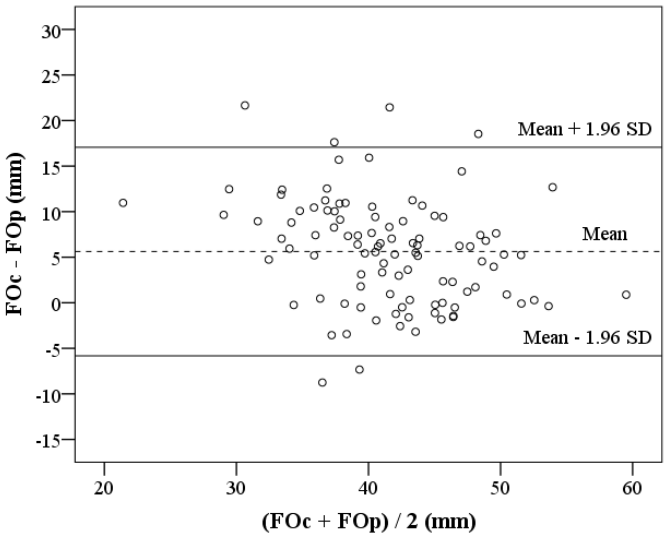
Group A: The scatter plot demonstrates a linear correlation between FO_p (y axis, mm) and FO_c (x axis, mm) (r=0.642, p<0.001). The line represents the least square fit.

From the regression analysis, Equation (1) was derived to predict FO as measured on CT from measurements on AP pelvis views:

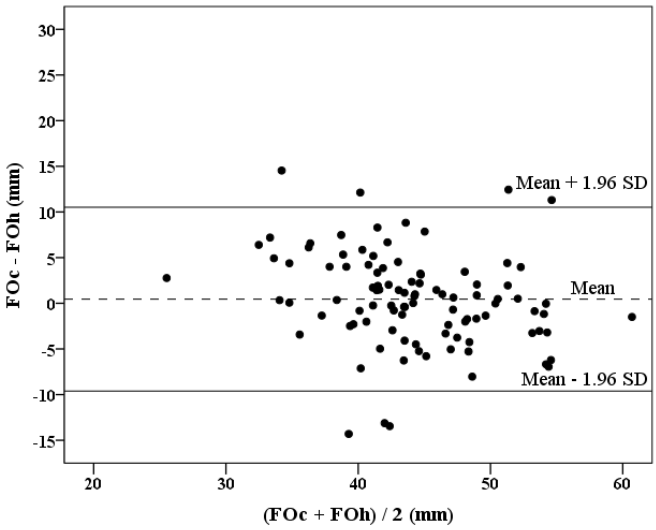
$$FO_c = 0.50 \times FO_p + 24.8 \ (R^2 = 0.412) \qquad \text{Equation (1)}$$

Bland-Altman plots demonstrated that the agreement between FO_p and FO_c was biased (mean bias: 5.6 mm, 95%CI: 4.5 to 6.8 mm). FO_h and FO_c showed good agreement (mean bias: 0.45 mm, 95%CI: -0.6 to 1.5 mm). Best agreement was seen between FO_{pred} and FO_c (bias: 0.2 mm, 95%CI: -0.1 to 1.1 mm, Figure 4.2).

A



B



C

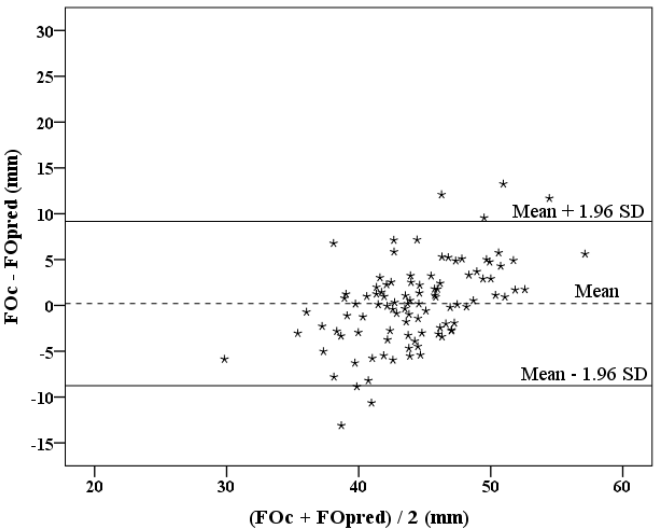


Figure 4.2

Bland-Altman plots illustrating the agreement in FO between CT and AP pelvis radiographs (A: FOc-FOp), CT and AP hip radiographs (B: FOc-FOh), and CT and predicted FO (C: FOc- FOpred) using Equation (1). Values are given in mm with the mean difference (mean), standard deviation (SD).

When considering males and females separately, corresponding FO_p and FO_c measurements demonstrated significant correlations for males ($r=0.537$, $p<0.001$) and for females ($r=0.660$, $p<0.001$). Gender specific regression analysis was performed to derive Equation (2) for males and Equation (3) for females:

$$FO_c = 0.39 \times FO_p + 31.9 \ (R^2 = 0.288) \qquad \text{Equation (2)}$$

$$FO_c = 0.45 \times FO_p + 25.4 \ (R^2 = 0.436) \qquad \text{Equation (3)}$$

Prediction of FO in group B using Equation (1) resulted in a highly significant under-estimation by 2.3 mm (95%CI: 1.2 to 3.5 mm, 5.2%, $p<0.001$) in males and in a significant over-estimation by 1.5 mm (95%CI: -2.8 to -0.3 mm, 3.6%, $p=0.013$) in females. Using gender specific prediction Equations (2, males) and (3, females), no significant difference between FO_{pred} and FO_c was observed for neither males (-0.2 mm, 95%CI: -1.4 to 0.9 mm, 0.5%, $p=0.689$, Figure 4.3, Table 4.4) nor females (-0.3 mm 95%CI: -1.5 to 0.9 mm 0.7%, Figure 4.4, Table 4.4).

	Group B (n=100)	Males (n=45)	Females (n=55)
FO_p	38.8 (range: 15.9-59.1) (95%CI: 37.3-40.2)	41.2 (range: 24.2-59.1) (95%CI: 38.9-43.4)	36.8 (range: 15.9-47.2) (95%CI: 34.9-38.6)
FO_h	43.9 (range: 24.1-61.5) (95%CI: 42.5-45.3)	47.2 (range: 33.1-61.5) (45.2-49.2)	41.3 (range: 24.1-51.0) (95%CI: 39.5-43.0)
FO_c	44.4 (range: 26.9-60.3) (95%CI: 43.2-45.6)	47.7 (range: 33.9-60.3) (95%CI: 46.1-49.4)	41.6 (range: 26.9-53.5) (95%CI: 40.3-43.0)
FO_{pred} using Equation (1) [0.50*FO_p+24.8] (mm)	44.2 (range: 32.8-54.3) (95%CI: 43.4-44.9)	45.4 (range: 36.9-54.3) (95%CI: 44.2-46.5)	43.2 (range: 32.8-48.4) (95%CI: 42.3-44.1)
FO_c – FO_{pred} (mm)	0.2 (range: -13.1-13.3) (95%CI: -0.7-1.1)	2.3 (range: -3.4-13.3) (95%CI: 1.2-3.5)	-1.5 (range: -13.1-7.1) (95%CI: -2.8-(-0.3)
FO_c – FO_{pred} (%)	0.5	5.2	3.7
p values (FO_c – FO_{pred})	0.660	< 0.001	0.013
FO_{pred} using Equation (2) [0.39*FO_p+31.9] (mm)	---	48.0 (range: 41.3-54.9) (95%CI: 47.1-48.8)	---
FO_c – FO_{pred} (mm)	---	-0.2 (range: -7.5-10.5) (95%CI: -1.4-0.9)	---
FO_c – FO_{pred} (%)	---	0.5	---
p values (FO_c – FO_{pred})	---	0.689	---
FO_{pred} using Equation (3) [0.45*FO_p+25.4] (mm)	---	---	42.0 (range: 32.6-46.6) (95%CI: 41.1-42.8)
FO_c – FO_{pred} (mm)	---	---	-0.3 (range: -11.7-8.0) (95%CI: -1.5-0.9)
FO_c – FO_{pred} (%)	---	---	0.7
p values (FO_c – FO_{pred})	---	---	0.607

Table 4.4

Prediction of true femoral offset (FOc) as measured on CT scans using regression equations for the entire group B, males and females. Predicted FO (FOpred) was calculated using regression equations (1, 2 and 3).

Compared to FO_c, FO_p demonstrated a clinically relevant under-estimation (>12%) in 53% of all cases in group B. FO_h resulted in a relevant under-estimation in 13% but also in an over-estimation in 10%. Equation (2) could predict FO_c more accurately for males with under-estimation rates of 7% and over-estimation rates of 2 % (males: 12% of FO_c=5.8 mm). However, equation (3) did not improve the prediction in females, as under-estimation

of gender-specific FO_{pred} occurred in 13% and over-estimation in 11% (females: 12% of FO_c=5.1 mm).

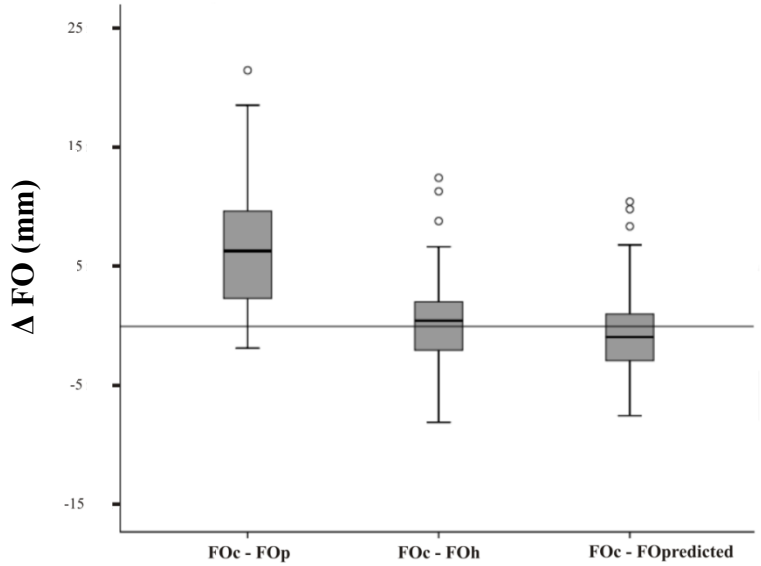


Figure 4.3

Male patients:
Differences (mm) in femoral offset (FO) between CT and AP pelvis radiographs (FO-FOp), CT and AP hip radiographs (FOc-FOh), and CT and FOpred using the gender specific regression equation (2) (FOc-FOpred) as boxplots.

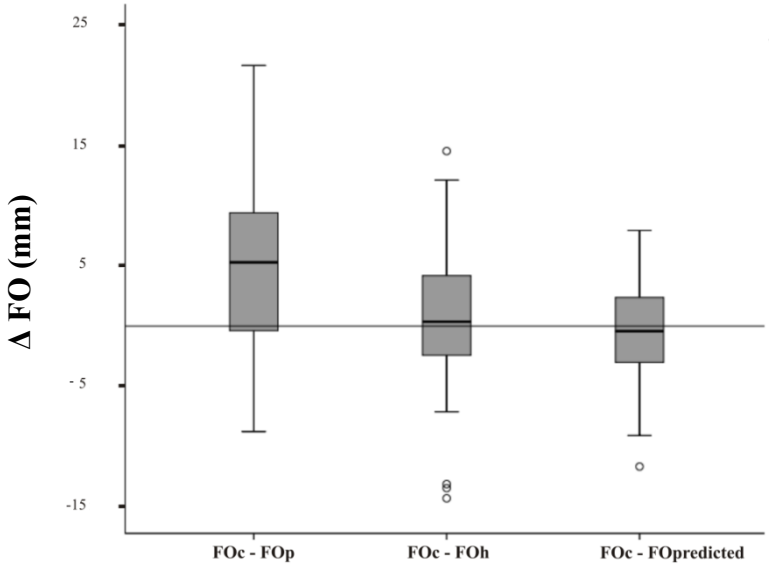


Figure 4.4

Female patients:
Differences (mm) in femoral offset (FO) between CT and AP pelvis radiographs (FOc-FOp), CT and AP hip radiographs (FOc-FOh), and CT and FOpred using the gender specific regression equation (3) (FOc-FOpred) as boxplots.

A stepwise regression model performed for group A identified patient height (m) as the only other significant independent variable ($p<0.05$); all other tested variables were not significant ($p>0.05$). The following gender specific regression equations (males: equation (4), females: equation (5)) including height (m) were derived. The coefficient of determination (R^2) improved slightly, however, this did not improve the accuracy of the prediction in group B.

$$FO_c = 0.38 \times FO_p + 14.41 \times \text{height} + 6.81 \quad (R^2 = 0.299) \qquad \text{Equation (4)}$$

$$FO_c = 0.34 \times FO_p + 14.43 \times \text{height} + 2.03 \quad (R^2 = 0.458) \qquad \text{Equation (5)}$$

4.4 Discussion

The present study evaluated the accuracy and reliability of predicting 3D femoral offset from standardised AP pelvis radiographs based on the underlying observation of a linear relationship between corresponding FO measurements performed on AP pelvis radiographs and CT scans.

To predict 3D FO from AP pelvis measurements and assess the accuracy compared to CT, the entire cohort was randomly split into subgroups A and B. Gender specific regression equations were derived from group A (245 patients) and then applied to FO_p measurements performed in group B (100 patients).

Measurements of FO on both radiography and CT scans showed excellent intra- and inter-observer reliability, and a linear correlation of corresponding FO measurements on all three modes of imaging was seen. Calculating FO_{pred} with use of gender specific regression equations, no significant difference between mean FO_{pred} and FO_c was seen in group B. Therefore, the present study suggests that 3D femoral offset may be accurately predicted from FO measurements performed on AP pelvis views with use of the provided equations. Moreover, the results demonstrate that the given equations reduce the occurrence of clinically relevant over- or underestimation (>12% of FO^{20}) that occurs when measuring FO_h.on AP hip radiographs.

The present study has a number of limitations:

Firstly, the target population of the present study were patients with primary end-stage hip OA. Care should therefore be taken when applying the provided equations to patients with secondary forms of OA or advanced deformity. However, for patients with primary OA, the present cohort can be considered as representative with regard to patient demographics.

This limitation should be put into perspective as the leading diagnosis for THA is primary OA[95]. In the present cohort, 16 patients had retroverted femora with mean FA of -2.7 degrees (range: -6.7 to 3.5 degrees, 95%CI: -3.9 to -1.4 degrees). Mean difference between FO_{pred} and FO_c was 0.4 mm for males (n=3, 95%CI: -7.0-7.7 mm) and -0.2 mm for females (n=13, 95%CI: -1.9-1.7 mm), suggesting that mild retroversion did not lead to an increased error of prediction.

Second, for FO measurements on CT, the long axis of the femur (centroid of proximal femoral metaphysis to centre of knee) was not used, as reported previously[152]. In the present study, FO_c measurements were performed based on the longitudinal axis of the proximal femur (centroid of proximal femoral metaphysis to centre of femoral isthmus) in order to represent femoral offset measurements as performed on plain radiography. In the entire study cohort, the observed absolute mean values for FO_c (44.6 mm) and FA (14.0 degrees) on CT scans compare well with reported values in the literature[29,39,153]. Third, patients whose affected hip was elevated for the AP hip radiographs to compensate for external rotation contracture cannot retrospectively be identified. Elevation seems beneficial to bring the femoral neck into the coronal plane to minimise the effect of rotation; however, this may have affected the object-to-film distance and might therefore be the cause of the observed overestimation of FO (>5mm) on AP hip radiographs in 13% of patients in group B .

This is the first study that demonstrates the validity and accuracy of predicting true 3D femoral offset from plain radiography in patients with primary hip OA. CT remains the gold standard in the assessment of proximal femoral geometry as the provided approach does not entirely account for imprecision in measurement on plain radiographs. Yet, the present findings support the surgeon in pre-operative planning on AP pelvis radiographs

and may improve femoral offset and limb length restoration in THA without the routine need for additional AP hip radiographs or CT. The suggested method of using predictive equations reduces radiation exposure and per-patient costs.

In conclusion, the work presented in this chapter confirms that a linear relationship between femoral offset measurements on corresponding AP pelvis radiographs and CT scans exists. The provided regression equations account for the adverse effects of positioning inconsistencies and beam divergence in conventional radiography and limit the occurrence of clinically relevant over- or underestimation of FO on AP hip radiographs. Although, CT clearly remains the most accurate option to assess pelvic and femoral anatomy, true 3D femoral offset can be accurately and reliably predicted from AP pelvis radiographs in patients with primary OA.

4.5 Summary

The aim of the present study was to evaluate the accuracy and reliability of predicting three-dimensional (3D) FO from standardised AP pelvis radiographs.

The work presented in this chapter suggests that femoral offset can be accurately and reliably predicted from AP pelvis radiographs in patients with primary end-stage hip osteoarthritis. This supports the surgeon in pre-operative templating on AP pelvis radiographs and may improve offset and limb length restoration in THA without the routine performance of additional radiographs or CT.

Chapter 3 and 4 have focused on femoral offset as a surrogate parameter for proximal femoral geometry. As described in Chapter 2, the assessment of proximal femoral canal shape in pre-operative templating for THA is, however, equally important. In an analogous manner to Chapter 3, the next chapter aims to determine differences in the radiographic

appearance of the proximal femoral canal between AP hip and AP pelvis radiographs with reference to CT using Active Shape Modelling (ASM).

5. ASSESSMENT PROXIMAL FEMORAL CANAL SHAPE

5.1 Introduction

Accurate pre-operative templating is an essential requirement in contemporary total hip arthroplasty (THA) as it aids the surgeon in the selection of appropriate implant geometry and size, and suggests positioning of prosthetic components[30,31].

Unlike cemented femoral components, in which a geometric mismatch between the femoral component and the medullary canal of the proximal femur is required for fixation, cementless femoral reconstruction aims for a close geometric fit between the implant and the endosteal surface of the proximal femur[97,98]. Stable primary fixation is achieved by press-fit implantation of a slightly oversized implant into the prepared medullary canal[99]. Primary stability is essential to minimise micro-motion at the implant bone interface and it allows secondary biologic fixation of the implant (osteointegration)[25,26]. A number of studies have highlighted the importance of metaphyseal stem fit to reduce micro-motion at the implant bone interface[97,100], and to minimise stress-shielding[101,102]. Despite promising long-term results of some cementless stem designs[103,160-162], an increased risk of aseptic loosening has been reported for undersized femoral components[105], and there is still is concern that progressive peri-prosthetic bone loss may compromise long-term stem performance[19]. This is particularly crucial with regard to a rising number of THAs performed in young and active patients[106] and the development of novel stem designs that aim for a metaphyseal fixation.

It has been shown that the appearance of canal shape on plain radiographs may be misleading as a result of inaccurate patient positioning and the difficulty to control femoral rotation[27,36].

The objective of the work presented in this chapter was to investigate which radiographic view allows the most accurate assessment of proximal femoral canal shape in patients with primary hip OA. This chapter aimed to determine (1) whether differences in the radiographic appearance of the proximal femoral canal exist between corresponding AP ***pelvis*** and AP ***hip*** radiographs, and (2) whether quantitative radiographic assessment of canal shape is accurate with reference to canal shape determined from computed tomography (CT).

5.2 Materials and Methods

5.2.1 Study Cohort

A consecutive series of 152 patients who had undergone primary cementless THA for primary end-stage hip osteoarthritis (OA) between July and December 2009 was retrospectively evaluated. For pre-operative templating, standardised AP pelvis radiographs, AP hip radiographs and CT scans of the affected hip were obtained. Details of the patient cohort, inclusion and exclusion criteria are given in section 3.2.1.

5.2.2 Imaging Protocols

The radiographic and CT imaging protocols are described in section 3.2.2 and 3.2.3.

5.2.3 Active Shape Modelling

In addition to the single geometric measures described previously, the present chapter aims to identify differences in proximal femoral canal shape on corresponding AP hip and AP pelvis radiographs with reference to CT using a more abstract, yet powerful technique, Active Shape Modelling (ASM). An overview of ASM is presented in section 2.3.

The model was built using a freely available ASM tool kit (Manchester University, Manchester, UK)[135].

To define the shape of the proximal femoral canal, the ASM template contained 33 points from a 67-point model of the proximal femur (Figure 5.1). Key points were placed at reliably identifiable features of the endosteal cortices (e.g. at the femoral isthmus, the lesser trochanter, the head neck junction), while the remaining points were spaced approximately evenly between features. Each key point was placed on the same feature on corresponding images to allow comparison between shapes and to perform point-based measurements.

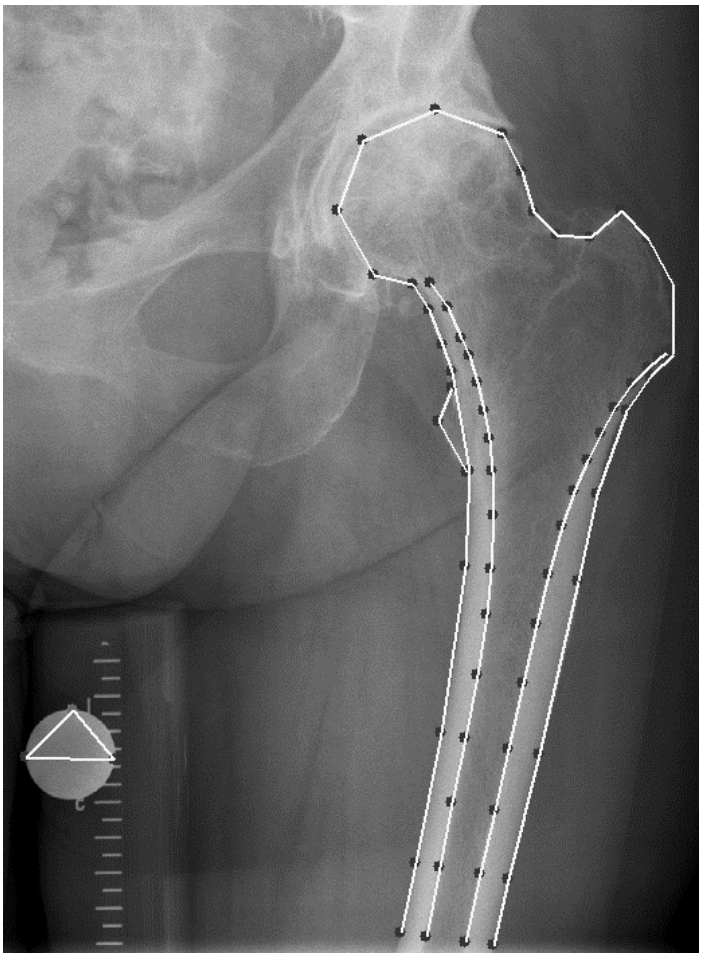


Figure 5.1

ASM template
The shape of the proximal femoral canal is described by 33 points placed on endosteal surface of the medial and lateral cortex.

For each mode in the model, mean and SD values for the entire dataset of corresponding AP pelvis and AP hip radiographs were calculated, and the mean value of each mode was scaled to zero. Mode scores for each radiograph were calculated and expressed how many standard deviations it lay from the mean value (zero) of that mode.

5.2.4 Curve Fitting

For comparison of the medial cortical flare between corresponding radiographs and CT, points on the endosteal surface were depicted as scatter plots (x-axis: femoral shaft axis (FSA), y-axis: perpendicular distance between endosteal cortex and FSA). Least squares curve fitting ($f(x) = ax^b+c$) was performed to quantify differences on corresponding modes of imaging.

On radiographs, endosteal dimensions were derived from the ASM template and scaled with reference to the calibration marker. The femoral shaft axis was defined as best fit line between the midpoints of the endosteal surface from a point 100 mm below the lesser trochanter to the midpoint at the lower aspect of the lesser trochanter.

On corresponding CT scans, measurements of endosteal dimensions were performed using the MATLAB [version 7.10, The MathWorks Inc., MA, USA] programme described in section 3.2.5. The programme enabled the user to select points from pre-selected axial CT slices and performed vector calculations in the 3D coordinate system of the CT scanner. Six slices were selected: S1 (head neck junction), S2 (centroid), S3 (proximal aspect of lesser trochanter), S4 (mid lesser trochanter), S5 (distal lesser trochanter), S6 (isthmus). The endosteal dimensions of the femoral canal were determined on each slice with a best fit ellipse. Endosteal distances were calculated in the plane of the femoral neck axis which was defined according to the single slice method described by Sugano[147], and

perpendicular to the femoral shaft axis which was defined as line between the centre of the femoral canal at the isthmus (S6) and at the lower aspect of the lesser trochanter (S5).

5.2.5 Measurement Reliability

For CT measurements, intra- and inter-observer reliabilities for determining canal diameters and the femoral neck axis were evaluated for 15 randomly selected patients by two independent observers using single-measure intra-class-correlation coefficients (ICC) with a two-way-random effects model for absolute agreement.

For placement of keypoints on the ASM template, the mean error was determined for 2 independent observers.

5.2.6 Statistical Analysis

In order to investigate differences in endosteal shape of the proximal femur between corresponding AP pelvis and AP hip radiographs, differences in normalised mode scores were tested for the first 10 modes using paired-samples t-tests. Results with p values <0.05 were considered as significant, p values of <0.001 as highly significant.

Coefficients of curve fits were calculated with 95% confidence intervals (95%CI), and goodness of curve fit was determined using R^2 values.

Statistical analysis was carried out using PASW Statistics 18 [SPSS Inc. an IBM company, IL, USA] and MATLAB [version 7.10, The MathWorks Inc., MA, USA].

5.3 Results

5.3.1 Measurement Reliability

For repeated CT measurements performed on 15 datasets, intra-observer ICCs ranged from 0.93 to 0.99, inter-observer ICC from 0.87 to 0.99, respectively.

The mean error for placement of keypoints on the radiographic ASM template for 15 datasets was <1 mm for both intra- (mean: 0.6 mm, 95%CI: 0.3 to 0.9 mm) and inter-observer (mean 0.9 mm, 95%CI: 0.5 to 1.4 mm) measurements.

5.3.2 Active Shape Modelling

ASM identified 10 independent shape modes that accounted for 96% of overall variation in the endosteal shape of the proximal femur. Mode scores from AP pelvis radiographs showed a higher scatter compared to those derived from AP hip views. For 7 out of 10 modes, significant differences in distribution of mode scores between corresponding AP hip and AP pelvis views were observed (range of p values 0.000-0.010, Table 5.1), indication that the shape of the same femur on corresponding AP pelvis and AP hip radiographs is significantly different.

The greatest variability of canal shape occurred in the medial femoral cortex between the lesser trochanter and the head neck junction. Modes 4 and 5 identified significant differences in the medial cortical flare ($p<0.001$) between corresponding AP pelvis and AP hip radiographs (Figure 5.2).

	AP hip	SD	AP pelvis	SD	Mean Difference	95% CI Lower	95% CI Upper	p-value
Mode 1	-0.448	0.5976	0.448	1.1171	-0.896	-1.1037	-0.6875	***< 0.001***
Mode 2	0.048	0.9026	-0.048	1.0912	0.096	-0.1357	0.3270	0.414
Mode 3	-0.472	0.6006	0.472	1.0954	-0.943	-1.1643	-0.7225	***< 0.001***
Mode 4	0.243	0.8299	-0.243	1.0966	0.485	0.3222	0.6482	***< 0.001***
Mode 5	0.173	0.8811	-0.173	1.0831	0.346	0.1604	0.5328	***< 0.001***
Mode 6	-0.116	0.7886	0.116	1.1667	-0.232	-0.5041	0.0404	0.094
Mode 7	-0.266	0.8763	0.266	1.0486	-0.532	-0.7735	-0.2897	***< 0.001***
Mode 8	0.108	0.9128	-0.108	1.0738	0.216	-0.0044	0.4381	0.055
Mode 9	-0.190	1.0125	0.190	0.9550	-0.380	-0.6563	-0.1041	***0.007***
Mode 10	-0.172	0.9185	0.172	1.0519	-0.344	-0.6031	-0.0855	***0.010***

Table 5.1

Differences in mode scores for corresponding AP hip and AP pelvis radiographs with standard deviation (SD) and 95% confidence intervals (95%CI).

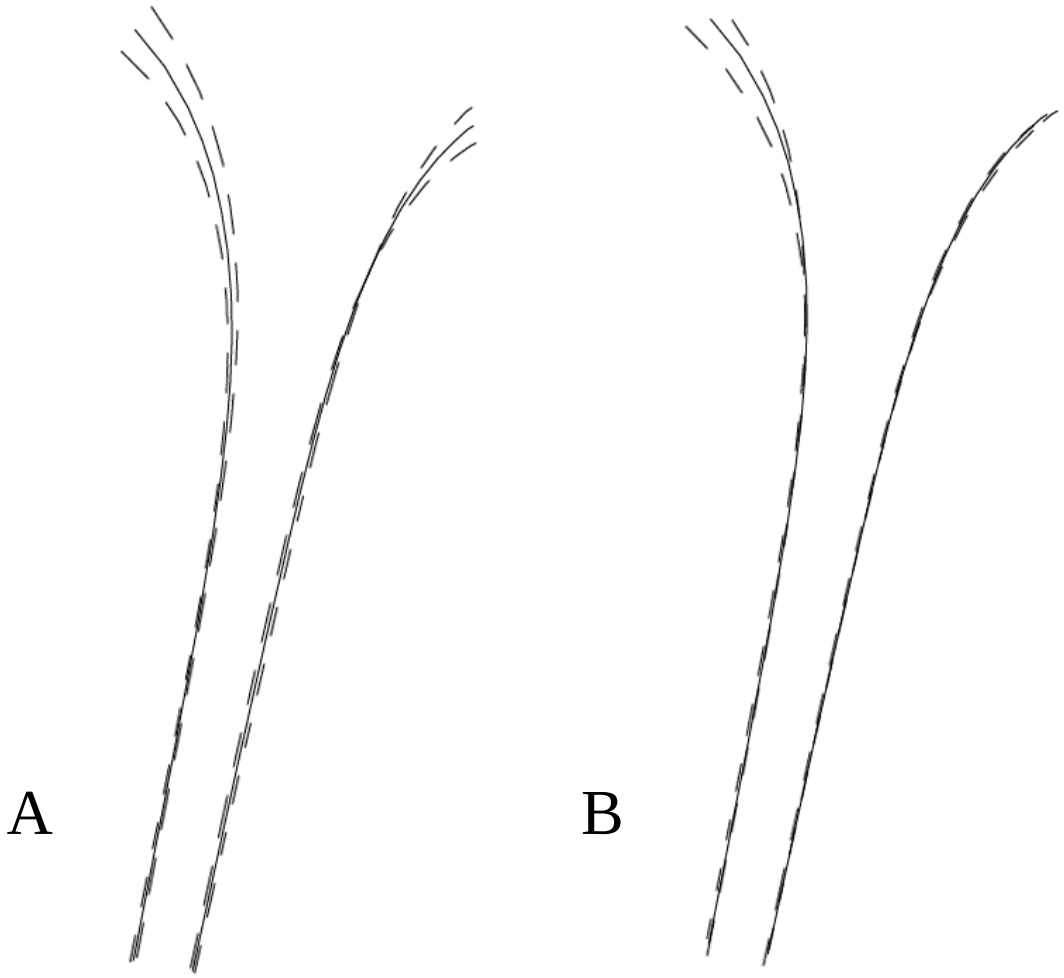


Figure 5.2

Overlay image of shape modes 4 (A) and 5 (B). The medial cortical flare shows greater variation than the lateral cortical flare. Modes scores for corresponding AP pelvis and AP hip radiographs were significantly different for both modes ($p<0.001$, Table 5.1). The solid line represents the mean shape, the dashed lines represent ±2 SDs.

5.3.3 Curve Fitting

Comparing the recovered average shapes of corresponding radiographs, the flare of the medial femoral cortex was underestimated on AP pelvis views with the calcar and neck region appearing in valgus orientation. On AP hip views, the medial cortical flare was more distinct and appeared in more varus orientation (Figure 5.3).

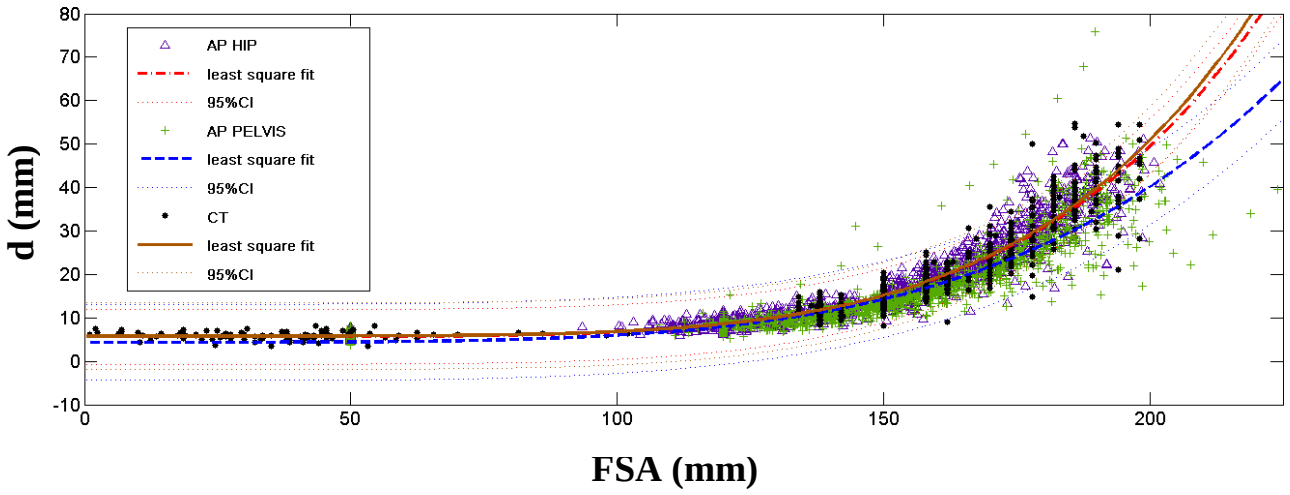


Figure 5.3

Scatter plot with least square fits for the endosteal flare of the medial femoral cortex. The femoral shaft axis (FSA) is aligned to the x-axis (y=0). The lesser trochanter is located at x=150 mm. The distance of points on the endosteal surface of the medial cortex with reference to the femoral shaft axis (d) is plotted on the y-axis (mm). Lines represent the least square fit ($f(x) = ax^b+c$) with 95% confidence intervals for corresponding AP pelvis radiographs, AP hip radiographs and CT.

The derived least square curve fits of the medial cortex demonstrated a good agreement between AP hip radiographs and CT. Agreement of the curve fit coefficients between AP pelvis radiographs and CT was less good (Figure 5.3, Table 5.2).

Coefficients	a	b	c	R^2
AP pelvis	1.98e-009	4.458	4.349	0.811
(95%CI)	(-7.953e-010-4.756e-009)	(4.193-4.722)	(3.620-5.078)	
AP hip	2.788e-011	5.3	5.62	0.904
(95%CI)	(-4.62e-012-6.038e-011)	(5.079-5.522)	(5.157-6.084)	
CT	1.264e-011	5.455	5.794	0.879
(95%CI)	(-9.747e-012-3.503e-011)	(5.119-5.791)	(4.987-6.602)	

Table 5.2

Least squares fit coefficients ($f(x) = ax^b+c$) for the medial cortical flare on corresponding radiographs and CT with 95% confidence intervals (95%CI).

5.4 Discussion

In cementless THA, the endosteal fit of the femoral component is a major factor determining load transfer and consequently, peri-prosthetic bone remodelling. Accurate metaphyseal stem fit is essential to reduce micro-motion at the implant bone interface[97,100], and to minimise stress-shielding[101,102]. It has been shown that femoral fit predicts not only radiographic changes following THA[101,102], but also affects clinical results in terms of post-operative pain[163] and implant survival[105].

Therefore, accurate and reliable assessment of canal shape in pre-operative templating is essential. Although standardised recommendations of patient positioning during radiography with 15° of internal rotation of the lower limbs have been made[151] to ensure reproducible projection with the femoral neck in the coronal plane, several studies have demonstrated that radiographic assessment of femoral canal shape has limited reliability[29,33]. CT is considered as the gold standard as it represents the 3D shape and geometry of the proximal femur, and thus allows a more accurate selection of the implant and its position[33].

The present study demonstrates that the endosteal shape of the proximal femoral canal varies considerably, not only between individuals, but also between corresponding AP pelvis and AP hip radiographs. The greatest variation in femoral shape was observed in the proximal femoral metaphysis, predominately in the flare of the medial cortex.

On corresponding AP pelvis and AP hip radiographs, ASM identified significant differences in the flare of the proximal medial cortex, further indicating that the scatter of femoral canal flare was smaller and thus more reliably measured on AP hip radiographs. Comparing the medial cortical flare as measured on radiographs to corresponding CT scans, AP hip radiographs were more accurate than AP pelvis radiographs as shown by the provided curve fit equations. These findings may be explained by a better control of femoral rotation and the ability to compensate for external rotation contractures during positioning.

It is important to point out the limitations of the present study:

Firstly, the target population were patients with primary end-stage hip OA. Care should therefore be taken when applying the present results to patients with secondary forms of OA, i.e. advanced deformity. However, for patients with primary OA, the present cohort can be considered as representative with regard to patient demographics. This limitation should be put into perspective as the leading diagnosis for THA is primary OA[95].

Secondly, as stated previously, patients whose affected hip was elevated on AP hip radiographs cannot be retrospectively identified. Elevation appears to be beneficial in order to bring the femoral neck into the coronal plane and to minimise the adverse effect of external rotation contractures on radiographic projection. Recently, a study has highlighted the clinical relevance of palpating the greater trochanter to assess femoral neck version[164].

Lastly, the present study used active shape modelling (ASM) to assess the overall variation and differences in the appearance of the proximal femoral canal on corresponding AP pelvis and AP hip radiographs. This method enables measurement of the variation in a complex shape, such as the hip. In ASM, a mode does not just capture one aspect of variation in femoral canal shape, it is a combination of evident and/or subtle differences between femurs[137]. It can, therefore, be difficult to visually describe what aspect of shape variation each mode represents. However, at the same time this method is powerful and able to detect differences that are not necessarily evident with conventional radiographic measures (e.g. angles, distances or canal flare indices)[135].

Cadaver, radiographic and CT based studies have demonstrated that the anatomy of the femoral medullary canal is highly variable[35,39,40] and as a consequence, a great variety of cementless femoral stem designs and implant systems with different geometry, surface treatment and underlying principles of fixation are currently in clinical use. The growing popularity of bone preserving and minimally invasive procedures[128] has led to the development of novel "short" stem designs which aim for metaphyseal fixation and preservation of the femoral neck[129]. Moreover, implants with multiple shape options have been introduced to account for individual patient anatomy[123,124]. For these components, the intra-operative selection of the broach that provides the best fit is essential, but intra-operative assessment of endosteal cortical contact is difficult and can only be done radiographically with the broach *in situ*. Consequently, the surgeon has to make decisions prior to and during femoral canal preparation and needs to choose the broach that allows adequate fit with regard to individual patient anatomy. For third generation cementless stems, pre-operative templating of resection levels and implant fit may thus be even more critical than for straight tapered stems, since small inaccuracies in the pre-operative

assessment of canal shape may compromise proximal fixation and/or restoration of physiologic joint mechanics. Moreover, a mismatch of bone and implant shape may increase the risk for intra-operative peri-prosthetic fractures[165,166]. Therefore, the present findings of differences in femoral canal shape between corresponding radiographs are of clinical relevance.

This is the first study that demonstrates the reliability and accuracy in the assessment of proximal femoral canal shape on plain radiographs in patients with primary hip OA. CT remains the gold standard in the assessment of proximal femoral geometry and shape as the provided radiographic protocol for AP hip views does not entirely account for potential measurement imprecision. Yet, the work presented here confirms that AP hip radiographs allow a better assessment of proximal femoral anatomy compared to AP pelvis views and may improve pre-operative templating in THA.

In conclusion, AP hip radiographs allow a more accurate and more reliable assessment of canal shape than AP pelvis radiographs compared to CT. Although the ultimate decision of implant design, size and position must be made intra-operatively, standardised AP hip radiographs are a feasible option for pre-operative assessment of femoral canal shape in the frontal plane in patients with primary OA. The findings of this chapter support surgeons in pre-operative templating and may improve stem fit and restoration of joint geometry without the routine use of CT.

5.5 Summary

In cementless femoral reconstruction, accurate endosteal stem fit is essential for stability and proximal load transfer. The objective of the work presented in this chapter was to determine (1) whether differences in the radiographic appearance of the of the proximal femoral canal exist between corresponding AP pelvis and AP hip radiographs, and (2) whether quantitative radiographic assessment of canal shape is accurate with reference to canal shape determined from computed tomography (CT).

ASM identified significant differences in distribution of mode scores between corresponding AP hip and AP pelvis views. The greatest variability of canal shape occurred in the medial cortex of the proximal femoral metaphysis. Least squares curve fitting demonstrated a good agreement between AP hip radiographs and CT. Agreement of the curve fit coefficients between AP pelvis radiographs and CT was less good.

Thus, considering the results of Chapter 3, AP hip radiographs allow an accurate and reliable assessment of geometry ***and*** canal shape of the proximal femur.

In the next Chapter, a second ASM study is developed to determine the overall variation and underlying patterns in proximal femoral anatomy in a cohort of 345 patients with primary hip OA.

6. VARIATION AND PATTERNS OF PROXIMAL FEMORAL SHAPE AND GEOMETRY

6.1 Introduction

In cementless total hip arthroplasty (THA), the optimal femoral component should allow both accurate endosteal stem fit and individual restoration of physiologic joint mechanics. This poses a major surgical challenge, as the osseous anatomy of the proximal femur is highly variable[27,39,40], and most contemporary stem designs are limited in their potential to adjust femoral offset, version, and limb length intra-operatively. Moreover, due to the variability in the size and shape of the medullary canal, surgeons may be forced to compromise between the endosteal stem fit, which is critical to achieve stable fixation with proximal load transfer[97,100], and accurate restoration joint mechanics.

Several studies have described the variation in femoral anatomy over the last three decades. However, most reported values were obtained from cadaveric specimens or individuals with non-arthritic hip joints[39,40,153], or from cohorts with limited patient numbers. Differences in femoral morphology between males and females have been described[125,154], but there continues to be limited data on gender differences in primary OA. Furthermore, it is not clear whether the shape of the proximal femoral canal is associated with geometric or anthropometric measures and whether distinct patterns of shape and geometry exist; this important information would allow a comprehensive classification of femoral morphology in patients requiring THA.

Therefore, the objectives of the work presented in this chapter were (1) to investigate the variation and underlying patterns in proximal femoral anatomy and (2) to determine the

association of proximal femoral canal shape with geometric and anthropometric parameters in a cohort of patients with primary, end-stage hip OA.

6.2 Materials and Methods

6.2.1 Study Cohort

For the present retrospective cohort study, a consecutive series of 597 patients who had undergone primary THA for end-stage hip osteoarthritis (OA) with a custom-made cementless femoral component between June 2008 and December 2009 were reviewed. Each patient received standardised radiographs and a CT scan of the affected hip pre-operatively, and all images were retrieved in generic DICOM format.

In order to obtain normative values for the variation in femoral shape and geometry, only patients with primary hip osteoarthritis were considered for this study. According to the study criteria reported in section 4.2.1, 252 patients were excluded from the initial cohort, leaving 345 patients (146 males, 199 females, mean age 60 (range: 40-79) years, mean body- mass- index (BMI) 27 (range: 19-57) kg/m², Table 1) that were included in the present study. The study was approved by the institutional review board (reference S-272/2009).

6.2.2 Imaging Protocols

For all patients, standardised, low-centered AP hip radiographs and CT scans of the proximal femur were obtained in a supine position according to standardised protocols as described in section 3.2.2 to section 3.2.5.

6.2.3 Active Shape Modelling

The present study used Active Shape Modelling (ASM) to describe the variation in shape of the proximal femoral canal in the present cohort. The model was built using the freely

available ASM tool kit (Manchester University, Manchester, UK)[135,167]. Details of the ASM template and underlying principles of ASM are presented in section 5.2.3.

6.2.4 Cluster Analysis

Cluster Analysis is a mathematical approach to divide data, objects or observations into useful or meaningful groups (clusters) that should capture the natural structure of the data or the relationship of the objects of interest. The goal of cluster analysis is to identify and group similar objects which are different from or unrelated to objects of other groups[168-170].

In the present study, agglomerative hierarchical cluster analysis (Ward's method) of the mode scores (1-10) derived from ASM was performed to identify natural groupings of patients based on femoral canal shape[171]. This approach defines the proximity between two clusters by the increase in the sum of the squared error (SSE) that would result when two clusters are merged and attempts to minimise the sum of the squared Euclidean distance from each mode score to its cluster centroid in an n-dimensional space. The number of clusters that allowed the best separation was determined according to the Duda and Hart index[172].

6.2.5 Canal Flare

To quantify differences in shape between clusters, the radiographic canal flare index (CFI) as described by Noble[39] (Figure 6.1), the canal-to-calcar ratio (CCR) and the cortical thickness index (CTI) as described by Dorr[41] was calculated (Figure 6.1). In addition, CFIs of the medial and lateral cortex were calculated as ratio of the distances from the determined endosteal points perpendicular to the femoral shaft axis.

For comparison of the medial and lateral cortical flare with regard to gender and cluster membership, points on the endosteal surface were depicted as scatter plots (x-axis: femoral

shaft axis (FSA), y-axis: perpendicular distance between endosteal points and FSA). Least squares curve fitting was performed to quantify variation and differences in canal flare. Endosteal dimensions and point locations were derived from the ASM template perpendicular to the femoral shaft axis and scaled with reference to the calibration marker. The femoral shaft axis was defined as best fit line between the midpoints of the endosteal surface from a point 100 mm below the lesser trochanter to the midpoint at the lower aspect of the lesser trochanter.

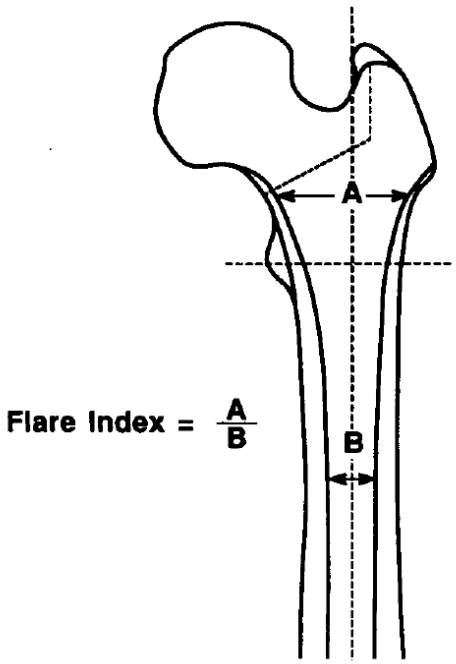


Figure 6.1

Canal flare index (CFI) according to Noble:
CFI is defined as the ratio of intra-cortical width of the femur at a point 20 mm proximal to the lesser trochanter and at the canal isthmus (source: Noble. et al., 1988[39]).

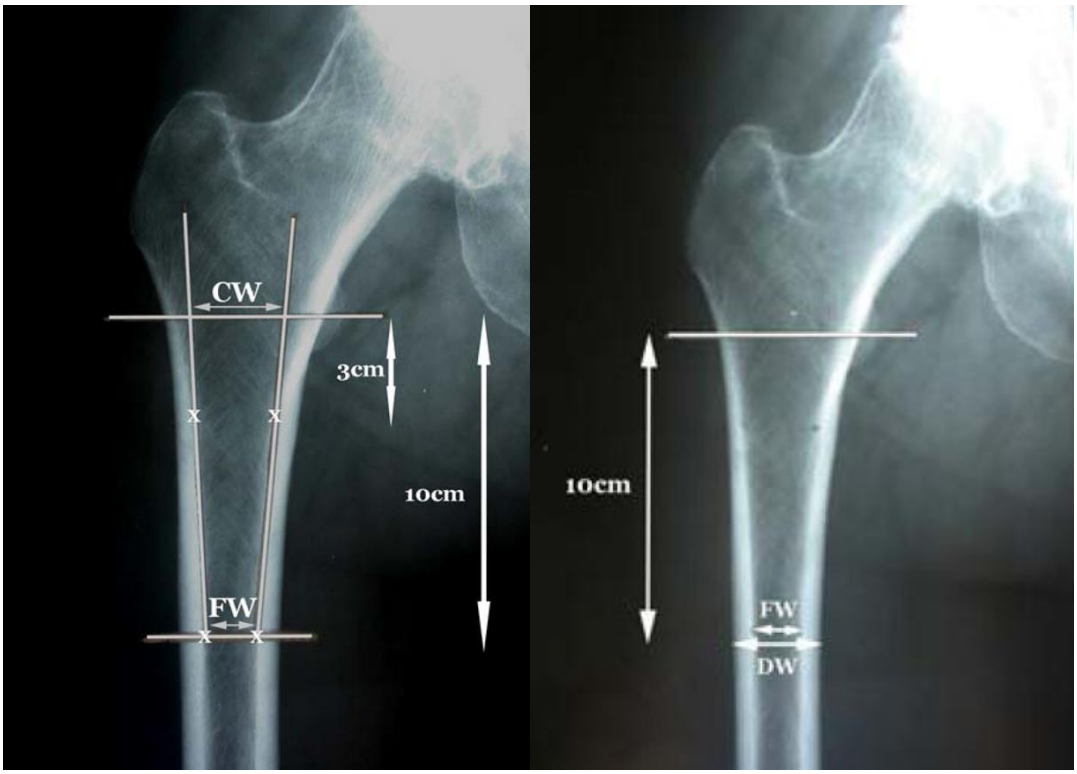


Figure 6.2

Canal-to-calcar Ratio [CCR= FW/CW] and the cortical thickness index [CTI=(DW-FW)/DW] as described by Dorr[41] (source: Sah et. al., 2007[173])

6.2.6 CT measurements

Femoral offset (FO) and femoral anteversion (FA) on the corresponding CT data was assessed as described in sections 3.2.5.

6.2.7 Measurement reliability

Intra- and inter-observer reliabilities for 15 randomly selected corresponding radiographs and CT scans were evaluated by two independent and blinded observers using single-measure intra-class-correlation coefficients (ICC) with a two-way-random effects model for absolute agreement. For placement of keypoints on the ASM template, the mean error was determined for 2 independent observers (see section 5.3.1).

6.2.8 Statistics

For descriptive analysis, absolute mean values and differences were expressed in mm or degrees (°) with standard deviations (SD). Differences between males and females and between clusters were expressed as mean values with 95% confidence intervals (95%CI).

The distributions of all variables were examined in an exploratory data analysis, and tested for normality using Kolmogorov-Smirnov tests. As not all variables met the criteria for a normal distribution, non-parametric tests were used. Differences between males and females were compared using Mann–Whitney U tests for unpaired observations. Differences in morphologic measures of the proximal femur and demographic parameters between the clusters were evaluated using Kruskal-Wallis or Chi-square tests, as appropriate. Spearman's correlation (r) was used to evaluate associations between continuous variables. Correlation was characterised as poor (0.00-0.20), fair (0.21-0.40), moderate (0.41-0.60) good (0.61-0.80), or excellent (0.81-1.00)[159].

Coefficients of curve fits ($f(x) = ax^b+c$) were calculated with 95% confidence intervals (95%CI). The goodness of curve fit was determined using R^2 values.

Results with p values <0.05 were considered as significant, p values of <0.001 were considered as highly significant. Statistical analysis was carried out using PASW Statistics 18 [SPSS Inc. an IBM company, IL, USA] and MATLAB [version 7.10, The MathWorks Inc., MA, USA].

6.3 Results

6.3.1 Measurement reliability

Intra-observer and inter observer ICCs of CT measurements and of mean errors for placement of keypoints on the radiographic ASM template have been reported in section 5.3.1.

6.3.2 Radiographic and CT measurements

FO_h was significantly higher in male (47.6 mm, SD: 6.30 mm) than in female patients (41.6 mm, SD: 6.30 mm, $p<0.001$). In the entire cohort, there was no significant difference between mean FO_c (44.6 mm, SD: 5.62 mm) and FO_h (44.1 mm, SD: 6.95 mm, $p=0.092$, Table 1). FO_c and FO_h demonstrated a good correlation ($r_s=0.75$, $p<0.001$) indicating that the present radiographic protocol allows accurate assessment of FO.

Mean NSA was 125° for both males (SD:5.6°) and females (SD: 6.3°, $p=0.692$). Females had a slightly higher femoral anteversion (FA: 15°, SD 10.5°) than males (FA: 13°, SD 8.3°), however, this finding was not statistically significant ($p=0.348$, Table 6.1).

The CFI of the medial cortex (4.45, SD: 0.536) was significantly higher than the CFI of the lateral cortex (3.5, SD: 0.514, $p<0.001$). No significant differences in radiographic canal shape parameters (CFI, CFI_{med}, CFI_{lat}, CCR, CTI) were observed between males and females (Table 6.1). No significant correlations between radiographic canal shape parameters (CFI, CFI_{med}, CFI_{lat}, CCR, CTI) and measures of patient size (HD, height, weight, BMI) were observed.

	Entire cohort	Males	Females	p-value
n %	345 (100)	146 (42)	199 (58)	
Age in [years]	60	60	60	0.764
SD	7.00	6.9	7.1	
range	40-79	43-72	40-79	
Height [m]	1.70	1.77	1.65	***<0.001***
SD	0.088	0.063	0.063	
range	1.46-1.97	1.60-1.97	1.46-1.88	
Weight [kg]	78.5	85.3	73.3	***<0.001***
SD	15.42	13.26	14.94	
range	46.0-173.0	54.0-138.0	46.0-173.0	
BMI [kg/m^2]	27.0	27.1	26.9	0.281
SD	4.51	3.76	5.00	
range	19.2-56.5	19.8-42.6	19.2-56.5	
NSA [degrees]	125	125	125	0.692
SD	6.0	5.6	6.3	
range	111-149	114-144	111-149	
HD [mm]	47.7	51.2	45.2	***<0.001***
SD	4.53	3.73	3.18	
range	35.0-59.8	41.4-59.8	35.0-53.8	
FO_h [mm]	44.1	47.6	41.6	***<0.001***
SD	6.95	6.30	6.30	
range	21.4-61.5	26.2-61.5	21.4-57.9	
FO_c [mm]	44.6	48.0	42.0	***<0.001***
SD	5.62	5.05	4.63	
range	26.9-66.2	33.9-66.2	26.9-61.0	
FA [º]	14	13	15	0.348
SD	9.6	8.3	10.5	
range	-7-57	-3-36	-7-57	
CTI	0.59	0.59	0.58	0.399
SD	0.040	0.038	0.041	
range	0.41-0.72	0.41-0.71	0.45-0.72	
CCR	0.45	0.45	0.45	0.872
SD	0.044	0.045	0.043	
range	0.32-0.70	0.34-0.70	0.32-0.60	
CFI	3.98	3.99	3.97	0.723
SD	0.433	0.428	0.437	
range	2.54-5.93	2.54-5.93	2.87-5.76	
CFI_{medial}	4.45	4.45	4.45	0.949
SD	0.536	0.476	0.578	
range	3.02-6.69	3.15-6.32	3.02-6.69	
$CFI_{lateral}$	3.50	3.52	3.49	0.659
SD	0.514	0.522	0.508	
range	1.94-5.55	1.94-5.55	2.02-5.13	

Table 6.1

Patient demographics and mean measurement parameters for the entire cohort, males and females with standard deviation (SD) and range.

6.3.3 Active Shape Modelling

In ASM, the first 10 independent shape modes accounted for 96% of overall variation in proximal femoral canal shape within the dataset.

Modes 2, 3 and 4 depicted the variation in cortical flare which has been previously characterised as stove pipe vs. champagne flute shape[41] (Figure 6.3). Distributions of mode scores between males and females were significantly different for mode 2 ($p<0.001$). Mode 3 showed a moderate correlation with FO ($r_s=0.48$, $p<0.001$), and a fair inverse correlation with NSA ($r_s=-0.38$, $p<0.001$); similarly, mode 4 showed a moderate correlation with NSA ($r_s=-0.49$, $p<0.001$) and a fair correlation with FO ($r_s=0.28$, $p<0.001$).

No significant correlations between shape modes and measures of size (HD, height, weight, BMI) were observed.

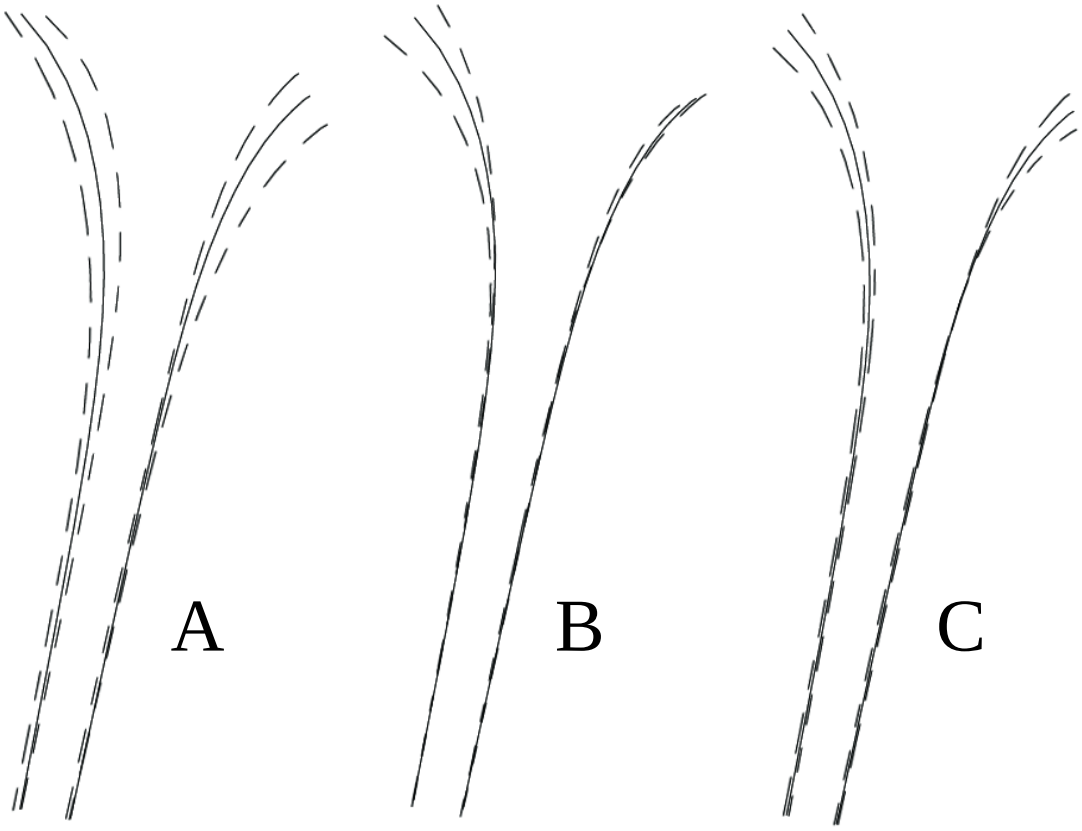


Figure 6.3

Overlay image of shape modes 2 (A), 3 (B) and 4 (C). The medial cortical flare shows greater variation than the lateral cortical flare. The solid lines represent the mean shape, the dashed lines represent ±2 SDs.

6.3.4 Cluster Analysis

Cluster Analysis identified 10 distinct shape clusters (Table 6.2) for which all 10 shape modes demonstrated a significantly different distribution ($p<0.001$). Significant differences in gender, BMI, HD, NSA, FO, $FO_{c,}$ and FA between the clusters were seen (Table 6.2). Similarly, CFI and CCR were significantly different between clusters. No significant differences with regard to patient age were observed.

Both medial and lateral (Figure 6.4) cortical flares demonstrated considerable differences between clusters. The derived least squares curve fits showed that the variation in flare was greater for the medial femoral cortex than for the lateral cortex. Least squares curve fit equation coeffficients for each cluster are reported in Appendix B.

Cluster	1	2	3	4	5	6	7	8	9	10	p-value
n (%)	35 (10)	39 (11)	41 (12)	19 (6)	49 (14)	61 (18)	21 (6)	38 (11)	14 (4)	28 (8)	---
Gender m:f	17:18	10:29	19:22	11:8	20:29	22:39	16:5	11:27	6:8	14:14	**0.011**
Age [years]	59	60	60	63	62	60	61	62	61	59	
SD	8.0	6.2	7.7	5.2	7.3	6.1	7.8	6.7	7.9	7.5	0.326
range	45-74	45-73	42-73	53-71	45-79	40-70	43-72	44-73	45-69	44-69	
BMI [kg/m^2]	25.9	27.0	25.7	27.6	26.9	27.6	26.0	28.7	26.2	26.6	
SD	7.0	4.8	3.6	4.9	3.4	4.3	3.5	5.1	6.2	6.9	**0.037**
range	21.3-32.7	19.4-42.2	19.5-36.3	19.2-36.3	20.8-35.7	19.4-44.6	20.3-34.0	19.5-41.1	19.7-42.6	20.3-56.5	
HD [mm]	50.1	46.2	47.6	49.7	47.3	46.8	50.6	46.9	47.1	48.0	
SD	4.36	3.97	4.18	5.10	4.50	4.04	3.97	4.36	4.89	5.04	**<0.001**
range	40.9-58.8	38.7-59.0	39.6-55.8	38.6-59.8	40.5-56.8	38.7-56.3	40.9-57.0	39.6-56.1	35.0-53.4	37.8-56.1	
NSA [degrees]	125	125	129	126	125	125	121	124	121	128	
SD	5.1	5.3	5.7	5.7	5.0	7.0	4.3	6.6	4.1	3.4	**<0.001**
range	113-137	114-135	117-147	116-138	113-141	111-149	114-128	112-141	115-128	122-136	
FO_h [mm]	47.7	44.6	42.1	44.8	45.4	41.6	51.3	44.1	45.4	39.7	
SD	5.9	6.3	7.3	6.1	5.6	6.9	5.8	6.9	6.4	4.6	**<0.001**
range	35.4-61.2	30.4-57.1	27.0-57.3	29.7-56.4	33.8-58.1	21.4-57.5	40.2-61.5	24.1-58.1	33.0-54.4	30.4-49.4	
FO_C [mm]	47.6	44.5	43.5	44.5	45.3	43.0	49.0	43.9	43.8	42.7	
SD	5.8	4.7	5.6	6.0	4.5	5.8	5.0	6.2	6.0	4.4	**<0.001**
range	38.5-66.2	35.2-56.7	33.5-54.0	35.4-56.0	38.6-61.0	30.9-61.2	40.3-60.0	26.9-60.3	33.9-53.5	34.8-51.1	
FA [degrees]	12	12	14	18	14	17	11	13	15	12	
SD	9.1	7.1	12.4	8.4	10.1	9.8	7.6	8.5	8.4	8.1	**0.049**
range	-2-33	0-26	-5-51	2-31	-5-36	-7-57	-4-33	-3-33	2-30	0.27	
CTI	0.60	0.59	0.57	0.55	0.61	0.59	0.60	0.58	0.56	0.57	
SD	0.037	0.036	0.034	0.041	0.037	0.033	0.035	0.027	0.070	0.030	**<0.001**
range	0.52-0.71	0.52-0.68	0.49-0.63	0.47-0.61	0.52-0.72	0.51-0.64	0.54-0.67	0.49-0.62	0.41-0.64	0.49-0.63	
CCR	0.43	0.47	0.45	0.46	0.46	0.45	0.44	0.47	0.47	0.43	
SD	0.039	0.031	0.037	0.032	0.047	0.042	0.043	0.043	0.083	0.034	**<0.001**
range	0.34-0.51	0.40-0.52	0.38-0.54	0.40-0.52	0.36-0.60	0.35-0.55	0.34-0.51	0.38-0.57	0.38-0.70	0.32-0.48	
CFI	4.33	3.87	3.92	3.67	4.13	3.96	4.13	3.76	3.77	4.04	
SD	0.516	0.380	0.332	0.319	0.430	0.381	0.457	0.283	0.593	0.360	**<0.001**
range	3.28-5.93	3.05-4.62	3.20-4.67	3.17-4.24	4.14-5.76	3.18-4.81	3.55-5.50	3.23-4.48	2.54-4.85	3.59-5.22	
CFI_{medial}	4.95	4.39	4.19	4.14	4.70	4.32	4.80	4.33	4.34	4.34	
SD	0.606	0.504	0.397	0.439	0.538	0.399	0.476	0.435	0.530	0.534	**<0.001**
range	3.92-6.32	3.27-5.41	3.36-5.19	3.48-4.89	3.44-6.69	3.02-5.20	3.90-5.89	3.24-5.44	3.15-5.37	3.45-5.78	
$CFI_{lateral}$	3.71	3.36	3.65	3.19	3.57	3.59	3.47	3.19	3.19	3.76	
SD	0.565	0.522	0.474	0.305	0.457	0.500	0.497	0.381	0.793	0.329	**<0.001**
range	2.57-5.55	2.02-4.41	3.04-5.13	2.47-3.59	2.64-4.84	2.75-4.75	2.78-5.12	2.39-4.15	1.94-5.15	3.24-4.66	

Table 6.2

Measurements of native femoral anatomy by cluster with standard deviation (SD) and range.

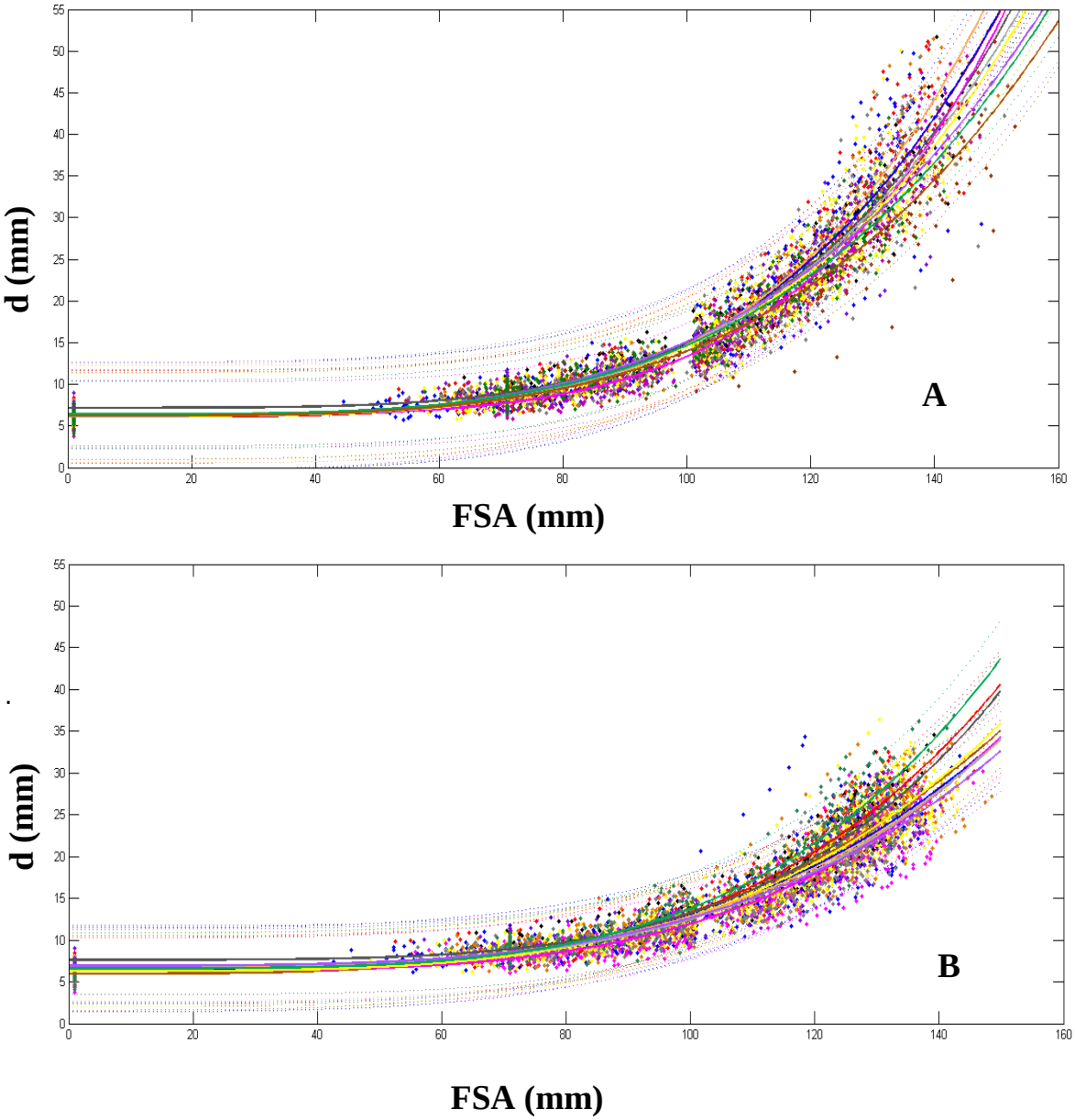


Figure 6.4

Scatter plot with least square fits for the endosteal flare of the medial (A) and lateral (B) femoral cortex. The femoral shaft axis (FSA) is aligned to the x-axis (y=0). The lesser trochanter is located at x=100 mm. The distance of points on the endosteal surface of the medial cortex with reference to the femoral shaft axis (d) is plotted on the y-axis (mm). Lines represent the least squares fit ($f(x) = ax^b+c$) with 95% confidence intervals.

6.4 Discussion

In cementless femoral reconstruction, the clinical outcome following THA is closely related to both femoral stem fit and the concomitant restoration of physiologic joint mechanics. A close geometric fit between the implant and the endosteal surface of the proximal femur[97,98] is essential to achieve primary stability and secondary osteointegration of the implant[25,26]. Previous studies have demonstrated that accurate metaphyseal stem fit reduces micro-motion at the implant-bone interface[97,100], and minimises stress-shielding[101,102]. An increased risk of aseptic loosening has been reported for undersized femoral components[105] and there is still is concern that progressive peri-prosthetic bone loss may compromise long-term stem performance[19]. As mentioned previously, there is substantial evidence that accurate restoration of femoral offset and soft tissue tension reduce risk for post-operative complications such as impingement, dislocation or wear failure[22,24,142,143]. Moreover, it is well accepted that the restoration of joint geometry provides patients with a better functional outcome in terms of improved abductor muscle strength[20,21] and greater range of motion[21,22,141].

The work presented in this chapter does not intend to emphasize absolute measurement values, its primary aim was to describe the variation in proximal femoral anatomy in patients with primary end-stage hip osteoarthritis. The native anatomy of the primary arthritic proximal femur in the present cohort is highly variable, which confirms previous findings of non-arthritic femora[39,40]. The greatest variation in the shape of the medullary canal occurred in the proximal femoral metaphysis, and specifically in the medial cortical flare. Males had significantly higher femoral offset than females. However, in contrast to previous studies[39,125], no difference in the distribution of NSA and FA and radiographic measures of cortical flare (CFI) between genders and with respect to age was detected

when looking at the entire patient cohort. This may be attributed to the strict exclusion criteria for all secondary forms of OA and the relatively homogeneous age of the cohort. As gender differences have been reported in other studies of non-arthritic femora[39], the present findings suggest that the native femoral anatomy of patients with primary OA may be different from those of healthy individuals[174].

Despite the overall variation and the lack of gender associated differences in the entire cohort, cluster analysis identified 10 shape clusters which were associated with significant differences in gender, BMI, geometric parameters (NSA, FO_h, FO_c, and FA), and measurements of canal shape (CFI, CCR, CTI). Interestingly, some clusters depicted expected configurations of shape and geometry while others did not. Cluster 7 was predominantly comprised of male patients with high FO, low NSA, low FA and a high flare of the medial cortex. In contrast, Cluster 10 depicted a typical configuration with low FO, high NSA and a low flare of the medial cortex. Interestingly, both males and females showed this configuration. A high FA was seen in Clusters 4 and 6, and patients demonstrated intermediate mean values for FO, NSA and medial and lateral cortical flare. A further interesting finding was that in cluster 7 the medial flare was high, but the lateral flare was quite low. The opposite configuration was seen in cluster 10. This indicates that it is important to consider the medial and lateral cortical flare separately, as the routinely used CFI for both the medial and lateral cortex does account for these variations and may be misleading.

The mean values for FO, NSA, FA and CFI in the present cohort compare well to reported values in the literature[39,40,175]. Similarly, the observed lack of correlation between measures of size (HD, height, BMI) and shape (mode scores) is consistent with previous findings[39].

The results of this chapter show that distinct patterns of femoral canal shape exist and that each pattern is associated with a specific set of geometric parameters, which highlights the association of shape and geometry seen in ASM.

This study has limitations: Firstly, the present study cohort was comprised of patients with primary end-stage hip OA. Care should be taken to apply the present findings to all patients who undergo THA, as the variation in patients with secondary forms of OA, such as dysplasia or other deformity, might be even greater. However, the present cohort can be considered as representative and findings should be put into perspective as the leading diagnosis for THA is primary OA[95].

Secondly, this work only assessed the shape of the proximal femur in the frontal plane and did not address the anterior-posterior bowing of the femur. However, pre-operative templating of implant size and position is performed on AP radiographs as the design of most femoral components aims for endosteal fit in the frontal plane. It has been previously shown that the present radiographic protocol for AP hip views allows accurate 2D assessment of proximal femoral geometry (Chapter 3) and shape (Chapter 5). Additionally, the accuracy of radiographic FO values compared to CT based FO values in the present cohort confirms this observation.

Lastly, the present study used active shape modelling (ASM) to assess the overall variation of the proximal femoral canal shape on AP hip radiographs. This method enables measurement of the variation in a complex shape, such as the hip. In ASM, a mode does not just capture one aspect of variation in femoral canal shape, it is a combination of evident and/or subtle differences between femurs[137]. It can, therefore, be difficult to visually describe what aspect of shape variation each mode represents. However, at the same time this method is powerful and able to detect differences that are not necessarily

evident with conventional radiographic measures (e.g. angles, distances or canal flare indices)[135]. Using ASM, the present work has contributed to a more subtle understanding of variation in proximal femoral geometry and shape anatomy in patients with primary hip OA.

Contemporary third generation implants are designed to closely approximate the functional anatomy of a normal hip joint. Besides material properties and manufacturing technology, the knowledge of variation in proximal femoral anatomy dictates the design of prosthetic components[120]. The issue of identifying the optimal femoral component has not yet been resolved, even with contemporary stem designs that have been introduced in order to account for anatomical variations in the proximal femur. The use of custom-made cementless stems[121] in primary OA is questionable due to higher costs and the need for CT. Off-the-shelf implants with multiple shape options and "short" stem designs have been recently introduced to account for individual patient anatomy[123,124], but long-term follow-up data for these novel components is not available. In addition, early failures of some designs have been reported[133,134]. Similarly, modular hip stems have gained growing popularity[123,125]. However, concerns have been raised that modularity increases the risk of fretting corrosion, concomitant metal ion release and early implant failure[126,127]. Moreover, previous studies have demonstrated that proximal loading cannot be entirely achieved with the use of current stem designs that aim for a proximal intertrochanteric fixation[176].

Therefore, the identification of distinct shape clusters is clinically relevant for the development of future femoral component designs that aim to account for optimal stem fit and concomitant reconstruction of individual hip anatomy.

The present study illustrates that Active Shape Modelling and subsequent cluster analysis have the potential to identify specific patterns of proximal femoral shape and geometry

despite the variability in proximal femoral anatomy. Understanding of variation and association of geometry and shape of the proximal femur is essential both for surgeons and for implant manufacturers in order to achieve the goals of accurate stem fit and restoration of individual joint mechanics.

In conclusion, the design of the femoral component should take into account both the variation in shape and its association with geometric parameters. The present findings highlight the great variability in native proximal femoral anatomy in patients with primary hip OA and consequently support the use of implant systems that enable independent adjustment of stem fit and reconstruction of joint geometry. The work of this chapter has identified 10 different types of femora in patients with primary OA, and the present data allow a comprehensive classification of variation in proximal femoral shape and geometry. This may improve future designs of femoral components that will optimise stem fit and simultaneously enable individual restoration of physiological biomechanics of the hip.

6.5 Summary

In uncemented total hip arthroplasty (THA), the optimal femoral component should allow both optimal endosteal fit with proximal load transfer and accurate restoration of individual joint biomechanics. This is often compromised due to a high variability in proximal femoral anatomy. The aim of the work presented in this chapter was to assess the variation in proximal femoral canal shape and its association with geometric and anthropometric parameters in primary hip OA.

The present study illustrates that active shape modelling and subsequent cluster analysis have the potential to identify specific patterns of shape and geometry of the proximal femur despite the variability in proximal femoral anatomy. Ten distinct patterns of proximal femoral canal shape in end-stage hip OA have been identified. The present findings allows a comprehensive classification of variation in proximal femoral shape and its association with joint geometry.

The present data has the potential to improve future designs of cementless femoral components that will optimise stem fit and simultaneously allow individual restoration of physiological biomechanics of the hip, regardless of individual anatomic variations.

7. CONCLUSIONS, CLINICAL RELEVANCE AND FUTURE WORK

7.1 Review of Objectives and Conclusions

The aims of the present work were (1) to improve pre-operative planning in THA and (2) to provide information for future femoral component design accounting for individual patient anatomy by quantifying the variation in proximal femoral canal shape and its association with geometric and anthropometric parameters in primary end-stage hip osteoarthritis.

A review of the literature (Chapter 2) demonstrated that the success of primary THA is dependent on stem fixation and the restoration of physiologic joint mechanics. Hence, accurate pre-operative assessment of proximal femoral canal shape and geometry is essential. It has been shown that pre-operative planning performed on AP pelvis radiographs has limited reliability which can be explained by a considerable variation in proximal femoral (patho-) anatomy of arthritic hips. Despite an increasing popularity of cementless femoral reconstruction and the development of novel short and modular stem designs, the current knowledge of the variation in proximal femoral geometry and canal shape in arthritic hips is very limited. Additionally the association between geometry and canal shape is poorly understood.

Chapter 3 assessed differences in femoral offset on corresponding AP ***pelvis*** radiographs, AP ***hip*** radiographs and CT scans in patients who actually underwent THA for primary end-stage hip osteoarthritis. Femoral offset (FO) was taken as a surrogate parameter to represent proximal femoral geometry. In the study cohort, FO was significantly underestimated on AP ***pelvis*** radiographs which confirmed previous findings. It was,

however, concluded that standardised AP ***hip*** radiographs allow better control of femoral rotation during radiography, reduce the projection effects of beam divergence and consequently are an accurate and reliable method to assess femoral offset, comparable to 3D measurements performed on CT data.

Chapter 4 confirmed the linear relationship between FO measurements made on corresponding modes of imaging as described in Chapter 3, and provided gender specific regression equations to predict 3D femoral offset from AP pelvis radiographs.

In Chapter 5, Active Shape Modelling (ASM) was used to determine differences in the radiographic appearance of the proximal femoral canal between AP hip and AP pelvis radiographs. In an analogous manner to Chapter 3, it was demonstrated that, in contrast to AP ***pelvis*** radiographs, standardised AP ***hip*** radiographs allow a more accurate and reliable assessment of the medial cortical flare of the proximal femur.

In Chapter 6, a second ASM study was developed to determine the variation and underlying patterns in proximal femoral anatomy in a cohort of 345 patients with primary OA. An association between endosteal canal shape and joint geometry was observed. Ten distinct shape patterns of the proximal femoral canal were identified in primary OA; each pattern was associated with a specific set of geometric parameters. The presented data allows a comprehensive classification of proximal femoral geometry and shape in patients with primary OA.

7.2 Clinical Relevance

The work presented in this thesis is informative and clinically relevant for both hip surgeons and developers of hip replacement implants in several ways:

- Orthopaedic surgeons need to be aware that the assessment of the proximal femoral geometry and canal shape may be misleading on AP ***pelvis*** radiographs. With regard to the rising popularity of cementless fixation, modularity and short stem designs, pre-operative templating becomes even more critical as small inaccuracies in the assessment of proximal femoral shape and geometry may compromise the goals of fixation, proximal load transfer and restoration of physiologic mechanics.
- Standardised AP ***hip*** radiographs are a practical, cost-effective and readily available method to accurately and reliably assess femoral offset and canal shape without the routine performance of CT. These findings have the potential to aid surgeons in the selection of an appropriate design, size and intra-operative positioning of femoral implants. Consequently, it is recommended to routinely obtain additional AP hip radiographs to improve pre-operative templating in THA.
- When AP ***hip*** radiographs are not available for templating, the provided gender specific regression equations have the potential to compensate for positioning inconsistencies and beam divergence on AP ***pelvis*** radiographs. Thus, the present findings support surgeons in pre-operative templating on AP ***pelvis*** radiographs without the routine performance of additional radiographs or CT.
- The present findings of the variation in proximal femoral anatomy have implications for cementless femoral component designs that aim to achieve optimal metaphyseal stem fit and concomitant restoration of individual patient anatomy. The observed variability in proximal femoral anatomy in patients with primary OA supports the use of implant systems that enable independent adjustment of fixation and reconstruction of individual joint geometry.

7.3 Strengths and Limitations

The present study cohort has to be critically examined to appraise the findings of this study. In order to exclusively assess patients with primary OA, rigid exclusion criteria for all secondary form of hip OA were applied. This justifies questioning the approach of creating such a homogeneous cohort which does not necessarily represent all patients in clinical practise. While the strict exclusion criteria for all secondary forms of OA contribute to the internal validity of this work, the exclusion of patients with secondary hip OA can be seen as a limitation as variables of geometry and shape are highly important and even more critical for this subgroup of patients. This objection is put into perspective when looking at the Swedish Hip Arthroplasty Register data from 2010, where Hailer et al.[95] reported primary OA as leading diagnosis for THA in 76% of all patients, followed by hip fracture in 13% of cases. Primary osteoarthritis is the commonest form of arthritis[68], and the distribution of gender and age in the study cohort further implies that the study cohort represents the typical patient undergoing primary THA. Finally, this study is based on substantial patient numbers (n=345) which further strengthens the quality and relevance of the described results.

The focus on primary OA, however, restricts the application of the present findings to patients with this diagnosis; this is a limitation of the present study. The presented results therefore allow no direct conclusions to be made concerning patients with more complex hip deformities due to secondary OA. In these patients, accurate radiographic measurements are particularly difficult and consequently CT scans are a reasonable option. As the present study cohort represents the natural variation in proximal femoral anatomy in primary end-stage osteoarthritis in Caucasian patients, care should be taken to apply the present findings to non-Caucasian patients.

If patients with secondary OA, or patients from other ethnical or geographic backgrounds had been included, one would assume that the variation of geometry and canal shape would have been even greater than that determined by the present work.

A second limitation to be discussed is that the present assessment of canal shape did not include the region of the greater trochanter in the ASM template. This information may be critical for novel, short stems designs that aim for isolated placement and fixation in the femoral neck and inter-trochanteric region. However, as the greater trochanteric region is extremely variable in shape, an inclusion might have added further and unnecessary complexity to the proposed classification of shape clusters.

Lastly, 3D CT data were used as gold standard when comparing differences in canal shape and proximal femoral geometry on corresponding AP hip and AP pelvis radiographs. The reported differences in femoral offset between radiographs and CT showed few subjects in whom FO was overestimated on radiographs outside the precision of the measurement. This can be attributed to inaccurate positioning of the patient and/or the calibration sphere, or inadequate elevation of the affected hip during radiography. An altered object-to-film distance might therefore be the cause of the observed overestimation of FO. Although a standardised positioning protocol was administered, the described method for obtaining the radiographs remains a potential source of bias as it depends on the judgment of the technician to compensate for the magnitude of femoral anteversion and external rotation contracture.

7.4 Future work

Considering the limitations described in section 7.3, the present work has raised relevant aspects that need further investigation. Future research into the variation in femoral and

acetabular anatomy including patients with secondary forms of OA and patients from other ethnic/geographic backgrounds is required. Sound understanding of the variation in patient anatomy and the association between canal shape and joint geometry of the arthritic hip is essential for both surgeons and implant developers in order to achieve the goal of accurate stem fit and restoration of individual anatomy. Moreover, it is essential to further improve pre-operative planning and to overcome present disadvantages of contemporary implant designs. In addition, evidence-based clinical studies investigating the association of stem fit, reconstruction of joint mechanics and clinical outcome following THA beyond implant survivorship are needed to justify the increasing use of novel implant designs.

On the basis of the present work, further research will be pivotal for the development of future implant designs that have the potential to minimise the occurrence of adverse clinical outcome and to improve implant survivorship, joint function and patient satisfaction following THA.

References

1. Charnley J. Arthroplasty of the hip. A new operation. *Lancet 1961;1-7187:1129-32.*
2. Amstutz HC. *Hip arthroplasty.* New York: Churchill Livingstone, 1991:xix, 1001 p.
3. Learmonth ID, Young C, Rorabeck C. The operation of the century: total hip replacement. *Lancet 2007;370-9597:1508-19.*
4. National Joint Registry. 2010.
5. Birrell F, Johnell O, Silman A. Projecting the need for hip replacement over the next three decades: influence of changing demography and threshold for surgery. *Ann Rheum Dis 1999;58-9:569-72.*
6. Kurtz S, Ong K, Lau E, Mowat F, Halpern M. Projections of primary and revision hip and knee arthroplasty in the United States from 2005 to 2030. *J Bone Joint Surg Am 2007;89-4:780-5.*
7. Anakwe RE, Jenkins PJ, Moran M. Predicting dissatisfaction after total hip arthroplasty: a study of 850 patients. *J Arthroplasty;26-2:209-13.*
8. Mahomed NN, Liang MH, Cook EF, Daltroy LH, Fortin PR, Fossel AH, Katz JN. The importance of patient expectations in predicting functional outcomes after total joint arthroplasty. *J Rheumatol 2002;29-6:1273-9.*
9. Gurney B, Mermier C, Robergs R, Gibson A, Rivero D. Effects of limb-length discrepancy on gait economy and lower-extremity muscle activity in older adults. *J Bone Joint Surg Am 2001;83-A-6:907-15.*
10. Nercessian OA, Piccoluga F, Eftekhar NS. Postoperative sciatic and femoral nerve palsy with reference to leg lengthening and medialization/lateralization of the hip joint following total hip arthroplasty. *Clin Orthop Relat Res 1994-304:165-71.*
11. Stone RG, Weeks LE, Hajdu M, Stinchfield FE. Evaluation of sciatic nerve compromise during total hip arthroplasty. *Clin Orthop Relat Res 1985-201:26-31.*
12. Friberg O. Clinical symptoms and biomechanics of lumbar spine and hip joint in leg length inequality. *Spine 1983;8-6:643-51.*
13. Aldinger PR, Jung AW, Pritsch M, Breusch SJ, Thomsen m, Ewerbeck V, Parsch D. Fifteen to Twenty year Results of Uncemented Gritblasted Straight Tapered Titanium Stems in Patients Younger than 55 Years of Age. *J Bone Joint Surg Am (accepted) 2009.*
14. McLaughlin JR, Lee KR. Total hip arthroplasty in young patients. 8- to 13-year results using an uncemented stem. *Clin Orthop Relat Res 2000-373:153-63.*
15. Parsch D, Jung AW, Thomsen M, Ewerbeck V, Aldinger PR. Good survival of uncemented tapered stems for failed intertrochanteric osteotomy: a mean 16 year follow-up study in 45 patients. *Arch Orthop Trauma Surg 2008;128-10:1081-5.*
16. Callaghan JJ, Forest EE, Sporer SM, Goetz DD, Johnston RC. Total hip arthroplasty in the young adult. *Clin Orthop Relat Res 1997-344:257-62.*
17. Pollard TC, Baker RP, Eastaugh-Waring SJ, Bannister GC. Treatment of the young active patient with osteoarthritis of the hip. A five- to seven-year comparison of hybrid total hip arthroplasty and metal-on-metal resurfacing. *J Bone Joint Surg Br 2006;88-5:592-600.*
18. Achten J, Parsons NR, Edlin RP, Griffin DR, Costa ML. A randomised controlled trial of total hip arthroplasty versus resurfacing arthroplasty in the treatment of young patients with arthritis of the hip joint. *BMC Musculoskelet Disord 2010;11:8.*
19. Engh CA, Jr., Young AM, Engh CA, Sr., Hopper RH, Jr. Clinical consequences of stress shielding after porous-coated total hip arthroplasty. *Clin Orthop Relat Res 2003-417:157-63.*

20. Asayama I, Chamnongkich S, Simpson KJ, Kinsey TL, Mahoney OM. Reconstructed hip joint position and abductor muscle strength after total hip arthroplasty. *J Arthroplasty 2005;20-4:414-20.*
21. McGrory BJ, Morrey BF, Cahalan TD, An KN, Cabanela ME. Effect of femoral offset on range of motion and abductor muscle strength after total hip arthroplasty. *J Bone Joint Surg Br 1995;77-6:865-9.*
22. Charles MN, Bourne RB, Davey JR, Greenwald AS, Morrey BF, Rorabeck CH. Soft-tissue balancing of the hip: the role of femoral offset restoration. *Instr Course Lect 2005;54:131-41.*
23. Little NJ, Busch CA, Gallagher JA, Rorabeck CH, Bourne RB. Acetabular polyethylene wear and acetabular inclination and femoral offset. *Clin Orthop Relat Res 2009;467-11:2895-900.*
24. Sakalkale DP, Sharkey PF, Eng K, Hozack WJ, Rothman RH. Effect of femoral component offset on polyethylene wear in total hip arthroplasty. *Clin Orthop Relat Res 2001-388:125-34.*
25. Cameron HU, Pilliar RM, MacNab I. The effect of movement on the bonding of porous metal to bone. *J Biomed Mater Res 1973;7-4:301-11.*
26. Haddad RJ, Jr., Cook SD, Thomas KA. Biological fixation of porous-coated implants. *J Bone Joint Surg Am 1987;69-9:1459-66.*
27. Husmann O, Rubin PJ, Leyvraz PF, de Roguin B, Argenson JN. Three-dimensional morphology of the proximal femur. *J Arthroplasty 1997;12-4:444-50.*
28. Nakahara I, Takao M, Sakai T, Nishii T, Yoshikawa H, Sugano N. Gender differences in 3D morphology and bony impingement of human hips. *J Orthop Res 2010.*
29. Sariali E, Mouttet A, Pasquier G, Durante E. Three-dimensional hip anatomy in osteoarthritis. Analysis of the femoral offset. *J Arthroplasty 2009;24-6:990-7.*
30. Della Valle AG, Padgett DE, Salvati EA. Preoperative planning for primary total hip arthroplasty. *J Am Acad Orthop Surg 2005;13-7:455-62.*
31. Gamble P, de Beer J, Petruccelli D, Winemaker M. The accuracy of digital templating in uncemented total hip arthroplasty. *J Arthroplasty 2010;25-4:529-32.*
32. Meermans G, Malik A, Witt J, Haddad F. Preoperative Radiographic Assessment of Limb-length Discrepancy in Total Hip Arthroplasty. *Clin Orthop Relat Res 2010.*
33. Sariali E, Mouttet A, Pasquier G, Durante E, Catone Y. Accuracy of reconstruction of the hip using computerised three-dimensional pre-operative planning and a cementless modular neck. *J Bone Joint Surg Br 2009;91-3:333-40.*
34. Sugano N, Ohzono K, Nishii T, Haraguchi K, Sakai T, Ochi T. Computed-tomography-based computer preoperative planning for total hip arthroplasty. *Comput Aided Surg 1998;3-6:320-4.*
35. Rubin PJ, Leyvraz PF, Aubaniac JM, Argenson JN, Esteve P, de Roguin B. The morphology of the proximal femur. A three-dimensional radiographic analysis. *J Bone Joint Surg Br 1992;74-1:28-32.*
36. Eckrich SG, Noble PC, Tullos HS. Effect of rotation on the radiographic appearance of the femoral canal. *J Arthroplasty 1994;9-4:419-26.*
37. Lee YS, Oh SH, Seon JK, Song EK, Yoon TR. 3D femoral neck anteversion measurements based on the posterior femoral plane in ORTHODOC system. *Med Biol Eng Comput 2006;44-10:895-906.*
38. Pasquier G, Ducharne G, Ali ES, Giraud F, Mouttet A, Durante E. Total hip arthroplasty offset measurement: is C T scan the most accurate option? *Orthop Traumatol Surg Res 2010;96-4:367-75.*

39. Noble PC, Alexander JW, Lindahl LJ, Yew DT, Granberry WM, Tullos HS. The anatomic basis of femoral component design. *Clin Orthop Relat Res 1988-235:148-65.*
40. Maruyama M, Feinberg JR, Capello WN, D'Antonio JA. The Frank Stinchfield Award: Morphologic features of the acetabulum and femur: anteversion angle and implant positioning. *Clin Orthop Relat Res 2001-393:52-65.*
41. Dorr LD, Faugere MC, Mackel AM, Gruen TA, Bognar B, Malluche HH. Structural and cellular assessment of bone quality of proximal femur. *Bone 1993;14-3:231-42.*
42. Noble PC, Box GG, Kamaric E, Fink MJ, Alexander JW, Tullos HS. The effect of aging on the shape of the proximal femur. *Clin Orthop Relat Res 1995-316:31-44.*
43. Wang SC, Brede C, Lange D, Poster CS, Lange AW, Kohoyda-Inglis C, Sochor MR, Ipaktchi K, Rowe SA, Patel S, Garton HJ. Gender differences in hip anatomy: possible implications for injury tolerance in frontal collisions. *Annu Proc Assoc Adv Automot Med 2004;48:287-301.*
44. Sariali E, Mouttet A, Pasquier G, Durante E. Three-Dimensional Hip Anatomy in Osteoarthritis Analysis of the Femoral Offset. *J Arthroplasty 2008.*
45. Sugano N, Noble PC, Kamaric E, Salama JK, Ochi T, Tullos HS. The morphology of the femur in developmental dysplasia of the hip. *J Bone Joint Surg Br 1998;80-4:711-9.*
46. Buckwalter JA, Saltzman C, Brown T. The impact of osteoarthritis: implications for research. *Clin Orthop Relat Res 2004-427 Suppl:S6-15.*
47. Benedek TG, Rodnan GP. A brief history of the rheumatic diseases. *Bull Rheum Dis 1982;32-6:59-68.*
48. Mankin HJB, K.D.; Shulman, L.E. Workshop on etiopathogenesis of osteoarthritis. *The Journal of Rheumatology 1986;13:1127-60.*
49. Altman R, Alarcon G, Appelrouth D, Bloch D, Borenstein D, Brandt K, Brown C, Cooke TD, Daniel W, Feldman D, et al. The American College of Rheumatology criteria for the classification and reporting of osteoarthritis of the hip. *Arthritis Rheum 1991;34-5:505-14.*
50. Murray RO. The aetiology of primary osteoarthritis of the hip. *Br J Radiol 1965;38-455:810-24.*
51. Ganz R, Leunig M, Leunig-Ganz K, Harris WH. The etiology of osteoarthritis of the hip: an integrated mechanical concept. *Clin Orthop Relat Res 2008;466-2:264-72.*
52. Harris WH. Etiology of osteoarthritis of the hip. *Clin Orthop Relat Res 1986-213:20-33.*
53. Solomon L. Patterns of osteoarthritis of the hip. *J Bone Joint Surg Br 1976;58-2:176-83.*
54. Leunig M, Beaule PE, Ganz R. The concept of femoroacetabular impingement: current status and future perspectives. *Clin Orthop Relat Res 2009;467-3:616-22.*
55. Aspden RM. Osteoarthritis: a problem of growth not decay? *Rheumatology (Oxford) 2008;47-10:1452-60.*
56. Aspden RM. Obesity punches above its weight in osteoarthritis. *Nat Rev Rheumatol 2010.*
57. Chitnavis J, Sinsheimer JS, Clipsham K, Loughlin J, Sykes B, Burge PD, Carr AJ. Genetic influences in end-stage osteoarthritis. Sibling risks of hip and knee replacement for idiopathic osteoarthritis. *J Bone Joint Surg Br 1997;79-4:660-4.*
58. Loughlin J, Mustafa Z, Smith A, Irven C, Carr AJ, Clipsham K, Chitnavis J, Bloomfield VA, McCartney M, Cox O, Sinsheimer JS, Sykes B, Chapman KE. Linkage analysis of chromosome 2q in osteoarthritis. *Rheumatology (Oxford) 2000;39-4:377-81.*

59. Mustafa Z, Chapman K, Irven C, Carr AJ, Clipsham K, Chitnavis J, Sinsheimer JS, Bloomfield VA, McCartney M, Cox O, Sykes B, Loughlin J. Linkage analysis of candidate genes as susceptibility loci for osteoarthritis-suggestive linkage of COL9A1 to female hip osteoarthritis. *Rheumatology (Oxford) 2000;39-3:299-306.*

60. Valdes AM, Arden NK, Tamm A, Kisand K, Doherty S, Pola E, Cooper C, Muir KR, Kerna I, Hart D, O'Neil F, Zhang W, Spector TD, Maciewicz RA, Doherty M. A meta-analysis of interleukin-6 promoter polymorphisms on risk of hip and knee osteoarthritis. *Osteoarthritis Cartilage 2010;18-5:699-704.*

61. Riancho JA, Garcia-Ibarbia C, Gravani A, Raine EV, Rodriguez-Fontenla C, Soto-Hermida A, Rego-Perez I, Dodd AW, Gomez-Reino JJ, Zarrabeitia MT, Garces CM, Carr A, Blanco F, Gonzalez A, Loughlin J. Common variations in estrogen-related genes are associated with severe large-joint osteoarthritis: a multicenter genetic and functional study. *Osteoarthritis Cartilage 2010;18-7:927-33.*

62. van der Kraan PM, van den Berg WB. Osteoarthritis in the context of ageing and evolution. Loss of chondrocyte differentiation block during ageing. *Ageing Res Rev 2008;7-2:106-13.*

63. Chitnavis JP. The Genetic Epidemiology of Severe Symptomatic Osteoarthritis of the Hip and Knee. Thesis. Vol. Master of Surgery: University of Cambridge, 2000.

64. Brandt KD, Radin EL, Dieppe PA, van de Putte L. Yet more evidence that osteoarthritis is not a cartilage disease. *Ann Rheum Dis 2006;65-10:1261-4.*

65. Buckwalter JA, Mankin HJ. Articular cartilage: degeneration and osteoarthritis, repair, regeneration, and transplantation. *Instr Course Lect 1998;47:487-504.*

66. Ghosh P, Smith M. Osteoarthritis, genetic and molecular mechanisms. *Biogerontology 2002;3-1-2:85-8.*

67. Altman RD. Classification of disease: osteoarthritis. *Semin Arthritis Rheum 1991;20-6 Suppl 2:40-7.*

68. Lawrence RC, Felson DT, Helmick CG, Arnold LM, Choi H, Deyo RA, Gabriel S, Hirsch R, Hochberg MC, Hunder GG, Jordan JM, Katz JN, Kremers HM, Wolfe F. Estimates of the prevalence of arthritis and other rheumatic conditions in the United States. Part II. *Arthritis Rheum 2008;58-1:26-35.*

69. Bremner JM, Lawrence JS, Miall WE. Degenerative joint disease in a Jamaican rural population. *Ann Rheum Dis 1968;27-4:326-32.*

70. Lau EM, Lin F, Lam D, Silman A, Croft P. Hip osteoarthritis and dysplasia in Chinese men. *Ann Rheum Dis 1995;54-12:965-9.*

71. Lawrence JS, Bremner JM, Bier F. Osteo-arthrosis. Prevalence in the population and relationship between symptoms and x-ray changes. *Ann Rheum Dis 1966;25-1:1-24.*

72. Solomon L, Beighton P, Lawrence JS. Osteoarthrosis in a rural South African Negro population. *Ann Rheum Dis 1976;35-3:274-8.*

73. Scott D. Osteoarthritis of the hip. *Clin Evid (Online) 2006;2006.*

74. Scott D, Kowalczyk A. Osteoarthritis of the knee. *Clin Evid (Online) 2007;2007.*

75. Lawrence RC, Helmick CG, Arnett FC, Deyo RA, Felson DT, Giannini EH, Heyse SP, Hirsch R, Hochberg MC, Hunder GG, Liang MH, Pillemer SR, Steen VD, Wolfe F. Estimates of the prevalence of arthritis and selected musculoskeletal disorders in the United States. *Arthritis Rheum 1998;41-5:778-99.*

76. Jordan JM, Helmick CG, Renner JB, Luta G, Dragomir AD, Woodard J, Fang F, Schwartz TA, Nelson AE, Abbate LM, Callahan LF, Kalsbeek WD, Hochberg MC. Prevalence of hip symptoms and radiographic and symptomatic hip osteoarthritis in African Americans and Caucasians: the Johnston County Osteoarthritis Project. *J Rheumatol 2009;36-4:809-15.*

77. Merx H, Dreinhofer KE, Gunther KP. [Socioeconomic relevance of osteoarthritis in Germany]. *Z Orthop Unfall 2007;145-4:421-9.*
78. Leardini G, Salaffi F, Caporali R, Canesi B, Rovati L, Montanelli R. Direct and indirect costs of osteoarthritis of the knee. *Clin Exp Rheumatol 2004;22-6:699-706.*
79. Yelin E, Murphy L, Cisternas MG, Foreman AJ, Pasta DJ, Helmick CG. Medical care expenditures and earnings losses among persons with arthritis and other rheumatic conditions in 2003, and comparisons with 1997. *Arthritis Rheum 2007;56-5:1397-407.*
80. Kotlarz H, Gunnarsson CL, Fang H, Rizzo JA. Insurer and out-of-pocket costs of osteoarthritis in the US: evidence from national survey data. *Arthritis Rheum 2009;60-12:3546-53.*
81. Fautrel B, Hilliquin P, Rozenberg S, Allaert FA, Coste P, Leclerc A, Rossignol M. Impact of osteoarthritis: results of a nationwide survey of 10,000 patients consulting for OA. *Joint Bone Spine 2005;72-3:235-40.*
82. van Dijk GM, Veenhof C, Lankhorst GJ, Dekker J. Limitations in activities in patients with osteoarthritis of the hip or knee: the relationship with body functions, comorbidity and cognitive functioning. *Disabil Rehabil 2009;31-20:1685-91.*
83. Ethgen O, Bruyere O, Richy F, Dardennes C, Reginster JY. Health-related quality of life in total hip and total knee arthroplasty. A qualitative and systematic review of the literature. *J Bone Joint Surg Am 2004;86-A-5:963-74.*
84. Thompson FR. An essay on the development of arthroplasty of the hip. *Clin Orthop Relat Res 1966;44:73-82.*
85. Charnley J. Surgery of the hip-joint: present and future developments. *Br Med J 1960;1-5176:821-6.*
86. Judet R, Siguier M, Brumpt B, Judet T. A noncemented total hip prosthesis. *Clin Orthop Relat Res 1978-137:76-84.*
87. Steinberg ME, ed. *The Hip and Its Disorders.* WB Saunders Company Ltd, 1991.
88. BVMed Bundesverband Medizintechnologie e. V., 2007.
89. Statistisches Jahrbuch 2010. *2010.*
90. Generationensterbetafeln für Deutschland, Modellrechnungen für die Geburtsjahrgänge von 1871 - 2004. *Statistisches Bundesamt 2006.*
91. Callaghan JJ, Templeton JE, Liu SS, Pedersen DR, Goetz DD, Sullivan PM, Johnston RC. Results of Charnley total hip arthroplasty at a minimum of thirty years. A concise follow-up of a previous report. *J Bone Joint Surg Am 2004;86-A-4:690-5.*
92. Kurtz S, Mowat F, Ong K, Chan N, Lau E, Halpern M. Prevalence of primary and revision total hip and knee arthroplasty in the United States from 1990 through 2002. *J Bone Joint Surg Am 2005;87-7:1487-97.*
93. Malchau H, Herberts P, Eisler T, Garellick G, Soderman P. The Swedish Total Hip Replacement Register. *J Bone Joint Surg Am 2002;84-A Suppl 2:2-20.*
94. Morshed S, Bozic KJ, Ries MD, Malchau H, Colford JM, Jr. Comparison of cemented and uncemented fixation in total hip replacement: a meta-analysis. *Acta Orthop 2007;78-3:315-26.*
95. Hailer NP, Garellick G, Karrholm J. Uncemented and cemented primary total hip arthroplasty in the Swedish Hip Arthroplasty Register. *Acta Orthop 2010;81-1:34-41.*
96. Merle C, Clarius M, Aldinger PR. [Long-term results of uncemented stems in total hip arthroplasty: analysis of survival rates with a minimum 15-year follow-up]. *Orthopade 2010;39-1:80-6.*
97. Callaghan JJ, Fulghum CS, Glisson RR, Stranne SK. The effect of femoral stem geometry on interface motion in uncemented porous-coated total hip prostheses.

Comparison of straight-stem and curved-stem designs. *J Bone Joint Surg Am 1992;74-6:839-48.*
98. Burke DW, O'Connor DO, Zalenski EB, Jasty M, Harris WH. Micromotion of cemented and uncemented femoral components. *J Bone Joint Surg Br 1991;73-1:33-7.*
99. Zweymuller KA, Lintner FK, Semlitsch MF. Biologic fixation of a press-fit titanium hip joint endoprosthesis. *Clin Orthop Relat Res 1988-235:195-206.*
100. Pilliar RM, Lee JM, Maniatopoulos C. Observations on the effect of movement on bone ingrowth into porous-surfaced implants. *Clin Orthop Relat Res 1986-208:108-13.*
101. Decking R, Puhl W, Simon U, Claes LE. Changes in strain distribution of loaded proximal femora caused by different types of cementless femoral stems. *Clin Biomech (Bristol, Avon) 2006;21-5:495-501.*
102. Weinans H, Huiskes R, Grootenboer HJ. Effects of fit and bonding characteristics of femoral stems on adaptive bone remodeling. *J Biomech Eng 1994;116-4:393-400.*
103. Aldinger PR, Jung AW, Breusch SJ, Ewerbeck V, Parsch D. Survival of the cementless Spotorno stem in the second decade. *Clin Orthop Relat Res 2009;467-9:2297-304.*
104. Merle C, Streit MR, Volz C, Pritsch M, Gotterbarm T, Aldinger PR. Bone remodeling around stable uncemented titanium stems during the second decade after total hip arthroplasty: a DXA study at 12 and 17 years. *Osteoporos Int 2010.*
105. Aldinger PR, Jung AW, Pritsch M, Breusch S, Thomsen M, Ewerbeck V, Parsch D. Uncemented grit-blasted straight tapered titanium stems in patients younger than fifty-five years of age. Fifteen to twenty-year results. *J Bone Joint Surg Am 2009;91-6:1432-9.*
106. Kurtz SM, Lau E, Ong K, Zhao K, Kelly M, Bozic KJ. Future young patient demand for primary and revision joint replacement: national projections from 2010 to 2030. *Clin Orthop Relat Res 2009;467-10:2606-12.*
107. Bowman KF, Jr., Fox J, Sekiya JK. A clinically relevant review of hip biomechanics. *Arthroscopy;26-8:1118-29.*
108. Bergmann G, Graichen F, Rohlmann A. Hip joint loading during walking and running, measured in two patients. *J Biomech 1993;26-8:969-90.*
109. Bergmann G, Graichen F, Rohlmann A. Hip joint contact forces during stumbling. *Langenbecks Arch Surg 2004;389-1:53-9.*
110. Lim LA, Carmichael SW, Cabanela ME. Biomechanics of total hip arthroplasty. *Anat Rec 1999;257-3:110-6.*
111. Lecerf G, Fessy MH, Philippot R, Massin P, Giraud F, Flecher X, Girard J, Mertl P, Marchetti E, Stindel E. Femoral offset: Anatomical concept, definition, assessment, implications for preoperative templating and hip arthroplasty. *Orthop Traumatol Surg Res 2009.*
112. D'Lima DD, Urquhart AG, Buehler KO, Walker RH, Colwell CW, Jr. The effect of the orientation of the acetabular and femoral components on the range of motion of the hip at different head-neck ratios. *J Bone Joint Surg Am 2000;82-3:315-21.*
113. Yoshimine F, Ginbayashi K. A mathematical formula to calculate the theoretical range of motion for total hip replacement. *J Biomech 2002;35-7:989-93.*
114. Kurtz WB, Ecker TM, Reichmann WM, Murphy SB. Factors affecting bony impingement in hip arthroplasty. *J Arthroplasty 2010;25-4:624-34 e1-2.*
115. Sendtner E, Tibor S, Winkler R, Worner M, Grifka J, Renkawitz T. Stem torsion in total hip replacement. *Acta Orthop 2010;81-5:579-82.*
116. Devane PA, Horne JG. Assessment of polyethylene wear in total hip replacement. *Clin Orthop Relat Res 1999-369:59-72.*

117. Little NJ, Busch CA, Gallagher JA, Rorabeck CH, Bourne RB. Acetabular Polyethylene Wear and Acetabular Inclination and Femoral Offset. *Clin Orthop Relat Res 2009.*

118. Tönnis D. Congenital dysplasia and dislocation of the hip in children and adults. *Springer Verlag 1987:167.*

119. Clohisy JC, Carlisle JC, Trousdale R, Kim YJ, Beaule PE, Morgan P, Steger-May K, Schoenecker PL, Millis M. Radiographic evaluation of the hip has limited reliability. *Clin Orthop Relat Res 2009;467-3:666-75.*

120. Siopack JS, Jergesen HE. Total hip arthroplasty. *West J Med 1995;162-3:243-9.*

121. Aldinger G, De Pellegrin M, Kusswetter W. The personalized hip prosthesis. *Ital J Orthop Traumatol 1988;14-4:429-33.*

122. Akbar M, Aldinger G, Krahmer K, Bruckner T, Aldinger PR. Custom stems for femoral deformity in patients less than 40 years of age: 70 hips followed for an average of 14 years. *Acta Orthop 2009;80-4:420-5.*

123. Omlor GW, Ullrich H, Krahmer K, Jung A, Aldinger G, Aldinger P. A stature-specific concept for uncemented, primary total hip arthroplasty. *Acta Orthop 2010;81-1:126-33.*

124. Yerasimides JG. Use of the Fitmore(R) hip stem bone-preserving system for the minimally invasive anterior-supine approach in hip replacement. *Am J Orthop (Belle Mead NJ) 2010;39-10 Suppl:13-6.*

125. Traina F, De Clerico M, Biondi F, Pilla F, Tassinari E, Toni A. Sex differences in hip morphology: is stem modularity effective for total hip replacement? *J Bone Joint Surg Am 2009;91 Suppl 6:121-8.*

126. Wright G, Sporer S, Urban R, Jacobs J. Fracture of a modular femoral neck after total hip arthroplasty: a case report. *J Bone Joint Surg Am 2010;92-6:1518-21.*

127. Wilson DA, Dunbar MJ, Amirault JD, Farhat Z. Early failure of a modular femoral neck total hip arthroplasty component: a case report. *J Bone Joint Surg Am 2010;92-6:1514-7.*

128. Berry DJ, Berger RA, Callaghan JJ, Dorr LD, Duwelius PJ, Hartzband MA, Lieberman JR, Mears DC. Minimally invasive total hip arthroplasty. Development, early results, and a critical analysis. Presented at the Annual Meeting of the American Orthopaedic Association, Charleston, South Carolina, USA, June 14, 2003. *J Bone Joint Surg Am 2003;85-A-11:2235-46.*

129. Rohrl SM, Li MG, Pedersen E, Ullmark G, Nivbrant B. Migration pattern of a short femoral neck preserving stem. *Clin Orthop Relat Res 2006;448:73-8.*

130. Kim YH, Kim JS, Joo JH, Park JW. A Prospective Short-Term Outcome Study of a Short Metaphyseal Fitting Total Hip Arthroplasty. *J Arthroplasty.*

131. Lombardi AV, Jr., Berend KR, Adams JB. A short stem solution: through small portals. *Orthopedics 2009;32-9.*

132. Goebel D, Schultz W. The Mayo cementless femoral component in active patients with osteoarthritis. *Hip Int 2009;19-2:206-10.*

133. Ishaque BA, Sturz H, Basad E. Fatigue fracture of a short stem hip replacement: a failure analysis with electron microscopy and review of the literature. *J Arthroplasty;26-4:665 e17-20.*

134. Ishaque BA, Donle E, Gils J, Wienbeck S, Basad E, Sturz H. [Eight-year results of the femoral neck prosthesis ESKA-CUT]. *Z Orthop Unfall 2009;147-2:158-65.*

135. Cootes TF, Taylor CJ, Cooper DH, Graham J. Active Shape Models - Their Training and Application. *Computer Vision and Image Understanding 1995;61-1:38-59.*

136. Cootes TF, Hill A, Taylor CJ. Medical image interpretation using active shape models: Recent advances. *Information Processing in Medical Imaging 1995;3:371-2 408.*

137. Waarsing JH, Rozendaal RM, Verhaar JA, Bierma-Zeinstra SM, Weinans H. A statistical model of shape and density of the proximal femur in relation to radiological and clinical OA of the hip. *Osteoarthritis Cartilage 2010;18-6:787-94.*

138. Gregory JS, Waarsing JH, Day J, Pols HA, Reijman M, Weinans H, Aspden RM. Early identification of radiographic osteoarthritis of the hip using an active shape model to quantify changes in bone morphometric features: can hip shape tell us anything about the progression of osteoarthritis? *Arthritis Rheum 2007;56-11:3634-43.*

139. Gregory JS, Testi D, Stewart A, Undrill PE, Reid DM, Aspden RM. A method for assessment of the shape of the proximal femur and its relationship to osteoporotic hip fracture. *Osteoporos Int 2004;15-1:5-11.*

140. Matsushita A, Nakashima Y, Jingushi S, Yamamoto T, Kuraoka A, Iwamoto Y. Effects of the femoral offset and the head size on the safe range of motion in total hip arthroplasty. *J Arthroplasty 2009;24-4:646-51.*

141. Sakai T, Sugano N, Ohzono K, Nishii T, Haraguchi K, Yoshikawa H. Femoral anteversion, femoral offset, and abductor lever arm after total hip arthroplasty using a modular femoral neck system. *J Orthop Sci 2002;7-1:62-7.*

142. Lecerf G, Fessy MH, Philippot R, Massin P, Giraud F, Flecher X, Girard J, Mertl P, Marchetti E, Stindel E. Femoral offset: anatomical concept, definition, assessment, implications for preoperative templating and hip arthroplasty. *Orthop Traumatol Surg Res 2009;95-3:210-9.*

143. Patel AB, Wagle RR, Usrey MM, Thompson MT, Incavo SJ, Noble PC. Guidelines for implant placement to minimize impingement during activities of daily living after total hip arthroplasty. *J Arthroplasty 2010;25-8:1275-81 e1.*

144. Nicholls AS, Kiran A, Pollard TC, Hart D, Arden CP, Spector T, Gill HS, Murray DW, Carr AJ, Arden NK. The association between hip morphology parameters and 19-year risk of end-stage osteoarthritis in the hip: A nested case-control study. *Arthritis Rheum 2011.*

145. Billing L. Roentgen examination of the proximal femur end in children and adolescents; a standardized technique also suitable for determination of the collum-, anteversion-, and epiphyseal angles; a study of slipped epiphysis and coxa plana. *Acta Radiol Suppl 1954;110:1-80.*

146. Murphy SB, Simon SR, Kijewski PK, Wilkinson RH, Griscom NT. Femoral anteversion. *J Bone Joint Surg Am 1987;69-8:1169-76.*

147. Sugano N, Noble PC, Kamaric E. A comparison of alternative methods of measuring femoral anteversion. *J Comput Assist Tomogr 1998;22-4:610-4.*

148. Bland JM, Altman DG. Statistical methods for assessing agreement between two methods of clinical measurement. *Lancet 1986;1-8476:307-10.*

149. Fackler CD, Poss R. Dislocation in total hip arthroplasties. *Clin Orthop Relat Res 1980-151:169-78.*

150. Malik A, Maheshwari A, Dorr LD. Impingement with total hip replacement. *J Bone Joint Surg Am 2007;89-8:1832-42.*

151. Clohisy JC, Carlisle JC, Beaule PE, Kim YJ, Trousdale RT, Sierra RJ, Leunig M, Schoenecker PL, Millis MB. A systematic approach to the plain radiographic evaluation of the young adult hip. *J Bone Joint Surg Am 2008;90 Suppl 4:47-66.*

152. Yoshioka Y, Siu D, Cooke TD. The anatomy and functional axes of the femur. *J Bone Joint Surg Am 1987;69-6:873-80.*

153. Unnanuntana A, Toogood P, Hart D, Cooperman D, Grant RE. Evaluation of proximal femoral geometry using digital photographs. *J Orthop Res 2010;28-11:1399-404.*
154. Atkinson HD, Johal KS, Willis-Owen C, Zadow S, Oakeshott RD. Differences in hip morphology between the sexes in patients undergoing hip resurfacing. *J Orthop Surg Res 2010;5:76.*
155. Wiberg G. Studies on dysplastic acetabula and congenital subluxation of the hip joint. *Acta Chir Scand 1939;58:5–135.*
156. Sharp IK. Acetabular dysplasia. The acetabular angle. *J Bone Joint Surg Br 1961;43:268-72.*
157. Murphy SB, Ganz R, Muller ME. The prognosis in untreated dysplasia of the hip. A study of radiographic factors that predict the outcome. *J Bone Joint Surg Am 1995;77-7:985-9.*
158. Steinberg EL, Shasha N, Menahem A, Dekel S. Preoperative planning of total hip replacement using the TraumaCad system. *Arch Orthop Trauma Surg 2010;130-12:1429-32.*
159. Altman DG. Practical Statistics for Medical Research. *Chapman and Hall, London 1991.*
160. Belmont PJ, Jr., Powers CC, Beykirch SE, Hopper RH, Jr., Engh CA, Jr., Engh CA. Results of the anatomic medullary locking total hip arthroplasty at a minimum of twenty years. A concise follow-up of previous reports. *J Bone Joint Surg Am 2008;90-7:1524-30.*
161. McLaughlin JR, Lee KR. Total hip arthroplasty with an uncemented tapered femoral component in patients younger than 50 years. *J Arthroplasty 2011;26-1:9-15.*
162. Suckel A, Geiger F, Kinzl L, Wulker N, Garbrecht M. Long-term results for the uncemented Zweymuller/Alloclassic hip endoprosthesis. A 15-year minimum follow-up of 320 hip operations. *J Arthroplasty 2009;24-6:846-53.*
163. Whiteside LA. The effect of stem fit on bone hypertrophy and pain relief in cementless total hip arthroplasty. *Clin Orthop Relat Res 1989-247:138-47.*
164. Chung CY, Lee KM, Park MS, Lee SH, Choi IH, Cho TJ. Validity and reliability of measuring femoral anteversion and neck-shaft angle in patients with cerebral palsy. *J Bone Joint Surg Am 2010;92-5:1195-205.*
165. Berry DJ. Epidemiology: hip and knee. *Orthop Clin North Am 1999;30-2:183-90.*
166. Lindahl H. Epidemiology of periprosthetic femur fracture around a total hip arthroplasty. *Injury 2007;38-6:651-4.*
167. Cootes TF, Taylor CJ. Anatomical statistical models and their role in feature extraction. *Br J Radiol 2004;77 Spec No 2:S133-9.*
168. Steinbach M, Tan P-N, Kumar V. *Introduction to data mining.* Harlow: Addison-Wesley, 2005:700 p.
169. Kaufman L, Rousseeuw PJ. *Finding groups in data : an introduction to cluster analysis.* Hoboken, N.J.: Wiley-Interscience, 2005:xiv, 342 p.
170. Everitt B, Landau S, Leese M. *Cluster analysis.* 4th ed. / Brian S. Everitt, Sabine Landau, Morven Leese. ed. London: Arnold ; New York : Oxford University Press, 2001:viii, 237 p.
171. Tan P-N, Steinbach M, Kumar V. *Introduction to data mining.* International ed. ed. Boston, Mass. ; London: Pearson Addison Wesley, 2006:xxi, 769 p.
172. Duda RO, Hart PE, Stork DG, Duda ROPc, scene a. *Pattern classification.* 2nd ed. / Richard O. Duda, Peter E. Hart, David G. Stork. ed. New York ; Chichester: Wiley, 2001:xx, 654 p.

173. Sah AP, Thornhill TS, Leboff MS, Glowacki J. Correlation of plain radiographic indices of the hip with quantitative bone mineral density. *Osteoporos Int 2007;18-8:1119-26.*
174. Tonnis D, Heinecke A. Acetabular and femoral anteversion: relationship with osteoarthritis of the hip. *J Bone Joint Surg Am 1999;81-12:1747-70.*
175. Bargar WL, Jamali AA, Nejad AH. Femoral anteversion in THA and its lack of correlation with native acetabular anteversion. *Clin Orthop Relat Res 2010;468-2:527-32.*
176. Aldinger PR, Sabo D, Pritsch M, Thomsen M, Mau H, Ewerbeck V, Breusch SJ. Pattern of periprosthetic bone remodeling around stable uncemented tapered hip stems: a prospective 84-month follow-up study and a median 156-month cross-sectional study with DXA. *Calcif Tissue Int 2003;73-2:115-21.*

List of Tables

Table 2.1	Classification for subsets of osteoarthritis	-12-
Table 2.2	Radiographic Tönnis classification for osteoarthritis of the hip	-20-
Table 3.1	Demographic data of the study cohort	-28-
Table 3.2	Mean values of geometric measures of the study cohort, males and females	-33-
Table 3.3	Mean differences in FO between radiographs and CT	-34-
Table 4.1	Demographic data of the entire cohort, male patients and female patients	-45-
Table 4.2	Inter-observer and intra-observer ICCs for all analysed parameters	-49-
Table 4.3	Mean values of geometric measures for the entire cohort, males and females	-51-
Table 4.4	Prediction of 3D FO as measured on CT using regression equations	-55-
Table 5.1	Differences in mode scores for corresponding radiographs	-68-
Table 5.2	Least squares fit coefficients for the medial cortical flare on corresponding radiographs and CT	-71-
Table 6.1	Patient demographics and mean parameters for the entire cohort, males and females	-83-
Table 6.2	Measurements of native femoral anatomy by cluster	-87-

List of Figures

Figure 2.1	Charnley's low-friction arthroplasty, Judet prosthesis	-15-
Figure 3.1	Radiographic femoral offset measurements	-30-
Figure 3.2	Selection of CT slices of the proximal femur for 3D calculations	-31-
Figure 3.3	Differences in FO between radiographs and CT as boxplots	-35-
Figure 3.3	Relationship between FO as measured on corresponding radiographs and CT	-35-
Figure 3.5	Bland-Altman plot illustrating the agreement between FOp and FOc	-37-
Figure 3.6	Bland-Altman plot illustrating the agreement between FOh and FOc	-37-
Figure 3.7	Geometrical illustration for differences in corresponding FO measurements	-40-
Figure 4.1	Group A: Scatter plot demonstrating the linear correlation between FOp and FOc	-52-
Figure 4.2	Bland-Altman plots illustrating the agreement between CT and FOp, FOc and FOpred	-53-
Figure 4.3	Male patients: Differences FO between CT, radiographs, and prediction	-56-
Figure 4.4	Female patients: Differences FO between CT, radiographs, and prediction	-56-
Figure 5.1	ASM template	-64-
Figure 5.2	Overlay image of shape modes 4 and 5	-69-
Figure 5.3	Least square fits for the endosteal flare of the medial femoral cortex	-70-
Figure 6.1	Canal flare index (CFI) according to Noble	-79-
Figure 6.2	Canal-to-calcar ratio (CCR) cortical thickness index (CTI) according to Dorr	-80-
Figure 6.3	Overlay image of shape modes 2, 3 and 4	-85-
Figure 6.4	Scatter plot with least square fits for the endosteal flare of the medial and lateral femoral cortex	-88-

Appendix A

Considering the transverse plane, the difference in FO measurements observed between AP ***pelvis*** and AP ***hip*** radiographs can be represented as the trigonometric relation between the focal length (*f*), angle between the femoral neck and the focal plane (θ), distance between the centre of the femoral head and the x-ray source (*x)*, true offset (*l*), and the distance between the femoral head and the focal plane (*h*).

Equations (1) and (2) can be applied to determine FO_p and FO_h, respectively, if all other parameters are known.

$$FOh = \frac{fl\cos\theta}{f - h + l\sin\theta} \qquad \text{Equation (1)}$$

$$FOp = \frac{fx + fl\cos\theta}{f - h + l\sin\theta} - \frac{fx}{f - h} \qquad \text{Equation (2)}$$

Through examination of the partial derivative of Equation (2) with respect to *x*, it is possible to analyse the effect of *x* on FOp, if all other parameters are kept constant (Equation (3)).

$$\frac{\partial FOp}{\partial x} = \frac{-fl\sin\theta}{(f - h)^2 + (f - h)l\sin\theta} \qquad \text{Equation (3)}$$

It can therefore be deduced that the relationship between FO_p and *x* is linear; and that for $x = 0$, FOp = FOh, the equation of the linear relationship can be written as Equation (4).

$$FOp = \frac{\partial FOp}{\partial x}x + FOh \qquad \text{Equation (4)}$$

Appendix B

Cluster	med $f(x) = ax^b+c$	lat $f(x) = ax^b+c$
1	a = 3.778e-008 (-6.323e-009 to 8.187e-008) b = 4.183 (3.947 to 4.419) c = 6.099 (5.487 to 6.711) R^2: 0.939	a = 8.247e-008 (-2.551e-008 to 1.904e-007) b = 3.961 (3.695 to 4.227) c = 6.385 (5.908 to 6.862) R^2: 0.925
2	a = 3.138e-008 (-1.105e-008 to 7.381e-008) b = 4.22 (3.945 to 4.495) c = 6.249 (5.616 to 6.882) R^2: 0.9053	a = 4.031e-007 (-2.754e-007 to 1.082e-006) b = 3.602 (3.26 to 3.944) c = 6.492 (5.92 to 7.064) R^2: 0.8516
3	a = 1.499e-007 (-1.348e-008 to 3.132e-007) b = 3.856 (3.637 to 4.075) c = 6.226 (5.666 to 6.787) R^2: 0.9264	a = 1.028e-006 (-1.892e-007 to 2.245e-006) b = 3.425 (3.186 to 3.663) c = 5.97 (5.434 to 6.506) R^2: 0.9051
4	a = 2.023e-008 (-9.42e-009 to 4.988e-008) b = 4.294 (3.998 to 4.59) c = 7.176 (6.46 to 7.893) R^2: 0.9499	a = 1.191e-008 (-1.45e-008 to 3.832e-008) b = 4.335 (3.884 to 4.785) c = 7.637 (6.953 to 8.322) R^2: 0.9067
5	a = 3.183e-009 (4.942e-010 to 5.871e-009) b = 4.67 (4.5 to 4.841) c = 6.355 (6.001 to 6.709) R^2: 0.9634	a = 7.027e-008 (-2.463e-008 to 1.652e-007) b = 3.953 (3.679 to 4.227) c = 6.285 (5.871 to 6.7) R^2: 0.8988
6	a = 7.155e-008 (2.057e-009 to 1.411e-007) b = 4.034 (3.837 to 4.231) c = 6.155 (5.7 to 6.609) R^2: 0.9237	a = 2.357e-007 (-1.782e-008 to 4.893e-007) b = 3.722 (3.505 to 3.94) c = 6.278 (5.871 to 6.686) R^2: 0.9051
7	a = 8.394e-009 (-4.949e-009 to 2.174e-008) b = 4.498 (4.177 to 4.819) c = 6.449 (5.636 to 7.261) R^2: 0.9391	a = 2.235e-007 (-1.864e-007 to 6.333e-007) b = 3.716 (3.346 to 4.085) c = 6.791 (6.117 to 7.464) R^2: 0.9106
8	a = 7.003e-008 (-2.715e-008 to 1.672e-007) b = 4.043 (3.763 to 4.324) c = 6.183 (5.477 to 6.89) R^2: 0.9013	a = 8.095e-008 (-5.956e-008 to 2.215e-007) b = 3.919 (3.566 to 4.271) c = 6.921 (6.394 to 7.447) R^2: 0.874
9	a = 2.96e-007 (-5.364e-007 to 1.128e-006) b = 3.739 (3.166 to 4.312) c = 6.224 (4.922 to 7.525) R^2: 0.8594	a = 2.017e-007 (-3.468e-007 to 7.502e-007) b = 3.725 (3.174 to 4.275) c = 6.943 (6.055 to 7.83) R^2: 0.871
10	a = 1.762e-007 (-6.402e-008 to 4.164e-007) b = 3.837 (3.559 to 4.114) c = 6.373 (5.774 to 6.972) R^2: 0.9301	a = 5.588e-008 (-3.134e-008 to 1.431e-007) b = 4.054 (3.737 to 4.372) c = 6.597 (5.993 to 7.2) R^2: 0.9186

Least squares fit curve equations by cluster for the medial and lateral cortical flare with 95% confidence intervals (95%CI).

Acknowledgements

Professor Dr. Peter R. Aldinger has been my mentor and supervisor for this project in Germany. I would like to thank him for his remarkable guidance and constant support over the past years. His friendship is of great importance to me.

Dr. Harinderjit S. Gill and Professor David W. Murray have been my supervisors at the University of Oxford. I thank them for warmly welcoming me to Oxford and for constantly challenging me in the process of this work. They have made exceptional efforts to help me understand the principles of orthopaedic science in a much clearer way. Their continuous questions, thoughts and guidance were of utmost importance for this endeavour.

During the course of this work, it has been a privilege for me to work with colleagues and staff at the Nuffield Department of Orthopaedics, Rheumatology and Musculoskeletal Sciences, University of Oxford. In particular, I would like to acknowledge the scientific contributions of cand. med. Wenzel Waldstein and Dr. Elise Pegg. I would further like to thank Mrs. Barbara Marks and Ms. Jo Copp for their organisational skills, humour and practical advice.

I am grateful to Dr. Jennifer S. Gregory, Simon R. Goodyear and Professor Richard M. Aspden, Bone and Musculoskeletal Research Programme, Division of Applied Medicine, University of Aberdeen, for support in shape modelling.

The completion of this work would not have been possible without the support of Professor Dr. Volker Ewerbeck, Department of Orthopaedic and Trauma Surgery, University of Heidelberg, Germany and the institutional funding obtained from the non-profit foundation ENDO-Stiftung, Hamburg, Germany.

This thesis is dedicated to my family. I am ever grateful to my parents, my wife and my daughter for their patience, their great support, and for all they have given me.